CHAPTER 4

APPLICATION OF THE SIMULATION MODEL TO LOS ANGELES FINE PRIMARY CARBON PARTICULATE AIR QUALITY

4.1 Introduction

In this chapter, the air quality model developed in Chapter 3 will be used to predict monthly averaged fine primary carbonaceous particulate matter concentrations for each month of 1982 in the central portion of the South Coast Air Basin. First, the data requirements of the simulation model will be outlined and satisfied. Then the air quality model results will be examined and verified based on comparisons between predicted concentrations and those observed during the 1982 field experiments described in Chapter 2.

4.2 Data Requirements for Model Application

In order to apply the air quality model to the task of simulating the emission and transport of fine primary carbonaceous particulate matter in the Los Angeles area, information is needed regarding the sources of emissions, meteorology, atmospheric dispersion parameters, deposition rates, and aerosol carbon background concentrations. In addition, the receptor grid system must be defined and the cell size chosen. The time step, Δt, used for numerical integration of the transport equations must be identified. Finally,

the 1982 air quality observations must be organized for comparison to model predictions.

4.2.1 Emission Source Related Data

A spatially resolved inventory of fine carbon particle emissions during 1982 was compiled for over 70 types of mobile and stationary sources. Emission estimates made within the 80X80-km (50X50-mile) grid system of Figure 4.1 are summarized in Tables 4.1 through 4.4. Details of the emissions estimation procedure are given in Appendix A (Tables A.1-A.4). A tabulation of emissions within the entire South Coast Air Basin (four counties) is presented in Appendix C. By comparing these sets of tables, it is seen that the majority of the aerosol carbon emissions in the South Coast Air Basin arise from sources located within the grid system. A summary of emissions in the 50X50-mile grid, organized by major source category, is shown in Figure 4.2 and in Table 4.5.

Emissions from major stationary fuel burning sources were placed within 2-mile X 2-mile grid cells corresponding to the actual locations of those sources (South Coast Air Quality Managment District 1983a). Emissions from residential sources were distributed spatially in proportion to population density. Highway vehicle emissions were allocated to the grid system in proportion to traffic densities for surface streets and freeways (see procedure of Cass, 1977, updated to the year 1982). Emissions from other mobile sources (ships, railroads, airplanes) likewise were allocated to the grid system based

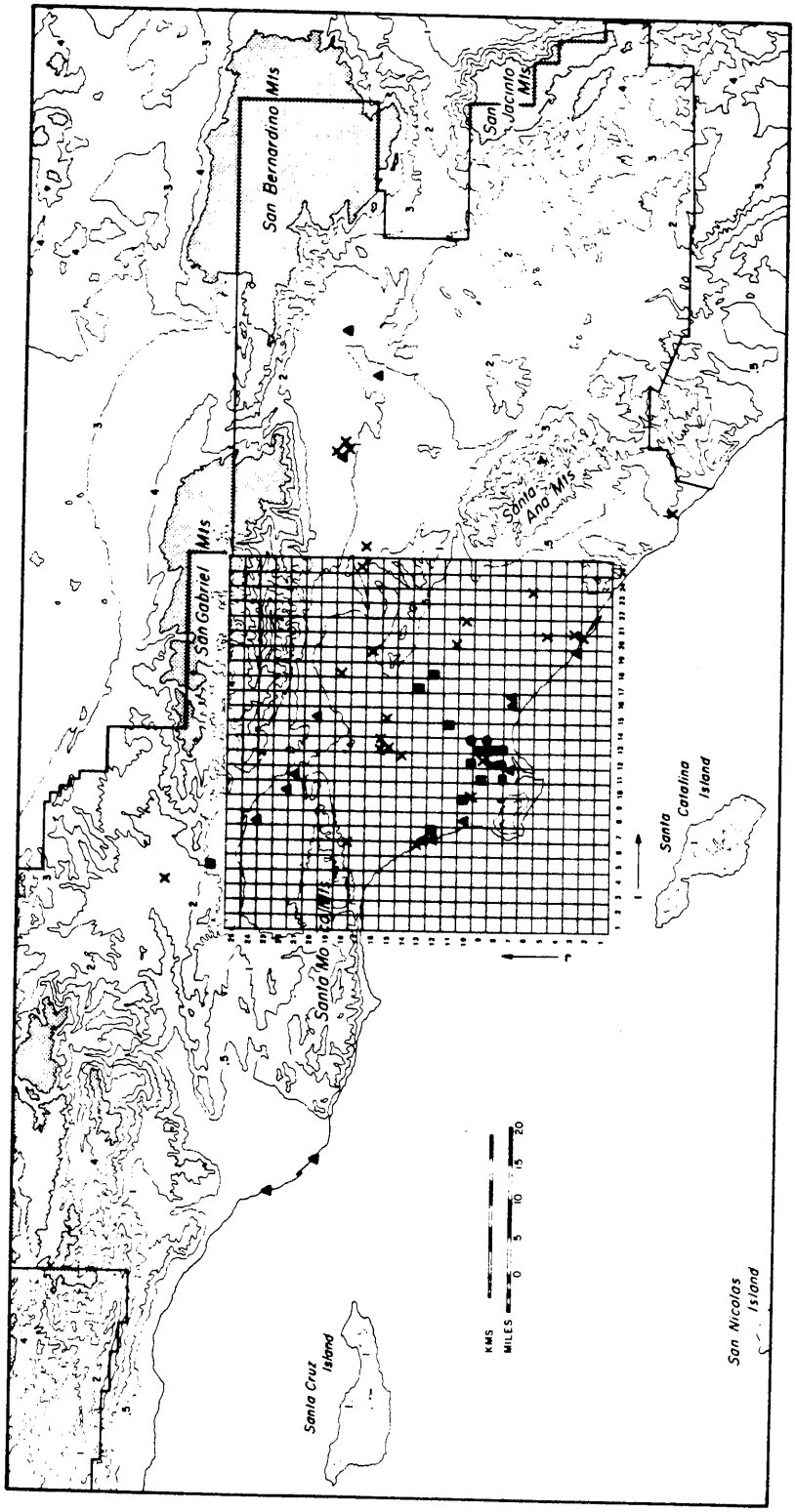

Figure 4.1 The central portion of the South Coast Air Basin showing the grid system used.

Table 4.1

Emissions Estimates for Mobile Sources
Within the 50X50-mile Grid 1982

	Source Class (a)	Fine (c) Total Carbon (kg/day)	Fine (c) Elemental Carbon (kg/day)
MOBILE SOURCES			
Highway Vehicles			
Catalyst Autos	1	466.9	210.1
Non-catalyst Autos	2	2971.0	632.8
Diesel Autos	3	931.9	713.8
Catalyst Light Trucks	1	87.7	39.5
Non-catalyst Light Trucks	2	558.0	118.8
Diesel Light Trucks	3	127.4	97.6
Catalyst Medium Trucks	4	55.3	24.9
Non-catalyst Medium Trucks	4	387.6	82.5
Gasoline Heavy Trucks	4	653.1	139.1
Diesel Heavy Trucks and Buses	5	6337.2	4854.3
Motorcycles	2	62.7	13.4
Civil Aviation			
Jet Aircraft	6,7,8 (b)	394.1	301.9
Aviation Gas	6	12.2	2.6
Commercial Shipping			
Residual Oil-fired Ships	9	82.8	16.6
Diesel Ships	10	179.9	137.8
Railroad			
Diesel Oil	11	899.4	689.0
Miscellaneous			
Off Highway Diesel Vehicles	12	1275.6	1206.9
Off Highway Gasoline Vehicles	13	82.1	17.5
TOTAL MOBILE SOURCES		15864.9	9299.1

(a) See Table D.38 for the definition of the 47 source classes used with the air quality model.

(b) Jet aircraft emissions supplied to the air quality model are divided into emissions located at three separate elevations.

(c) Fine particles below 2.1 μm.

Table 4.2

Emissions Estimates for Stationary Combustion Sources Within the 50X50-mile Grid 1982

	Source Class (a)	Fine (b) Total Carbon (kg/day)	Fine (b) Elemental Carbon (kg/day)
STATIONARY SOURCES			
Fuel Combustion			
Electric Utilities			
Natural Gas (boilers)	14	39.8	small
Natural Gas (turbines)	14	14.8	small
Residual Oil	14	193.6	38.7
Distillate Oil (turbines)	14	0.9	0.5
Digester Gas	14	0.04	small
Refinery Fuel			
Natural Gas	15	57.8	small
Refinery Gas	15	194.9	small
Residual Oil	15	9.2	1.8
Non-refinery Industrial/Low Priority Commercial Fuel			
Natural Gas	16	149.6	small
LPG	16	2.0	small
Residual Oil	16	12.8	2.6
Distillate Oil	16	90.2	52.3
Digester Gas (IC engines)	17	24.2	5.6
Coke Oven Gas	16	0 (c)	0 (c)
Gasoline (IC engines)	17	21.1	2.1
Distillate Oil (IC engines)	17	22.2	22.2
Residential/High Priority Commercial Fuel			
Natural Gas	18	642.1	211.9
LPG	18	11.6	3.8
Residual Oil	18	41.2	8.2
Distillate Oil	18	53.5	31.0
Coal	18	96.7	21.3
TOTAL FUEL COMBUSTION		1678.2	402.0

(a) See Table D.38 for the definition of the 47 source classes used with the air quality model.

(b) Fine particles below 2.1 μm.

(c) Sources located outside the 50X50-mile grid.

Table 4.3

Emissions Estimates for Industrial Processes
Within the 50X50-mile Grid 1982

	Source Class (a)	Fine (b) Total Carbon (kg/day)	Fine (b) Elemental Carbon (kg/day)
STATIONARY SOURCES			
Industrial Process Point Sources			
Petroleum Industry			
Refining (FCCU)	19	32.7	8.2
Other	20	278.2	0
Organic Solvent Use			
Surface Coating	21	1432.9	0
Printing	21	12.9	0
Degreasing	22	5.1	0
Other	22	106.2	0
Chemical			
Organic	23	736.2	44.2
Inorganic	43	0	0
Metallurgical			
Primary	24	228.4	0
Secondary	25	166.8	0
Fabrication	44	0	0
Mineral	26	212.0	54.3
Waste Burning	27	67.2	47.0
Wood Processing	28	85.6	11.1
Food and Agriculture	32	5.0	0
Asphalt Roofing	29	84.2	3.4
Textile	32	1.8	0
Rubber and Plastics	30	35.7	0
Coke Calciner	31	239.2	239.2
Miscellaneous Industrial	32	423.9	30.5
TOTAL PROCESS POINT SOURCES		4154.0	437.9

(a) See Table D.38 for the definition of the 47 source classes used with the air quality model.

(b) Fine particles below 2.1 μm.

Table 4.4

Emissions Estimates for Fugitive Sources
Within the 50X50-mile Grid 1982

	Source Class (a)	Fine (c) Total Carbon (kg/day)	Fine (c) Elemental Carbon (kg/day)
FUGITIVE SOURCES			
Road and Building Construction	45	0	0
Agricultural Tilling	46	0	0
Livestock Feedlots	33	20.4	0
Unpaved Road Dust	47	0	0
Paved Road Dust	34	5288.1	174.5
Tire Attrition	35	1001.4	330.5
Brake Lining Attrition	36	1804.8	324.9
Forest Fires (seasonal)	(b)	933.1	56.0
Structural Fires	37	92.8	29.7
Fireplaces	38	1612.6	343.0
Cigarettes	39	1376.9	41.3
Charcoal Broilers	41	4456.1	66.8
Agricultural Burning	40	2.8	0.3
Sea Salt	(b)	0	0
Roofing Tar Pots	42	753.2	0.8
TOTAL FUGITIVE SOURCES		17342.2	1367.8

(a) See Table D.38 for the definition of the 47 source classes used with the air quality model.

(b) Source class is not used with the air quality model.

(c) Fine particles below 2.1 μm.

Figure 4.2

FINE AEROSOL CARBON EMISSIONS IN THE 50×50 MI. MODELING REGION, 1982

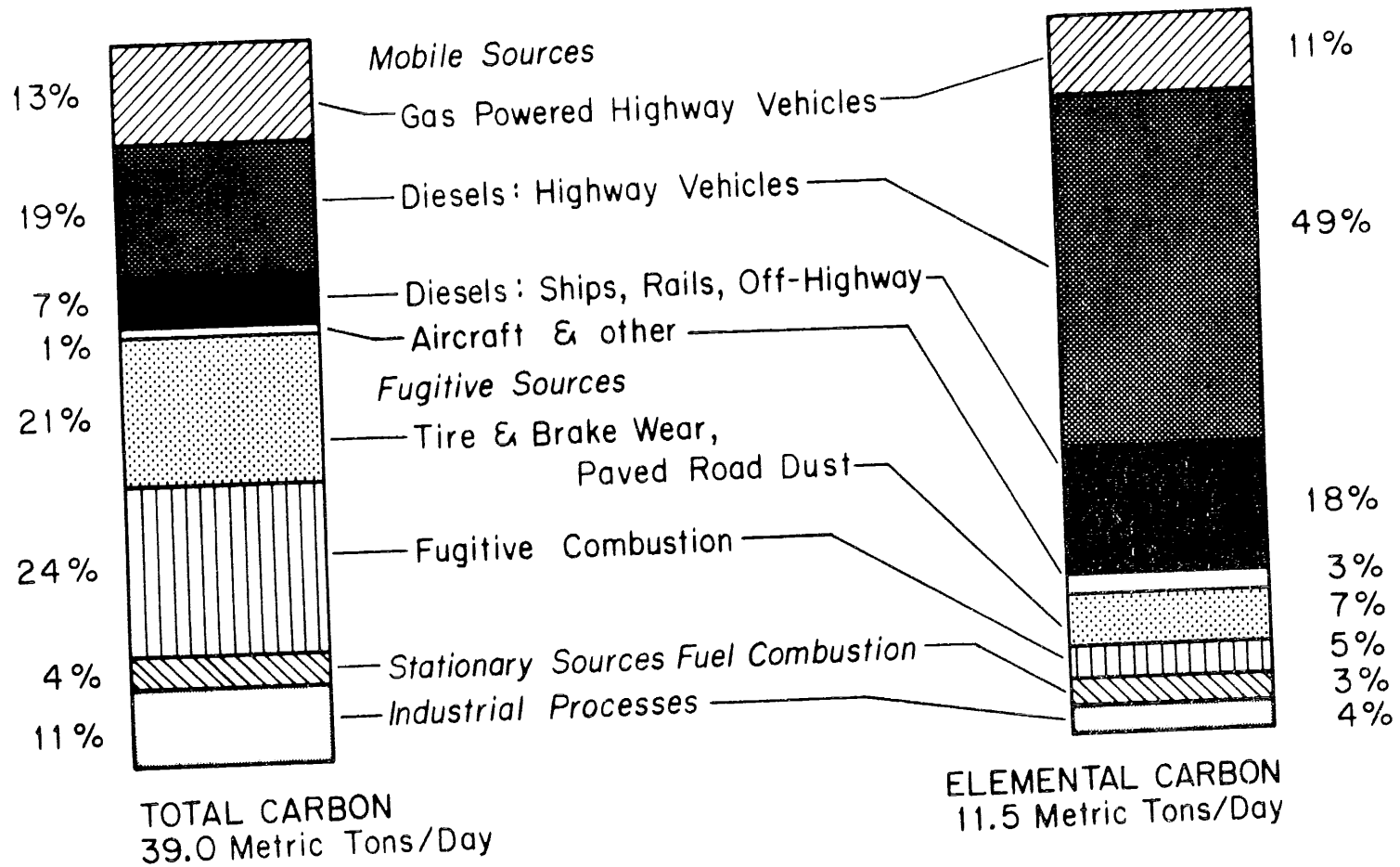

Table 4.5

1982 Annual Average Fine Particulate
Carbon Emissions Summary
Within the 50X50-mile grid

Major Source Category	Fine Total Carbon (kg/day) TC	Fine Elemental Carbon (kg/day) EC
Gasoline powered highway vehicles	5242.3	1261.1
Diesel: highway vehicles	7396.5	5665.7
Diesel: ships, rail, off-highway	2654.9	2033.7
Aircraft and other mobile	571.2	338.6
Highway fugitive (tire and brake wear; road dust)	8094.3	829.9
Other fugitive (fugitive combustion + livestock feedlots)	9247.9	537.9
Stationary source fuel combustion	1678.2	402.0
Industrial processes	4154.0	437.9
TOTAL	39039.3	11506.8

on travel patterns (see Cass 1977). Source location (by source class) was obtained for all other sources from a computerized emission inventory forecast provided by the California Air Resources Board (Ranzieri 1983). The spatial distribution of average daily emissions from all sources for December 1982 is illustrated in Figure 4.3 for total carbon emissions and in Figure 4.4 for elemental carbon

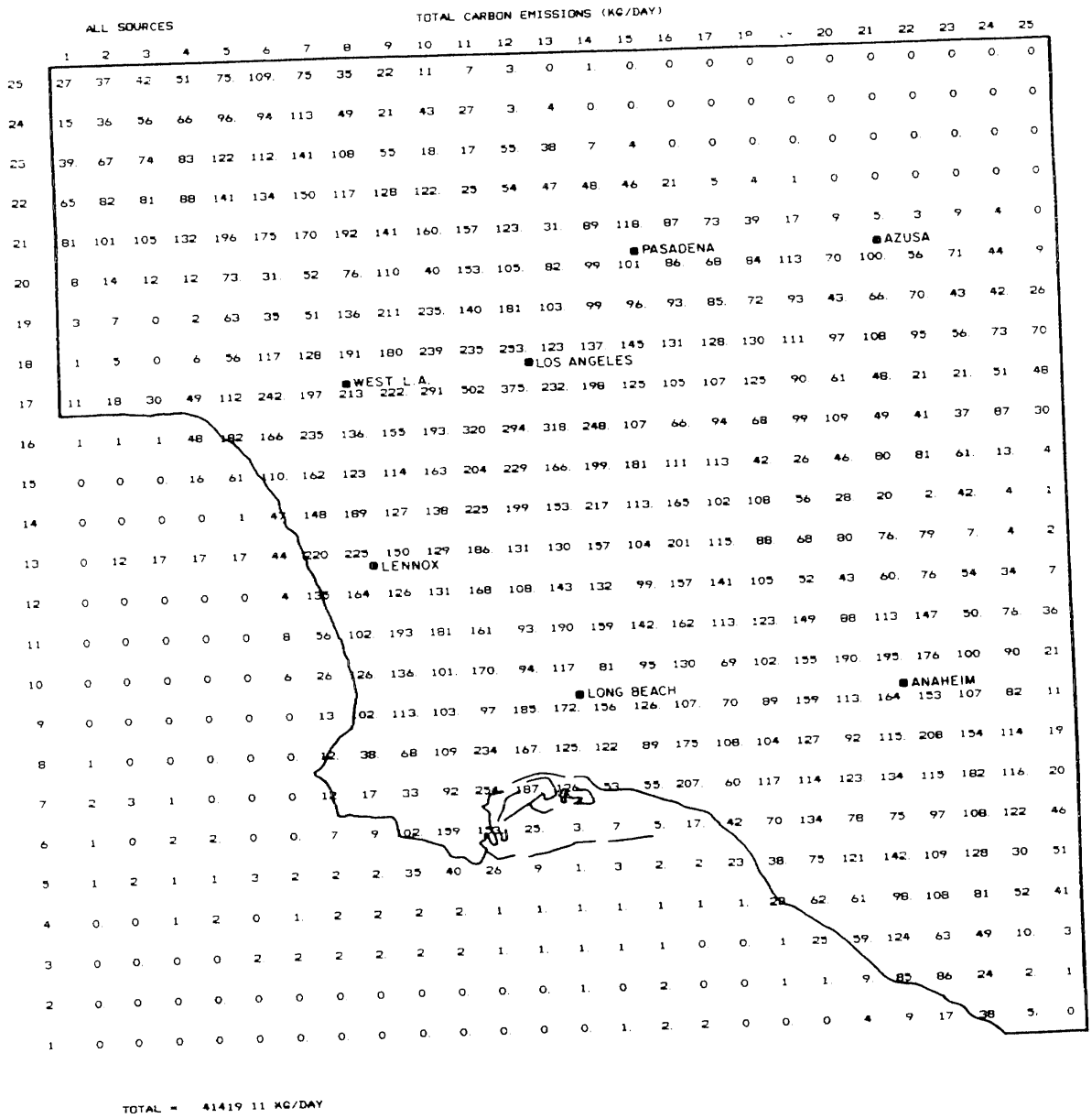

Figure 4.3 Fine total carbon emissions within the 50X50-mile grid during December 1982.

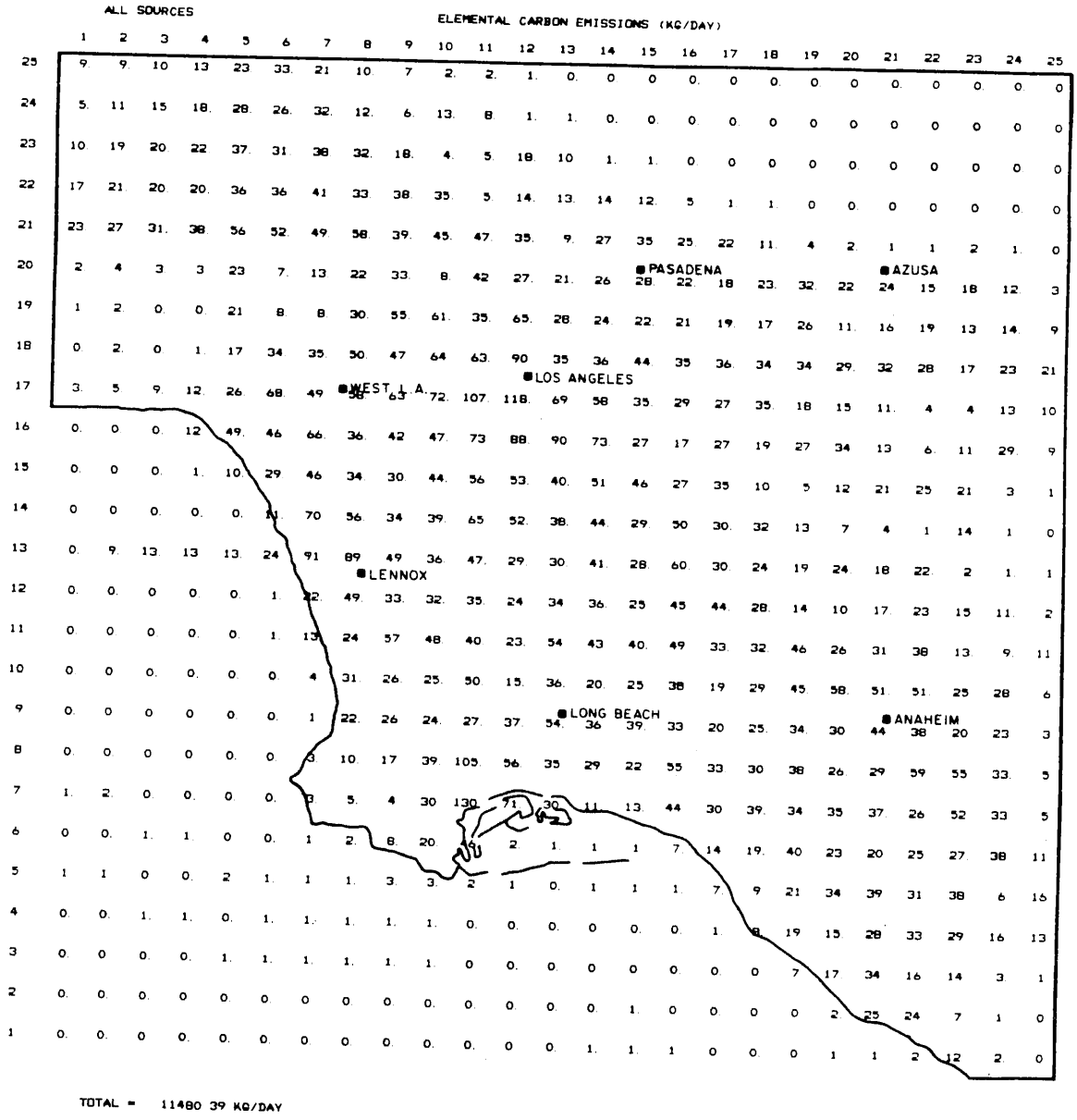

Figure 4.4 Fine elemental carbon emissions within the 50X50-mile grid during December 1982.

emissions. These gridded emissions maps were obtained by overlaying many similar maps, one developed for each source class. (Note that total carbon emissions in December slightly exceed the annual average value given in Table 4.5.)

Monthly fuel consumption data were used to determine seasonal trends in emissions for stationary fuel burning sources. The seasonal variation in emissions from fireplace combustion of wood is documented in Appendix A, Table A.9, note (b). All other source classes are assumed to operate without a pronounced seasonal variation.

The typical diurnal variation of emissions from vehicular traffic, airport operations, and electric utilities was specified based on the past studies of those sources (see Cass 1977). Local charcoal broiler establishments were surveyed to determine their level of operation at various times of day in order to approximate a typical diurnal pattern for emissions from this source class. The remaining source types were divided into two categories: (1) those that were assumed to operate at a uniform rate 24 hours per day and (2) those that were assumed to operate only during daylight hours. The latter group includes agricultural tilling, roofing tar pots, and off-road vehicles.

An effective stack height was specified for each source class which varies in accordance with hourly meteorological conditions. The Briggs plume rise formula (Briggs 1971) was used to compute plume rise as a function of wind speed for each source class. Plume rise was computed during each time step of the model's execution, depending on

the wind speed at that time step. Then computed plume rise was added to the physical stack height of the source to arrive at the effective stack height of emissions (see Cass 1977; Appendix A4).

All emissions from a given source class residing within a single grid cell are aggregated to form a single virtual source. To approximate an area source of particulate matter being released throughout the cell, the location of the virtual source is selected at random at each time step from a uniform distribution of possible horizontal locations within the grid cell.

Since the model performs a separate transport calculation for each source class, computation time may be shortened by combining several similar source types into a single source class. The sources must be similar, however, since all sources within a source class will have the same effective stack height and will experience an identical diurnal modulation of emissions strength within the model. Also, if too many source types are combined to form a single source class, information regarding the incremental contribution to air pollutant concentrations from individual source types will be lost. This information on source class contribution to downwind air quality is needed for control strategy analysis. The 74 separate source types listed in Tables 4.1 through 4.4 were grouped into 47 source classes, each of which will be handled separately during air quality modeling calculations. The members of each of these 47 source classes are indicated in the second column of Tables 4.1 through 4.4.

Although reasonable estimates of the chemical composition of

paved road dust may be made, it is difficult to assess the emission rate and the fraction of street dust that becomes airborne. For this source class only, a receptor modeling calculation was performed which then was used to replace the transport model as the method chosen to account for the paved road dust contribution to aerosol carbon levels. Fine particle road dust samples were taken that were analyzed chemically to determine their elemental composition, including the percentage of Al, Si, TC and EC in the road dust (Gray, Cass, and Turpin 1985). The ambient measurements of Al and Si taken at each monitoring site during 1982 each were used independently to estimate the maximum aerosol carbon concentrations that could be present due to paved road dust at the seven monitoring sites. Then the two estimates based on Al and Si were averaged. This calculation was performed separately for each month of the year at each monitoring site. (For an example of the receptor modeling technique applied to source apportionment in Los Angeles, see Cass and McRae [1983].) The ratio between receptor-modeled monthly average total carbon (or elemental carbon) and transport-modeled monthly average total carbon (using estimates of emissions of paved road dust from Table A.4) ranged from 0.12 to 0.53, with an average of 0.276. This indicates that the fine carbon particulate emissions from paved road dust presented in Table 4.4 that are based on present government estimates of road dust emissions may have been overestimated by as much as a factor of 8 but, more likely, closer to a factor of about 3 or 4. This emissions overestimate does not affect the model validation results because the

receptor model, rather than the transport model, was used to compute soil and road dust levels.

4.2.2 Meteorological Data

It is necessary to construct a time history of wind speed, wind direction, and inversion base motion for use with the air quality model presented in Chapter 3. It is also necessary to estimate the maximum retention time of air parcels within the grid system, τ_c.

After careful consideration of the available wind monitoring locations, the wind station operated by the South Coast Air Quality Management District at their central Los Angeles site was chosen (see Cass 1977, p. 157) to supply hourly averaged wind speeds and directions for use with the model (South Coast Air Quality Management District 1983b). A more detailed treatment would be needed in order to track the turning of the wind field around the Santa Monica Mountains as air parcels enter the San Fernando Valley. In order to avoid that problem, the model calculation will be restricted to predicting the concentration of carbonaceous particulate mater over the central flatlands of the Los Angeles basin and the adjoining San Gabriel Valley.

Inversion base motion above ground level is represented by a stylized diurnal cycle that passes through two daily measures of inversion base height. Early morning inversion base height is measured daily at the University of California at Los Angeles (UCLA), and maximum afternoon mixing depth over downtown Los Angeles is

calculated based on the morning sounding combined with data on the maximum ground level temperature reached at downtown Los Angeles. These two estimates of overnight and afternoon mixing depth were obtained from the South Coast Air Quality Management District (1983c) for each day during 1982, and then the mixing depth data were interpolated to form a diurnal cycle of the form shown in Figure 3.2 (from Cass 1977). Fresh emissions contribute to model-computed concentrations in inverse proportion to inversion base height. Examination of the monthly averaged diurnal cycle of model-computed elemental carbon concentrations shows early morning peaks and afternoon/evening lows in ratios similar to those found in observed concentrations of elemental carbon as inferred from km tape sampler data (Phadke et al. 1975, Cass et al. 1984). The use of this approximate diurnal cycle appears to adequately represent the mixing depth during computation of pollutant concentrations.

A selection of trajectory integration time, τ_c, must be made in order to determine how long each air parcel must be tracked. Cass (1981) observed that over 95% of the air parcels originating at major source locations within the 50X50-mile grid system will be outside the gridded area after 48 hours (using trajectories based on hourly averaged wind data from the years 1972 through 1974). Therefore, τ_c, is set to 48 hours for this model application.

4.2.3 Estimation of Atmospheric Diffusive Dispersion Parameters

Atmospheric turbulence causes small scale air parcel motions that are not resolvable from trajectory calculations based on mean wind speed and direction alone. The degree of air parcel dispersion in the i^{th} coordinate direction may be measured in terms of the standard deviation $\sigma_i(t)$ of the concentration distribution in that direction. Estimates of $\sigma_1(t)$ and $\sigma_2(t)$ are necessary for the simulation of horizontal eddy diffusion as described in Chapter 3, Section 3.3.1. Evaluation of a vertical dispersion parameter, $\sigma_z(t)$, is also required in order to account for incomplete vertical mixing of plumes at locations close to their source (see Chapter 3, Section 3.3.3).

4.2.3.1 Horizontal Dispersion Parameter In Chapter 3, Section 3.3.1, the assumption was made that the process of horizontal diffusion could be modeled by drawing displacements at random from a two-dimensional Gaussian distribution with mean zero and standard deviation $(\sigma_1(t),\sigma_2(t))$. If it is assumed that an expanding puff in the atmosphere remains symmetric with equal standard deviations in the downwind and crosswind directions, then $\sigma_1(t) = \sigma_2(t) = \sigma_y(t)$.

The most commonly employed estimates of atmospheric dispersion rates have been assembled based on observation of air parcels traveling over open countryside (see Pasquill 1961, Gifford 1961, Turner 1969). In urban areas, however, larger surface roughness and heat island effects result in a greater degree of dispersion than is

expected over open terrain. Cass (1977) summarized experimental observations on the rate of air parcel dispersion for long distance transport over the Los Angeles urban area, based on experiments by Drivas and Shair (1975) and Shair (1977), and for shorter distances in St. Louis by McElroy and Pooler (1968). The resulting equation for σ_y in meters and travel time in seconds, as graphed in Figure 4.5, is

$$\sigma_y(t) = 1.73\ t^{0.80} \qquad (4.1)$$

4.2.3.2 Vertical Dispersion Parameter McElroy and Pooler (1968), as part of their study of dispersion in St. Louis, collected data on the vertical dispersion parameter, σ_z, in terms of Pasquill-Turner stability class. From Figure 4.5, it can be observed that data on σ_y, collected in the Los Angeles basin, are in general agreement with similar estimates for St. Louis. Estimates of vertical dispersion rates based on experiments conducted in Los Angeles are not available. Therefore it is assumed that the estimates of σ_z presented by McElroy and Pooler for mixing over the St. Louis urban area may be used to represent the rate of vertical dispersion over the Los Angeles urban area. In practice, the values of σ_z only affect pollutant concentrations very close to their source because emissions within the model quickly become trapped between the ground and the elevated temperature inversion that persists over the Los Angeles basin.

The standard deviation of plume concentration in the vertical direction is presented by McElroy and Pooler (1968) for St. Louis as

either a function of travel time or downwind distance. Curves of σ_z versus downwind distance are plotted in Figure 4.6 from McElroy and Pooler (1968) for the Pasquill-Turner stability classes B through F. An estimate of σ_z may be obtained at given downwind distance once the Pasquill-Turner stability class has been determined. This stability class, in turn, is a function of surface wind speed and solar radiation or cloud cover. The stability categories are grouped into six classes. Class A is the most unstable, class F the most stable.

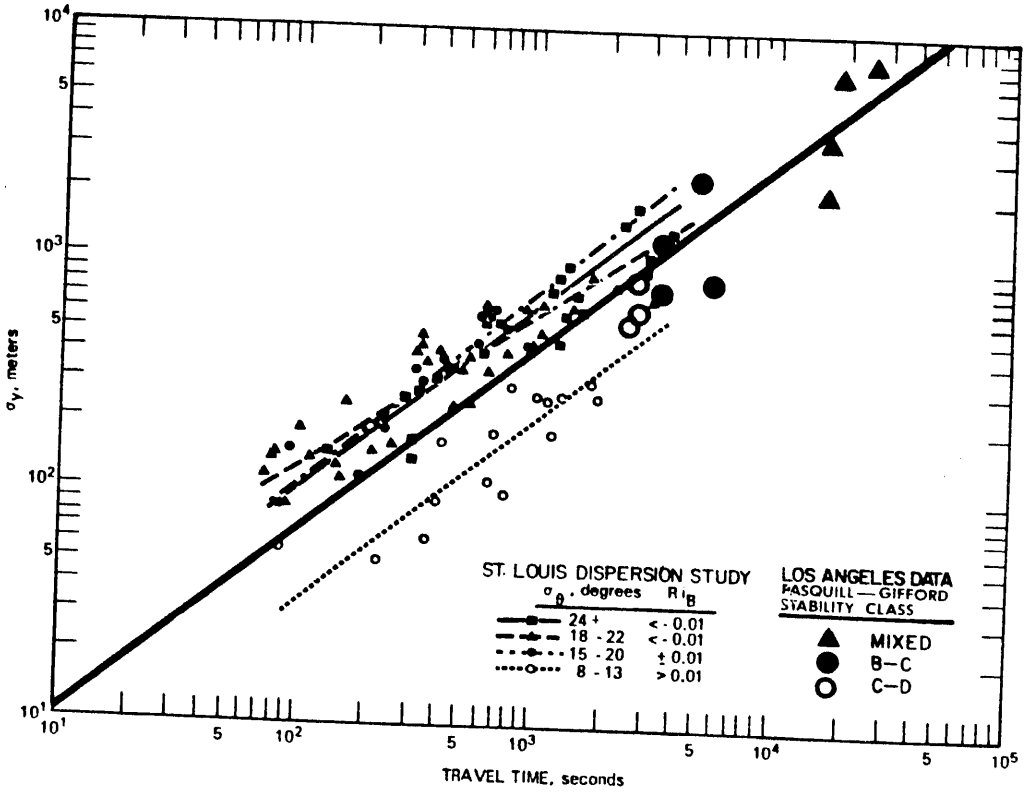

Figure 4.5 Cross-wind standard deviation of plume spread as a function of travel time. St. Louis data from McElroy and Pooler (1968). Los Angeles data from Drivas and Shair (1975) and Shair (1977). Heavy solid line represents function for $\sigma_y(t)$ fit to the Los Angeles data, from Cass (1977).

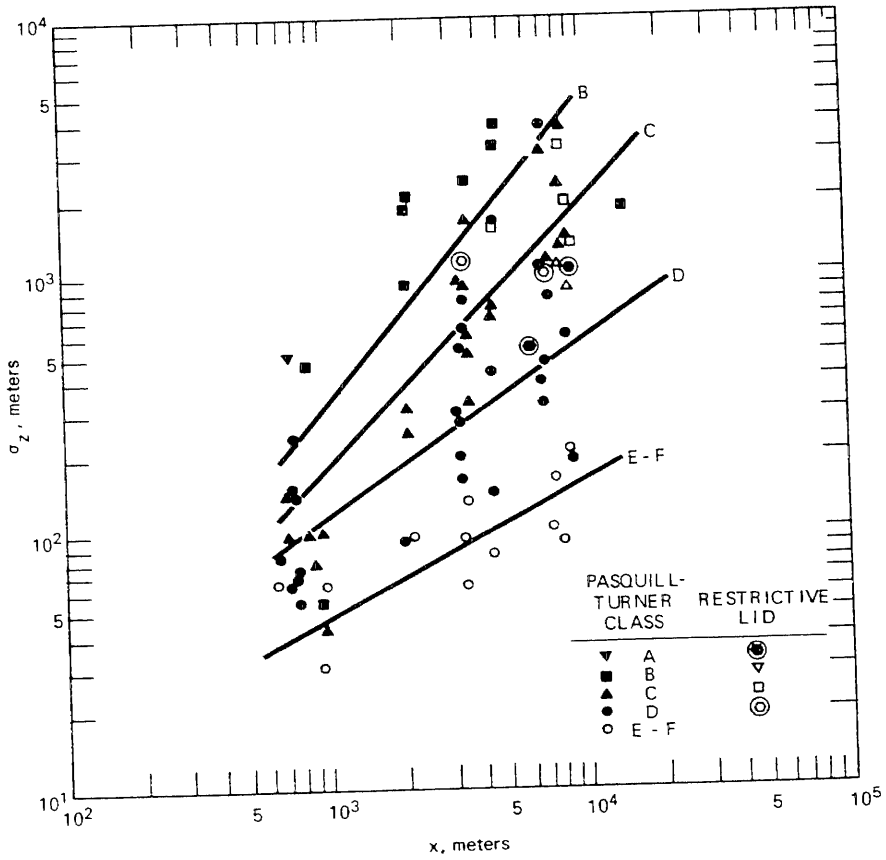

Figure 4.6 Effective vertical standard deviation of plume spread as a function of downwind distance in terms of Pasquill-Turner stability classes (from McElroy and Pooler, 1968).

A guide to the selection of stability categories is given in Table 4.6 (from Turner 1969).

Table 4.6

Key to Stability Categories (from Turner 1969)

Surface Wind Speed (m/sec)	Day			Night	
	Incoming Solar Radiation			Thinly Overcast or	
	Strong	Moderate	Slight	≥ 4/8 Low Cloud	≤ 3/8 Low Cloud
< 2	A	A–B	B	–	–
2–3	A–B	B	C	E	F
3–5	B	B–C	C	D	E
5–6	C	C–D	D	D	D
> 6	C	D	D	D	D

Selection of stablility classes for use during model calculations is accomplished by computing solar radiation intensity at every hour of the year from a solar simulator (McRae 1981) and then combining that information with hourly wind speed observations. For the current model application, only stability classes B, C, and D are used. Class A is not often encountered: McElroy and Pooler (1968) only recorded one example of class A conditions out of over 80 experimental data points. It was also assumed that due to heat island effects and the large effective surface roughness in urban areas, there would always exist sufficient vertical mixing near the surface such that class D would reasonably represent the minimum level of atmospheric mixing for a given downwind distance.

In general, the power law for σ_z as a function of downwind distance, x, may be expressed as:

$$\sigma_z = ax^b \qquad (4.2)$$

where both σ_z and x are in meters. Estimation of the coefficients a and b are summarized for the data of McElroy and Pooler (1968) in Table 4.7.

Table 4.7

Coefficients of $\sigma_z = ax^b$ by Stability Class, Fit to the Data of McElroy and Pooler (1968)

Stability Class	a	b
B	0.066	1.22
C	0.142	1.03
D	0.95	0.70
E-F	1.17	0.54

4.2.4 Estimation of Particulate Dry Deposition Velocity

Cass (1977) used a value for particulate sulfate dry deposition velocity of 0.03 cm/sec. This is within the range of experimental data collected by Davidson (1977), which indicated that sulfate deposition velocities in Los Angeles are in the range 0.01 to 0.1 cm/sec.

The deposition rate of atmospheric aerosols is dependent upon the size distribution of particulate matter in the surface layer near the ground. Both carbonaceous particulate matter and sulfates in the atmosphere are found predominantly in the fine particle fraction, so their dry deposition velocities would be expected to be similar. Therefore, a deposition velocity of 0.03 cm/sec will be used for this

model application. That value implies a time scale for removal of particulate from the mixed layer by dry deposition ranging from about a day to several weeks, depending on the depth of the mixed layer.

4.2.5 Background Concentrations of Fine Atmospheric Carbonaceous Particulate Matter

The prevailing wind direction in the South Coast Air Basin surrounding Los Angeles is from the southwest which means that most new air masses entering the air basin are of marine origin. Therefore, air pollutant concentrations measured at San Nicolas Island, a remote offshore island, should serve as satisfactory estimates of background air quality.

As reported in Chapter 2, fine aerosol concentrations (24-hour averages) were measured at San Nicolas Island for 47 days from March to December 1982. Monthly averaged fine total carbon and fine elemental carbon background concentrations based on the San Nicolas Island data are given in Table 4.8.

4.2.6 Selection of Time Step and Receptor Grid Cell Size

The selection of a time step and horizontal grid cell dimensions should be made simultaneously. One would like to keep the time step as large as possible to reduce the number of computations required to represent a one-year period. On the other hand, the time

Table 4.8

Fine Particulate Carbon
Background Concentrations (a)

	Fine Total Carbon ($\mu g/m^3$)	Fine Elemental Carbon ($\mu g/m^3$)
Jan (b)	2.30	0.35
Feb (b)	2.08	0.34
Mar	1.78	0.28
Apr	2.26	0.34
May	2.46	0.30
Jun	1.20	0.20
Jul	1.43	0.13
Aug	1.58	0.20
Sep	1.68	0.16
Oct	2.76	0.42
Nov	2.08	0.34
Dec	2.30	0.35

Notes:
(a) Monthly average concentrations from samples taken during 1982 at San Nicolas Island, a remote offshore island.
(b) No data were taken during January and February 1982. Concentrations are assumed to be equal to December and November 1982, respectively.

step must be kept small enough for enough statistical particles to be released to adequately estimate the probabilities of transition and, hence, pollutant concentrations. It is desirable to keep the grid cells small in order to attain a high level of spatial resolution in the computed pollutant concentrations. However, if the time step is very large and the grid cells are too small, an insufficient number of particles will reside within each cell. The result will be manifested by computed voids in some grid cells located within zones of

significant pollutant concentration. This is because the grid cells are too small and, hence, too numerous to have accumulated a statistically significant number of pollutant particles.

A time step of one hour is the largest time step possible without discarding useful meteorological information (wind speeds and directions are reported as hourly averages; see Section 4.2.2). Use of a grid cell size with the same dimensions as the 2 mile X 2 mile squares which make up the emissions grid (see Figure 4.1) was investigated by Cass (1977). It was determined that a one-hour time step coupled with τ_c = 48 hours (see Section 4.2.2) and a grid cell size of 2 miles X 2 miles would result in a smooth contour of monthly averaged concentrations from any single source location. Tests of the model simulation under typical 1982 conditions for a single source resulted in concentration distributions free of voids. Therefore, a time step, Δt, of one hour and horizontal grid cell dimensions (Δx_1,Δx_2) of 2 miles X 2 miles should result in concentration predictions which are smooth and accurate.

It may be noted that specification of a vertical cell dimension, Δx_3, is unnecessary. Examination of equations (3.10) and (3.35) through (3.38) reveals that Δx_3 cancels out.

4.2.7 Model Validation Data

During 1982, ambient elemental carbon concentrations were measured at a number of locations in the South Coast Air Basin, as reported in Chapter 2. Seven of these sites are located within the

receptor area that will appear later in Figure 4.23. These observations of monthly averaged elemental carbon air quality may be used to validate the model's prediction of monthly averaged fine elemental carbon concentrations. Verification of the model's performance may be found in the following section of this chapter.

4.3 Air Quality Model Results

4.3.1 Predicted versus Observed Fine Elemental Carbon Particle Concentrations

Elemental carbon is virtually inert in the atmosphere and is released only from primary emission sources. In order to avoid any ambiguity due to the presence of secondary organic aerosols, the accuracy of the predictions of the present air quality model can best be assessed by comparison of observed and predicted elemental carbon levels. Figures 4.7a through 4.13a present the results of the air quality simulation model for fine elemental carbon concentrations at each of the seven monitoring sites located within the receptor grid. The solid horizontal lines represent the monthly averaged concentrations predicted by the model. The small circles represent the arithmetical mean of concentrations observed at the monitoring sites during each month. The error bounds shown denote approximate 95% confidence intervals about each measured monthly mean value (see Cass [1977], Appendix B4, for standard error estimation procedure).

MONTHLY MEAN ELEMENTAL CARBON CONCENTRATION AT LENNOX

AIR QUALITY MODEL RESULTS VS. OBSERVED VALUES

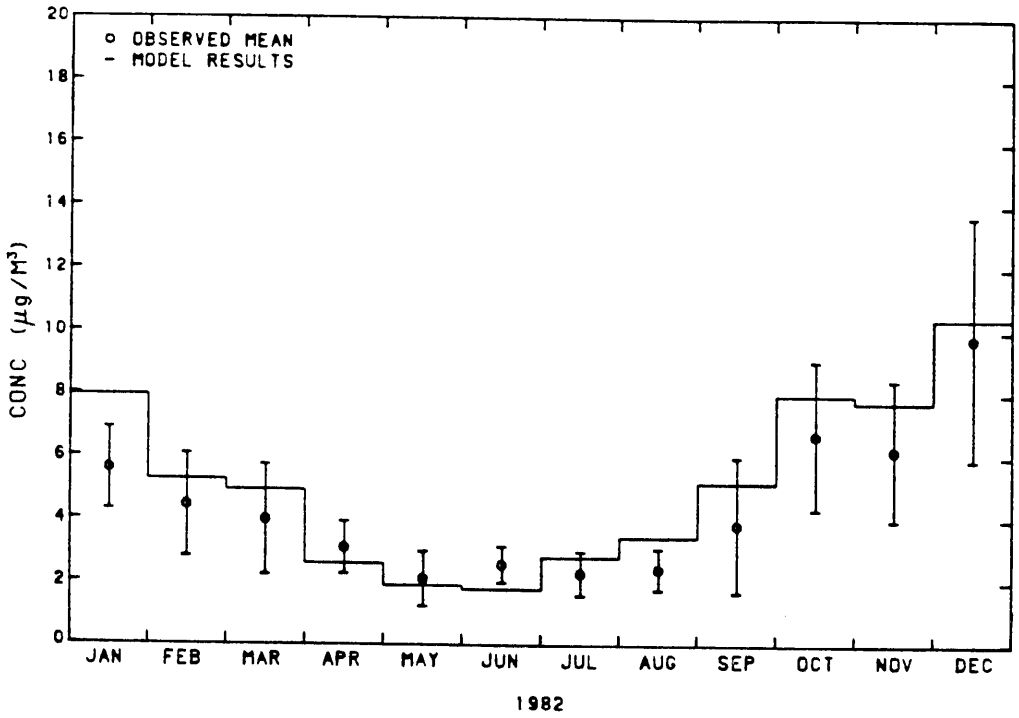

Figure 4.7a

SOURCE CLASS CONTRIBUTIONS TO ELEMENTAL CARBON CONCENTRATIONS AT LENNOX

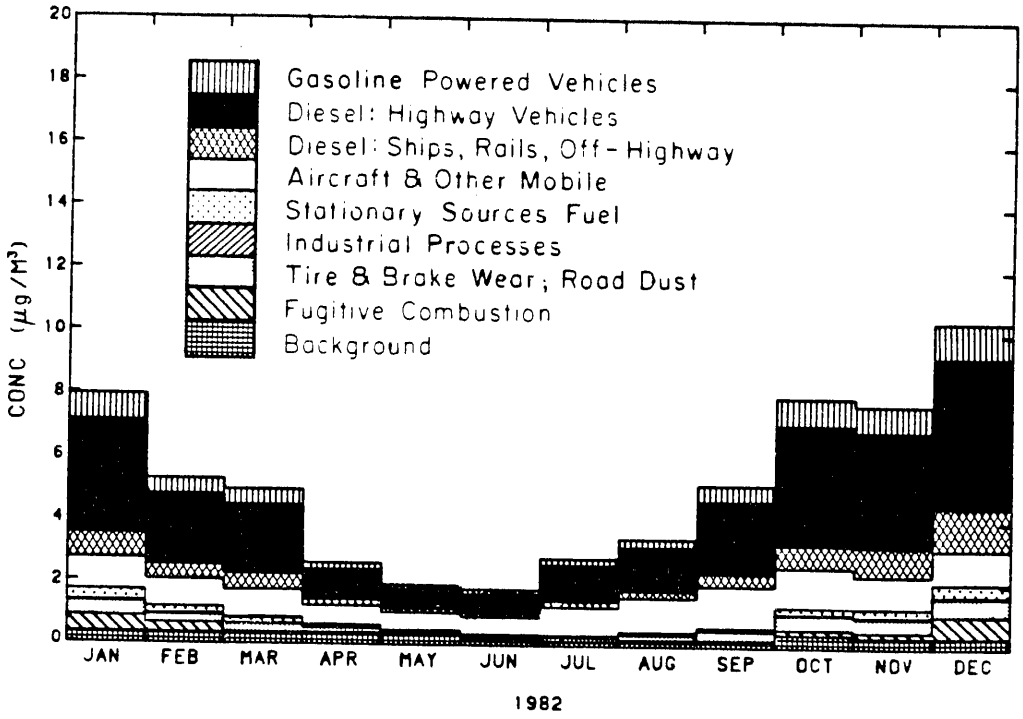

Figure 4.7b

MONTHLY MEAN ELEMENTAL CARBON CONCENTRATION AT LONG BEACH

AIR QUALITY MODEL RESULTS VS. OBSERVED VALUES

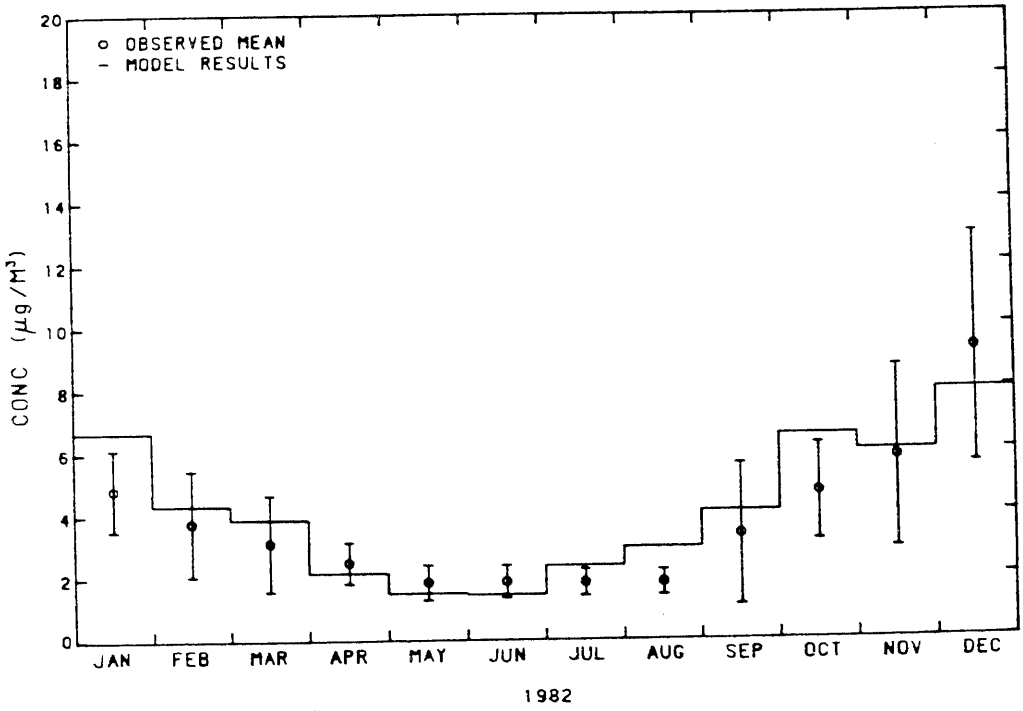

Figure 4.8a

SOURCE CLASS CONTRIBUTIONS TO ELEMENTAL CARBON CONCENTRATIONS

AT LONG BEACH

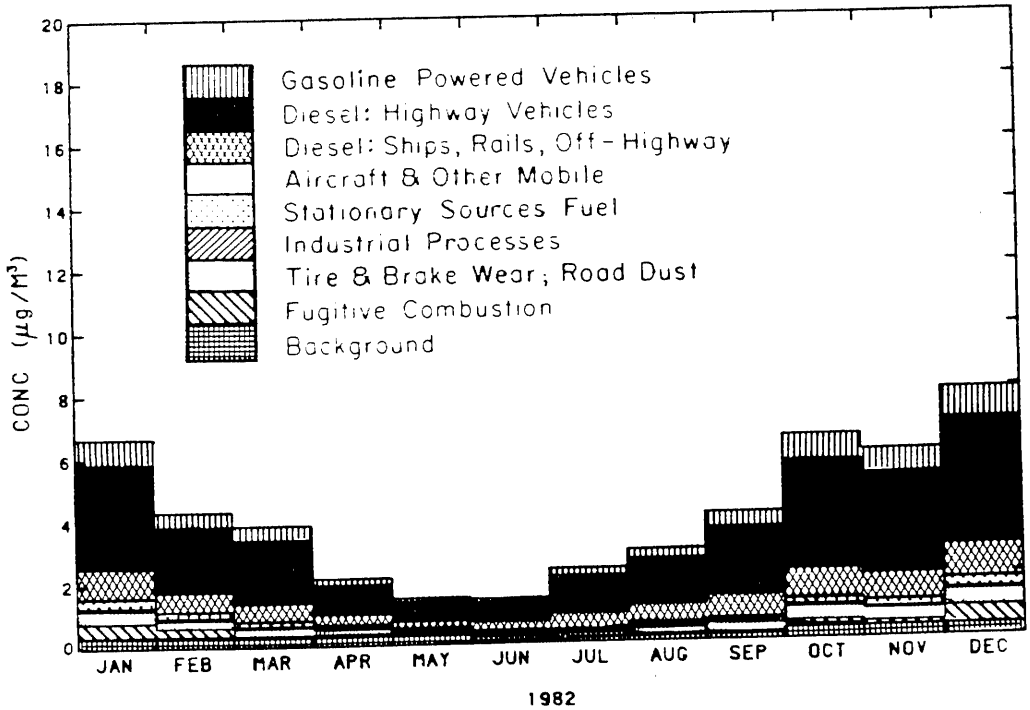

Figure 4.8b

MONTHLY MEAN ELEMENTAL CARBON CONCENTRATION AT WEST LOS ANGELES

AIR QUALITY MODEL RESULTS VS. OBSERVED VALUES

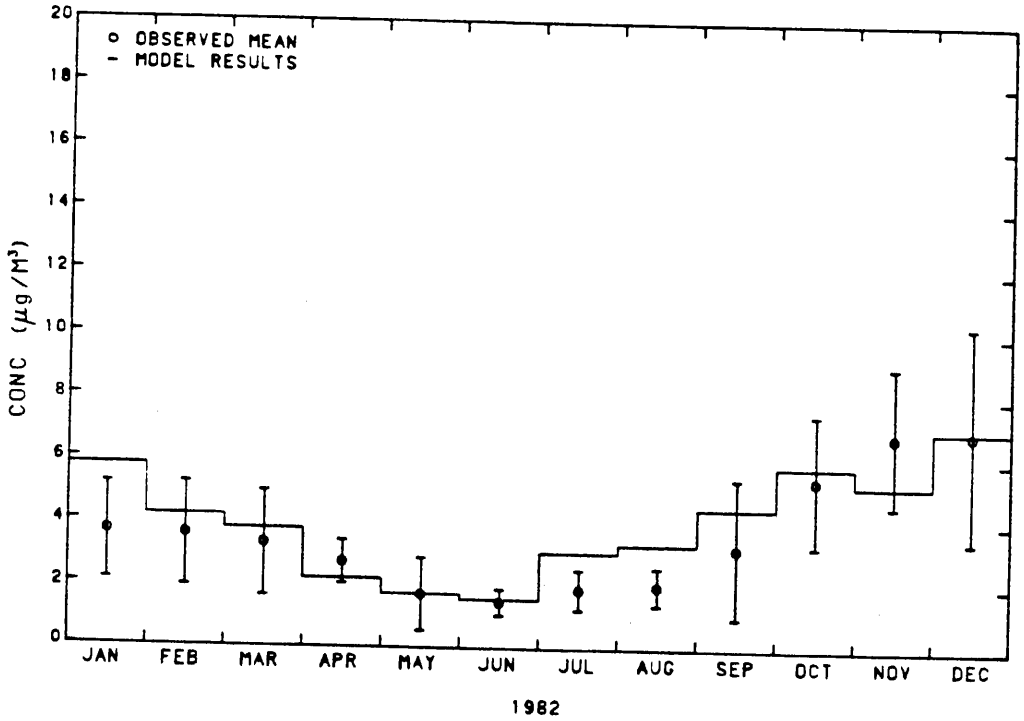

Figure 4.9a

SOURCE CLASS CONTRIBUTIONS TO ELEMENTAL CARBON CONCENTRATIONS

AT WEST LOS ANGELES

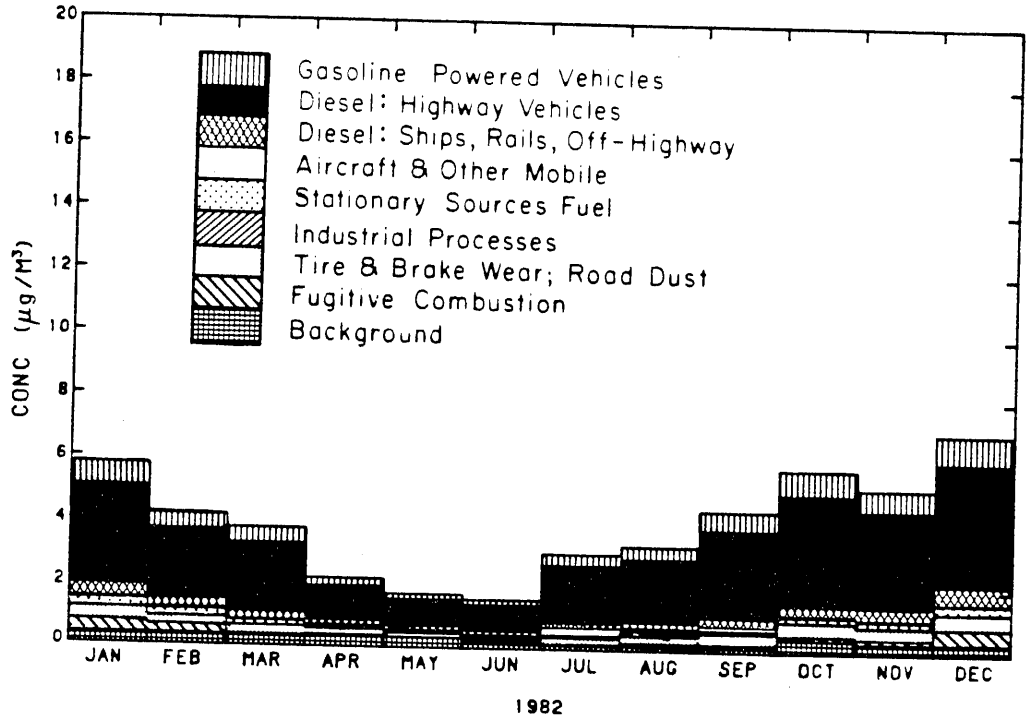

Figure 4.9b

MONTHLY MEAN ELEMENTAL CARBON CONCENTRATION AT LOS ANGELES

AIR QUALITY MODEL RESULTS VS. OBSERVED VALUES

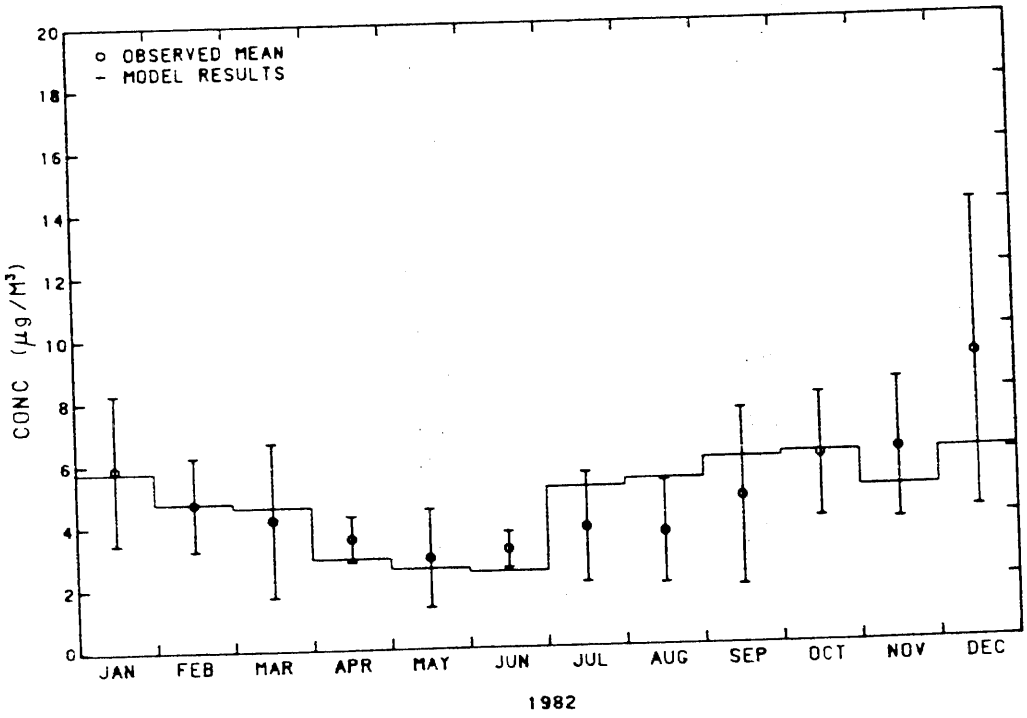

Figure 4.10a

SOURCE CLASS CONTRIBUTIONS TO ELEMENTAL CARBON CONCENTRATIONS

AT LOS ANGELES

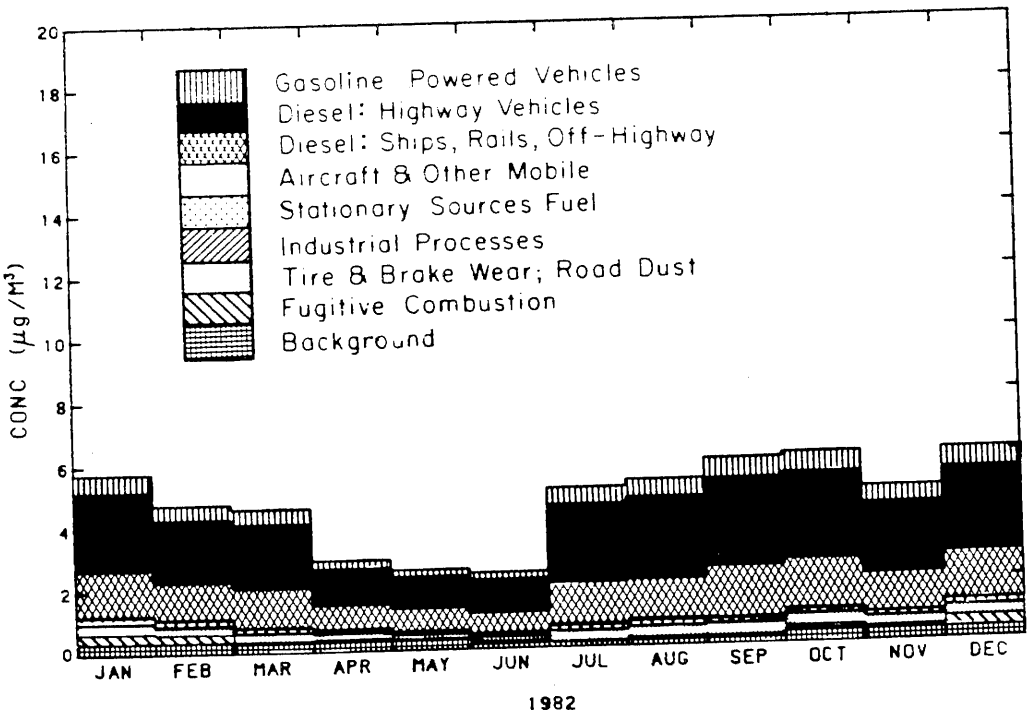

Figure 4.10b

MONTHLY MEAN ELEMENTAL CARBON CONCENTRATION AT ANAHEIM

AIR QUALITY MODEL RESULTS VS. OBSERVED VALUES

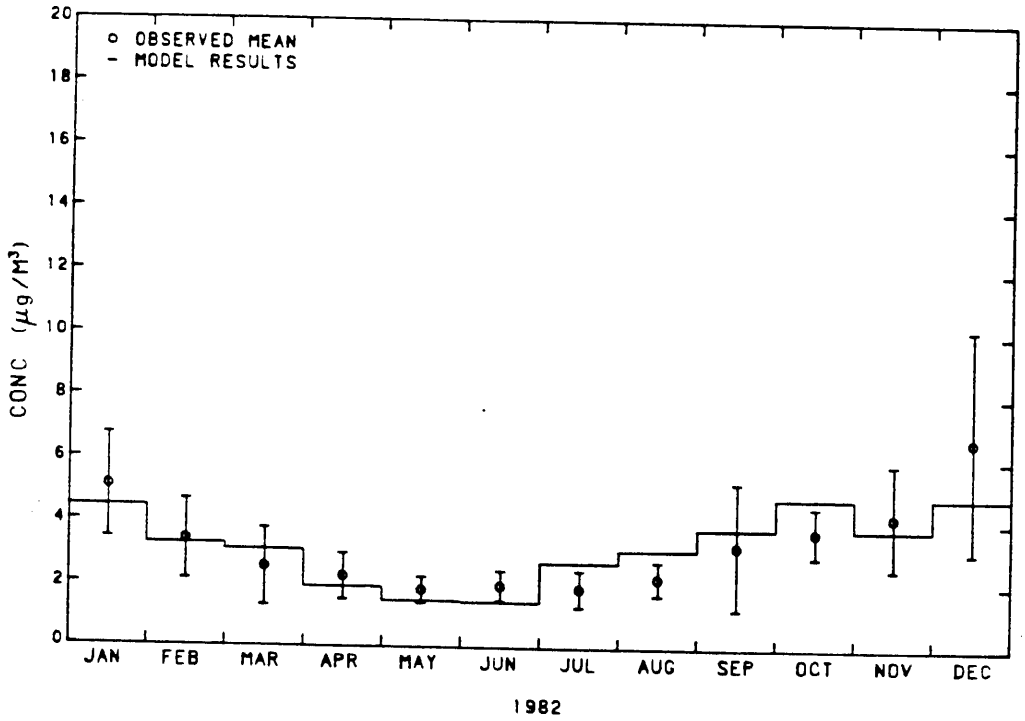

Figure 4.11a

SOURCE CLASS CONTRIBUTIONS TO ELEMENTAL CARBON CONCENTRATIONS AT ANAHEIM

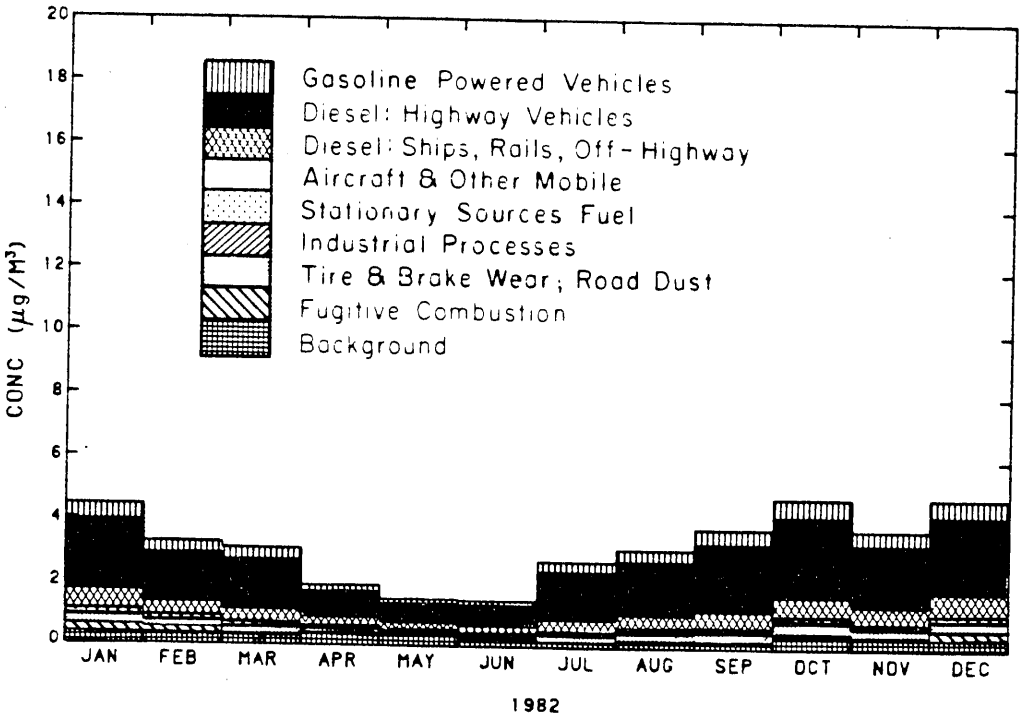

Figure 4.11b

MONTHLY MEAN ELEMENTAL CARBON CONCENTRATION AT PASADENA

AIR QUALITY MODEL RESULTS VS. OBSERVED VALUES

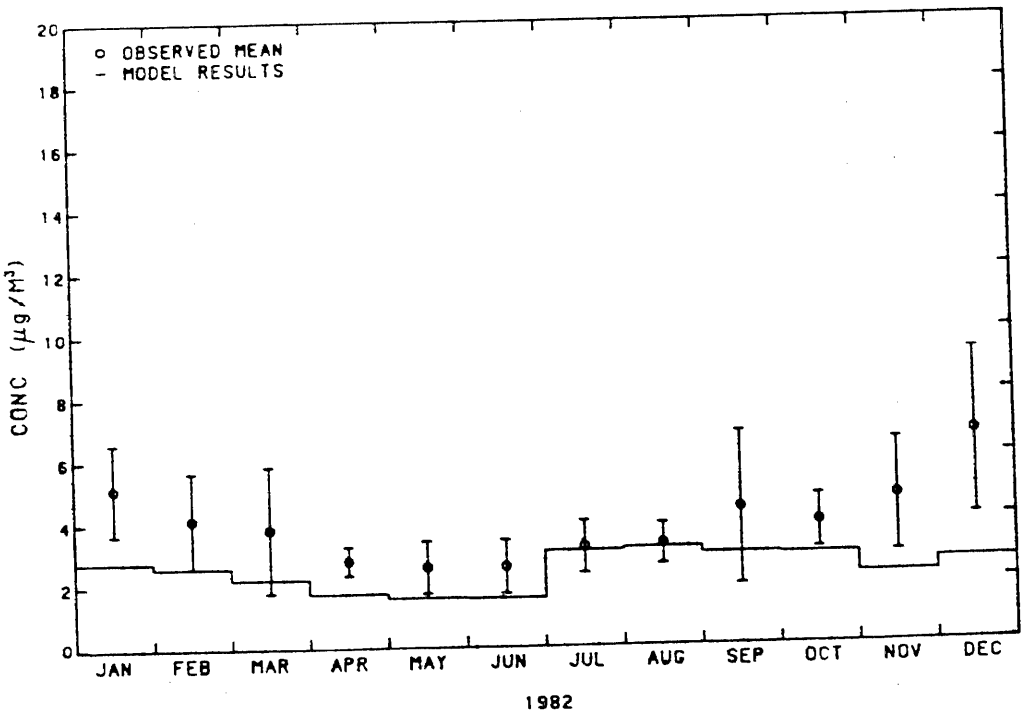

Figure 4.12a

SOURCE CLASS CONTRIBUTIONS TO ELEMENTAL CARBON CONCENTRATIONS AT PASADENA

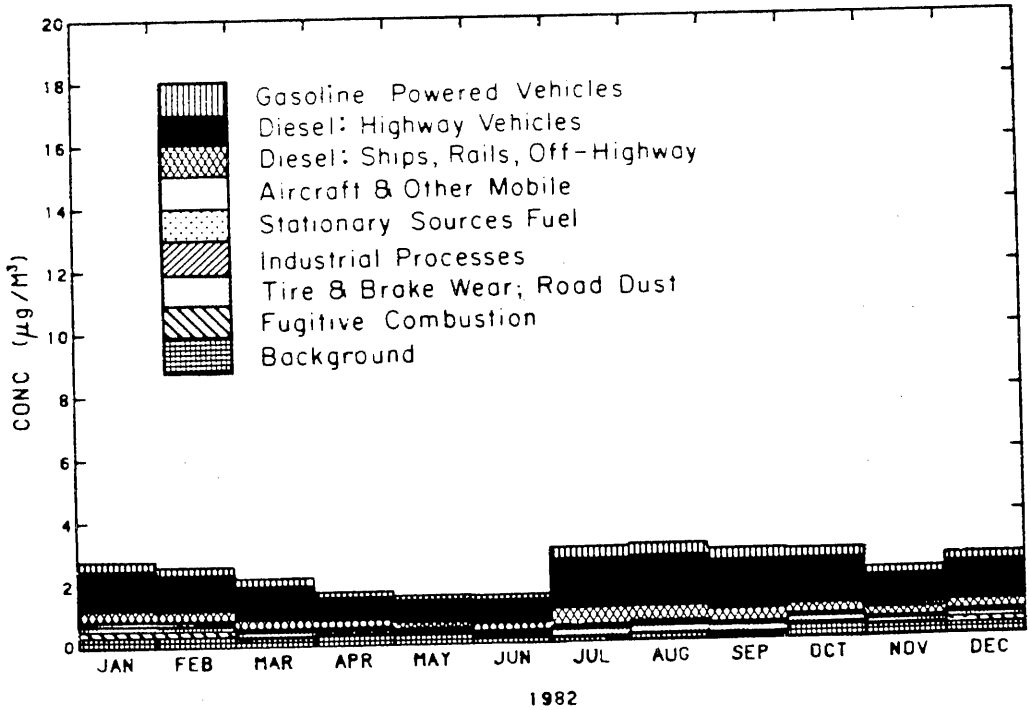

Figure 4.12b

MONTHLY MEAN ELEMENTAL CARBON CONCENTRATION AT AZUSA

AIR QUALITY MODEL RESULTS VS. OBSERVED VALUES

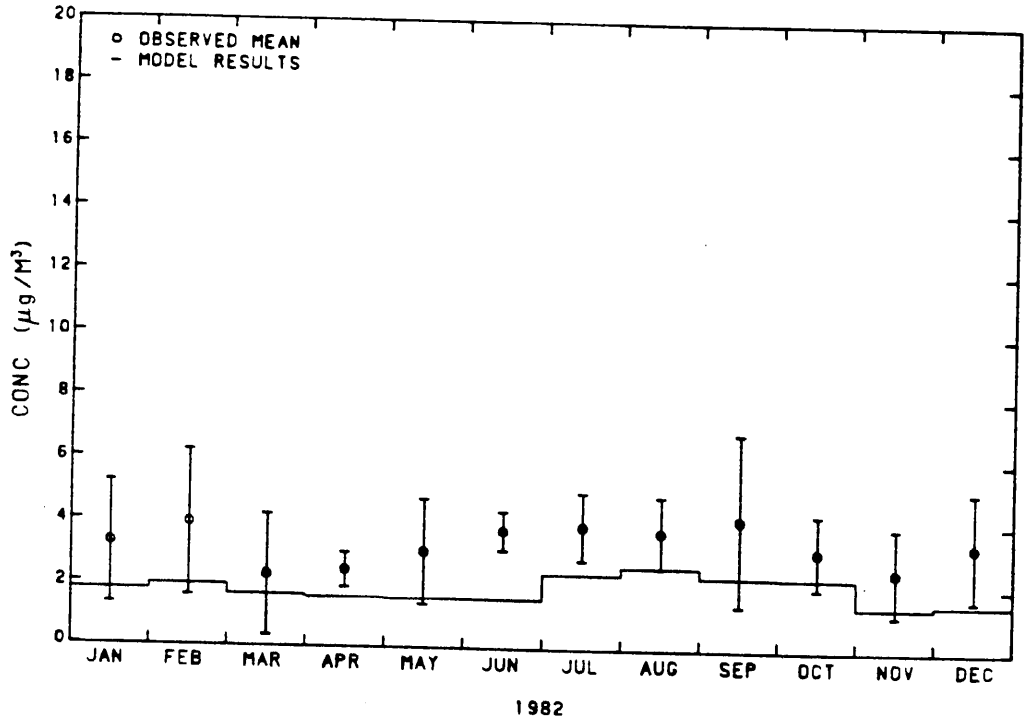

Figure 4.13a

SOURCE CLASS CONTRIBUTIONS TO ELEMENTAL CARBON CONCENTRATIONS AT AZUSA

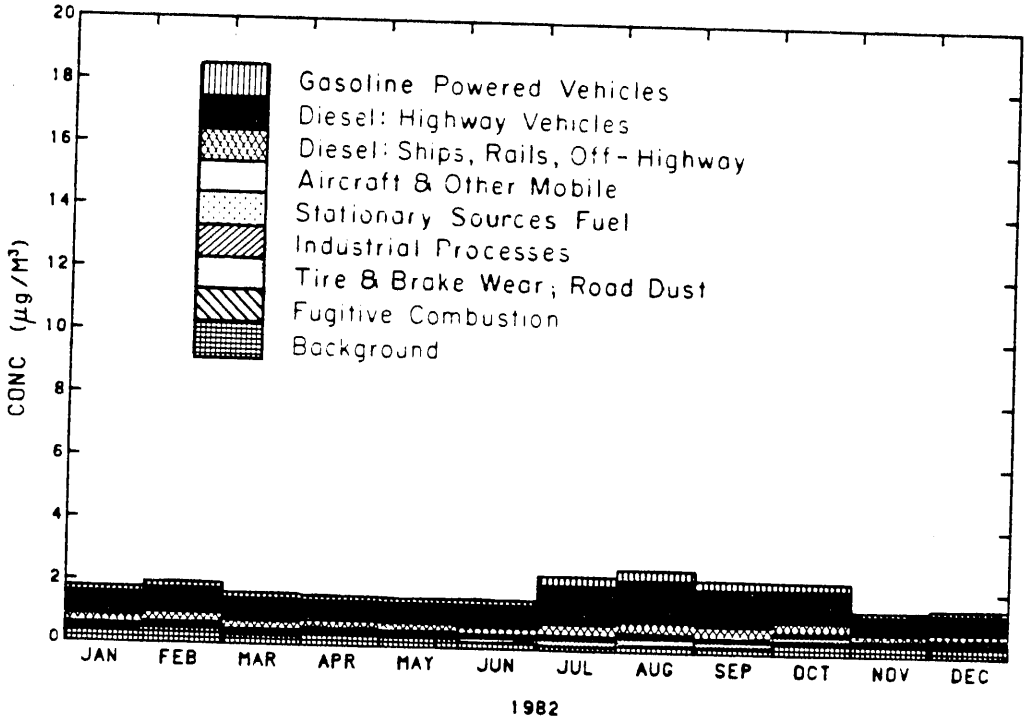

Figure 4.13b

These uncertainties in observed monthly average concentrations are due almost entirely to the facts that atmospheric concentrations fluctuate from day to day and that not all days in each month were sampled. Therefore, the true mean may not have been observed. Any model-predicted monthly average concentration that is within those error bounds is statistically indistinguishable from the measured monthly mean concentration. Fine monthly average elemental carbon particle concentrations predicted by the model are within the error bounds of the observations approximately 68% of the time. Annual average elemental carbon concentration predictions are compared to observations in Table 4.9. At all monitoring sites except Pasadena and Azusa, the annual average prediction is within the 95% confidence interval for the corresponding observation. Examination of Figures 4.7a through 4.13a shows that the model captures the major seasonal features of observed elemental carbon levels. At coastal sites like Lennox, predictions and observations are characterized by high winter concentrations and much lower summer values. At inland sites like Azusa, predicted and observed elemental carbon concentrations remain at about the same level year-round.

4.3.2 Spatial-Temporal Correlation between Predicted and Observed Fine Elemental Carbon Particle Concentrations

Predicted monthly average fine elemental carbon particle concentrations are compared graphically to air quality observations in Figure 4.14. Each data point represents a predicted monthly average

Table 4.9

Observed versus Predicted 1982 Annual Average
Fine Elemental Carbon Concentrations
(concentrations in $\mu g/m^3$)

	Air Quality Observations					Model Results	
	Sample arithmetic mean $\bar{y}$	Sample arithmetic standard deviation σ	Number of 24-hr. samples	Lower confidence limit on $\bar{y}$ (2.5%ile)	Upper confidence limit on $\bar{y}$ (97.5%ile)	Arithmetic mean from air quality model	Prediction is within confidence interval of observations?
Azusa	3.30	1.87	60	2.86	3.74	1.88	No
Long Beach	3.75	3.00	59	3.05	4.46	4.16	Yes
Lennox	4.51	3.16	61	3.78	5.23	5.17	Yes
Pasadena	3.95	2.07	60	3.46	4.43	2.43	No
West Los Angeles	3.61	2.78	58	2.94	4.27	4.01	Yes
Los Angeles	4.87	3.24	61	4.12	5.62	4.71	Yes
Anaheim	3.18	2.31	57	2.62	3.74	3.22	Yes
7 locations	3.88	2.68	416	3.64	4.12	3.66	Yes

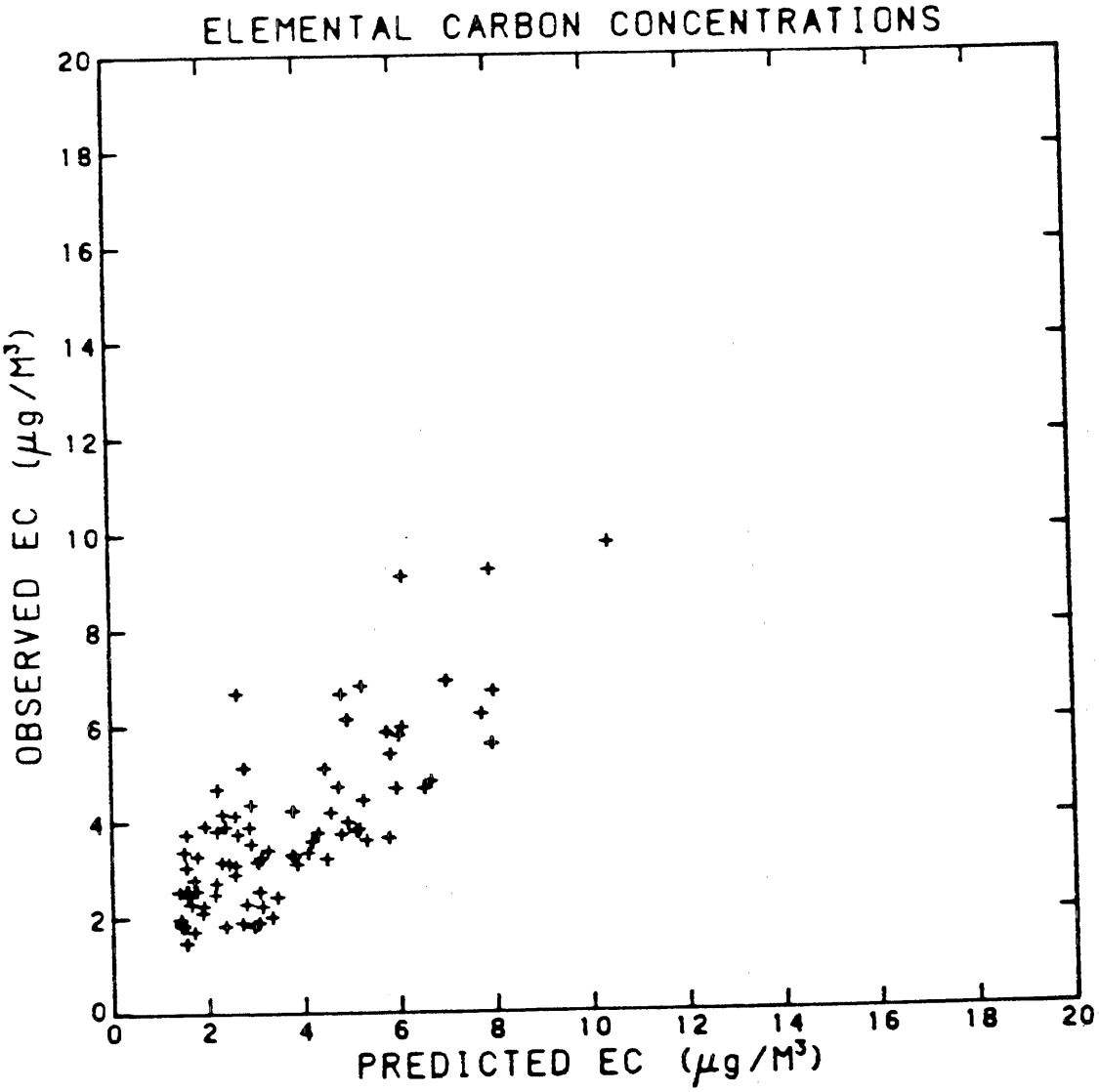

Figure 4.14 Monthly average fine elemental carbon particle concentrations at seven monitoring sites--observations vs. predictions.

concentration at one of the seven monitoring sites versus the corresponding monthly mean of measured concentrations. The correlation between observed and predicted elemental carbon concentrations is 0.78.

The model's ability to predict observed concentrations may be assessed by performing a goodness-of-fit test. The sum of squares of the difference between model predictions and observations, each square normalized by the observed concentration, approximately follows a chi-square distribution. The null hypothesis is that the model predicts elemental carbon concentrations accurately. This hypothesis will be rejected at the α level of significance only if the summation results in a value larger than χ^2_α (where the degrees of freedom equal the number of comparisons minus one); see Walpole and Myers (1978, p. 265) for a discussion of the goodness-of-fit test.

The comparison of predicted and observed annual average elemental carbon concentrations at the seven monitoring sites results in a goodness-of-fit statistic of 1.38. The value is well below $\chi^2_{.05}$ = 12.59 (degrees of freedom = 6), so the null hypothesis may not be rejected at the 0.05 level of significance. This implies that the model is a good predictor of annual average elemental carbon concentrations.

A more severe test involves performing the goodness-of-fit test on predicted monthly averages. The result for monthly average elemental carbon concentrations produces a statistic of 31.55. The chi-square value, $\chi^2_{.05}$ (degrees of freedom = 83), is approximately

105.0 (approximation for χ^2 with large degrees of freedom from Benjamin and Cornell [1970]; Table A.2, note 3); hence, the null hypothesis cannot be rejected at the 0.05 level of significance. The conclusion is that the model provides a good fit to the observed data; therefore, the model may be considered a good predictor of monthly average elemental carbon particle concentrations.

4.3.3 Comparison of Primary Fine Total Carbon Concentration Predictions and Fine Total Carbon Air Quality Observations

The air quality model employed in this study is capable of predicting the primary aerosol contribution to total carbon concentrations, given the inventory of primary aerosol carbon emissions presented in Section 4.2.1. A complete assessment of total aerosol carbon levels cannot be predicted by this model because no provision is made for secondary organic aerosol production due to chemical reaction of gas phase hydrocarbons present in the atmosphere. However, as noted in Chapter 2, a variety of evidence is available that suggests that secondary organics were not the overwhelming determinant of aerosol carbon levels in the Los Angeles area during the year 1982. Therefore, primary aerosol total carbon concentrations predicted by the air quality model may come close to explaining the origin of most of the total carbon levels observed over long averaging times in the atmosphere in that year.

MONTHLY MEAN TOTAL CARBON CONCENTRATION AT LENNOX

AIR QUALITY MODEL RESULTS VS. OBSERVED VALUES

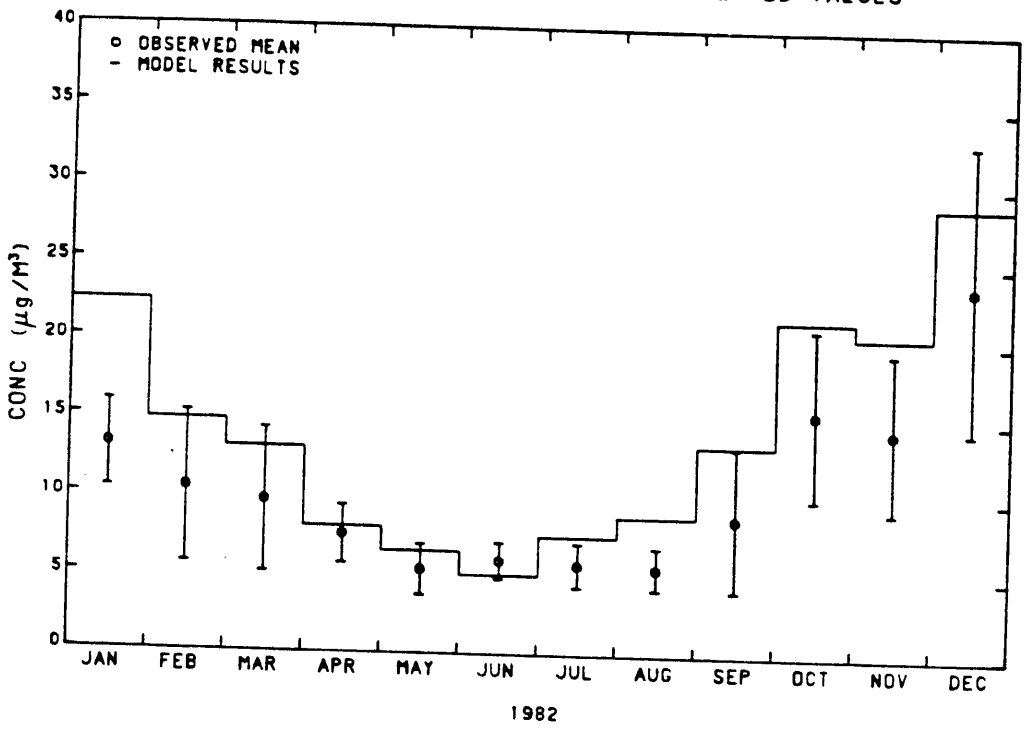

Figure 4.15a

SOURCE CLASS CONTRIBUTIONS TO TOTAL CARBON CONCENTRATIONS AT LENNOX

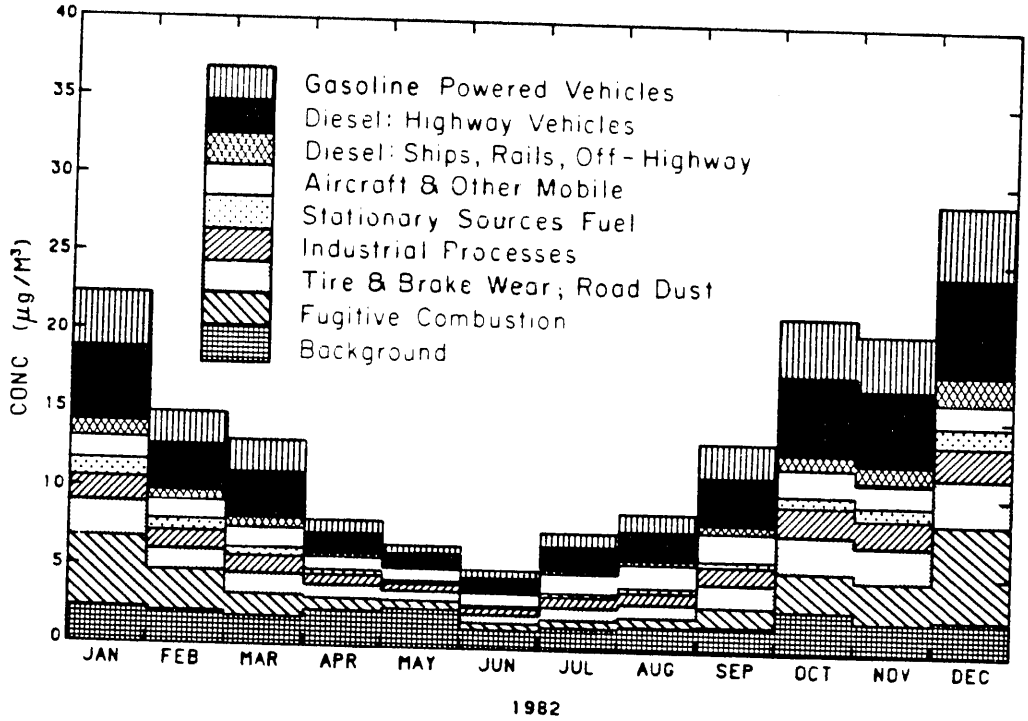

Figure 4.15b

MONTHLY MEAN TOTAL CARBON CONCENTRATION AT LONG BEACH

AIR QUALITY MODEL RESULTS VS. OBSERVED VALUES

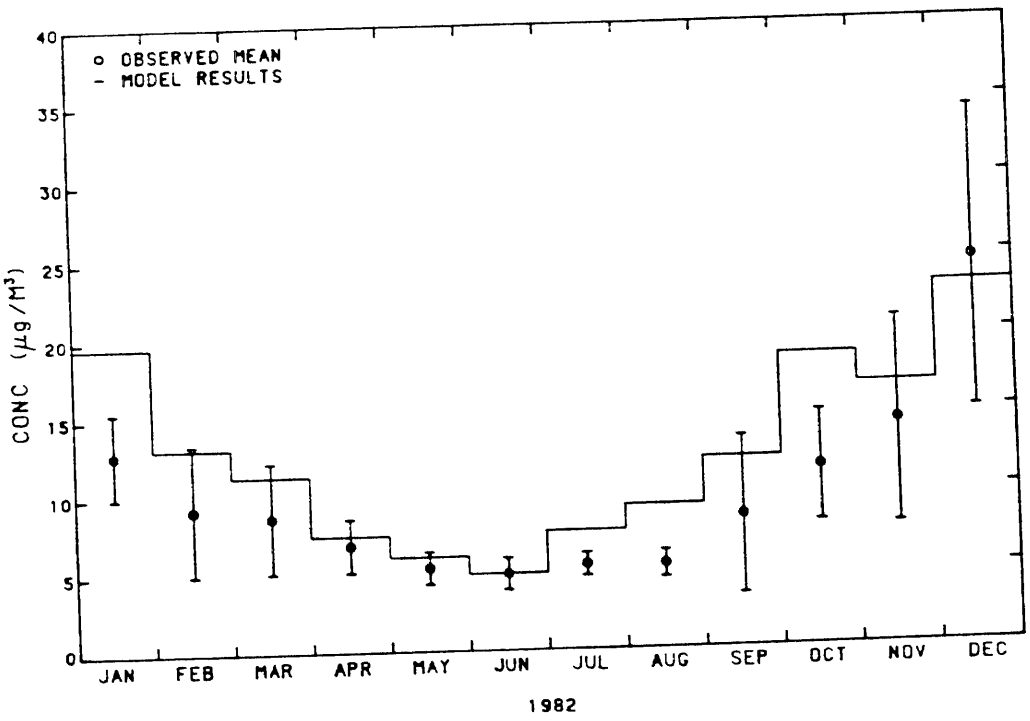

Figure 4.16a

SOURCE CLASS CONTRIBUTIONS TO TOTAL CARBON CONCENTRATIONS

AT LONG BEACH

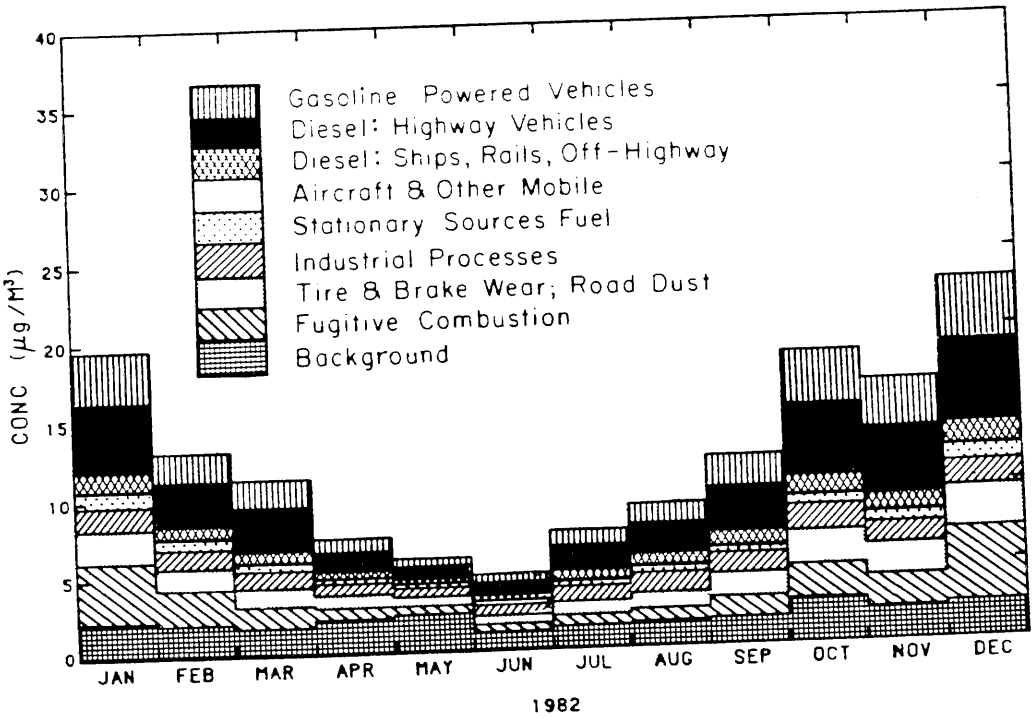

Figure 4.16b

MONTHLY MEAN TOTAL CARBON CONCENTRATION AT WEST LOS ANGELES

AIR QUALITY MODEL RESULTS VS. OBSERVED VALUES

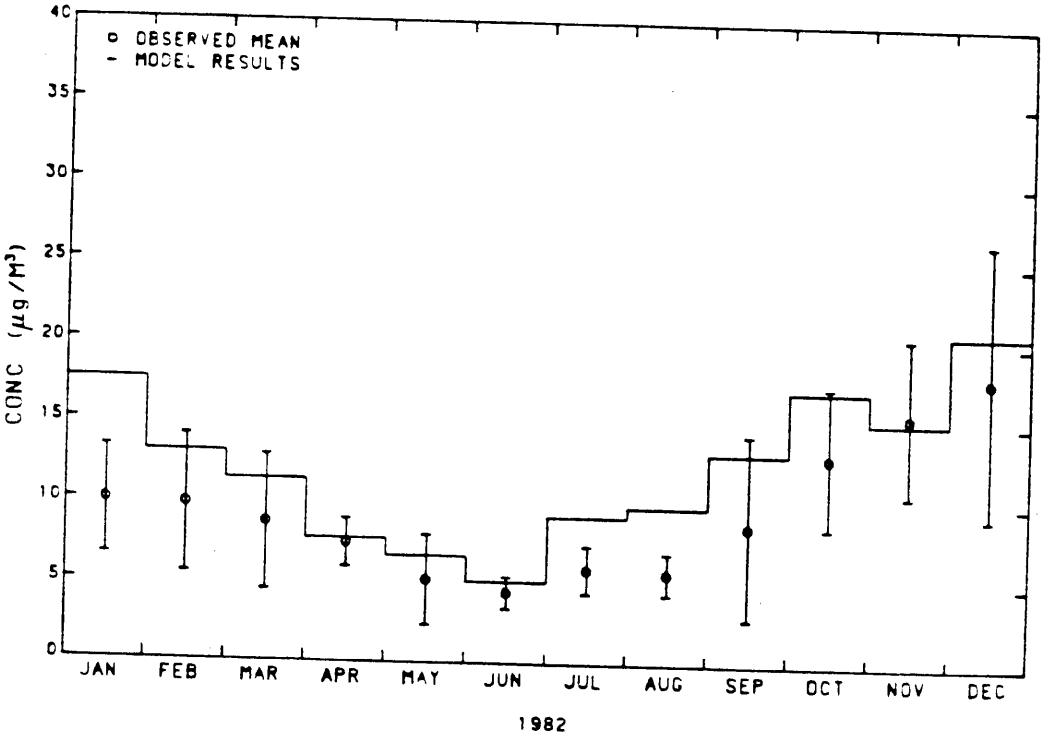

Figure 4.17a

SOURCE CLASS CONTRIBUTIONS TO TOTAL CARBON CONCENTRATIONS

AT WEST LOS ANGELES

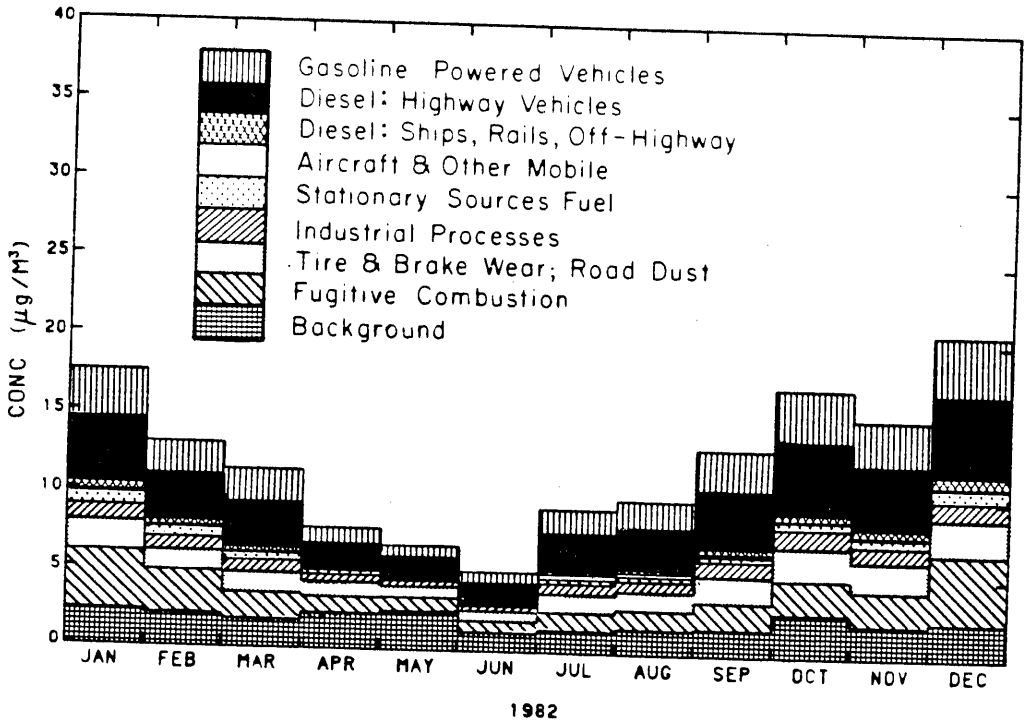

Figure 4.17b

MONTHLY MEAN TOTAL CARBON CONCENTRATION AT LOS ANGELES

AIR QUALITY MODEL RESULTS VS. OBSERVED VALUES

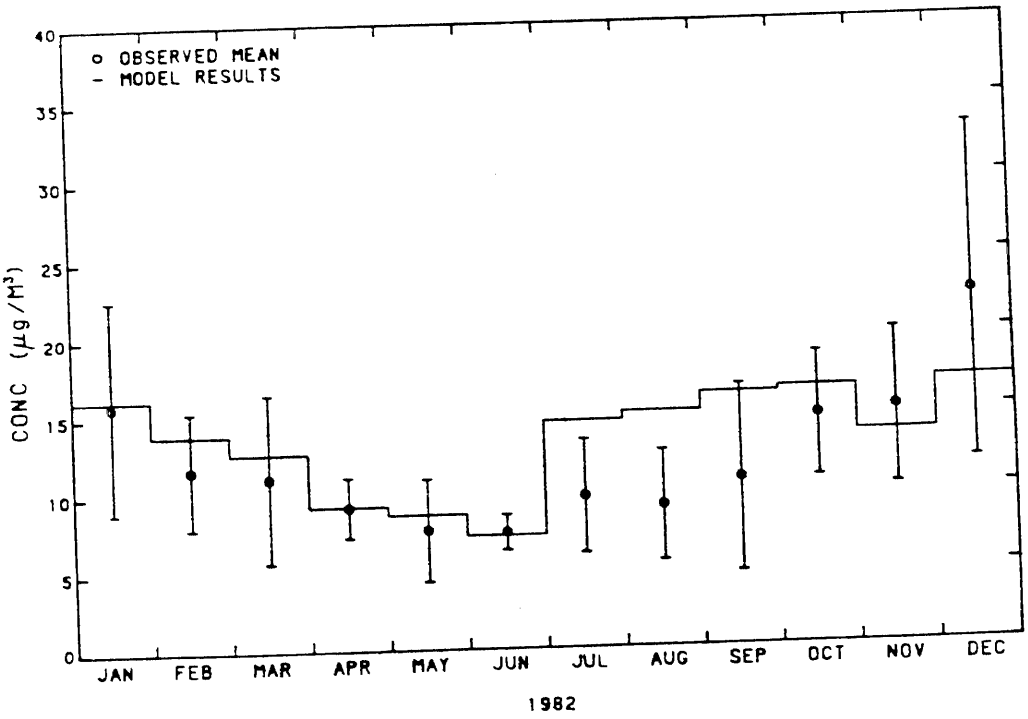

Figure 4.18a

SOURCE CLASS CONTRIBUTIONS TO TOTAL CARBON CONCENTRATIONS

AT LOS ANGELES

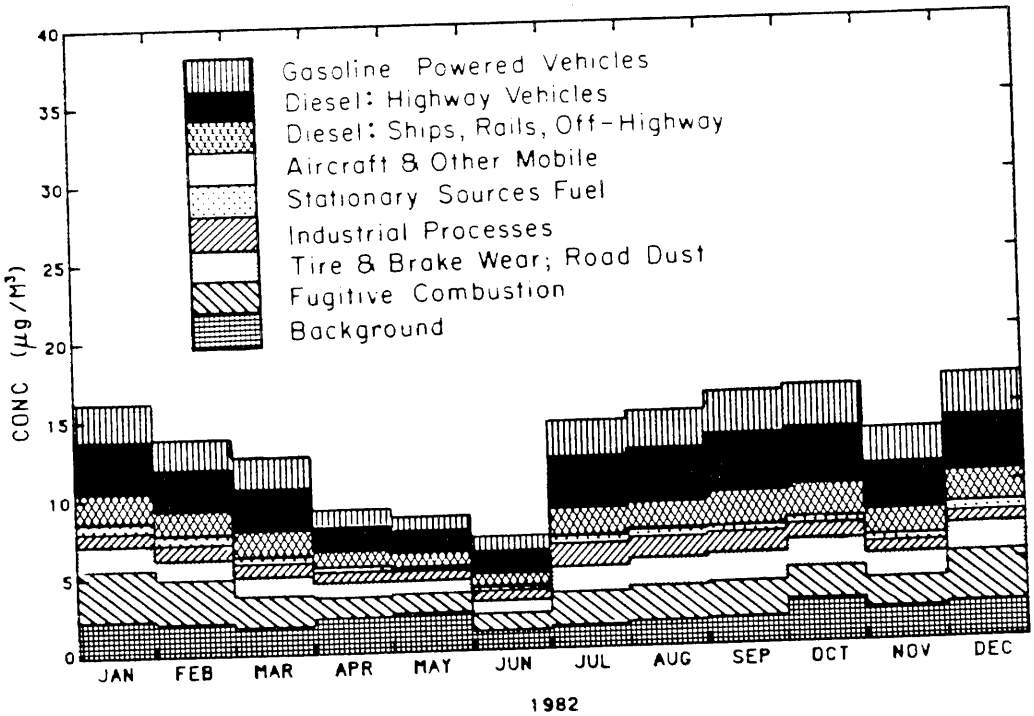

Figure 4.18b

MONTHLY MEAN TOTAL CARBON CONCENTRATION AT ANAHEIM

AIR QUALITY MODEL RESULTS VS. OBSERVED VALUES

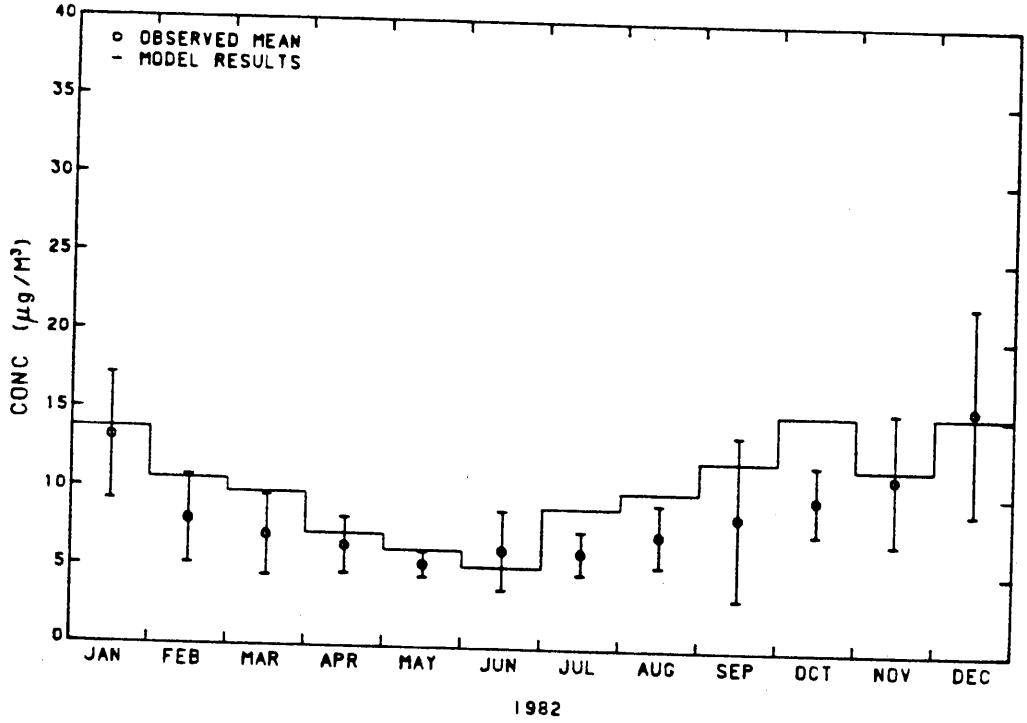

Figure 4.19a

SOURCE CLASS CONTRIBUTIONS TO TOTAL CARBON CONCENTRATIONS AT ANAHEIM

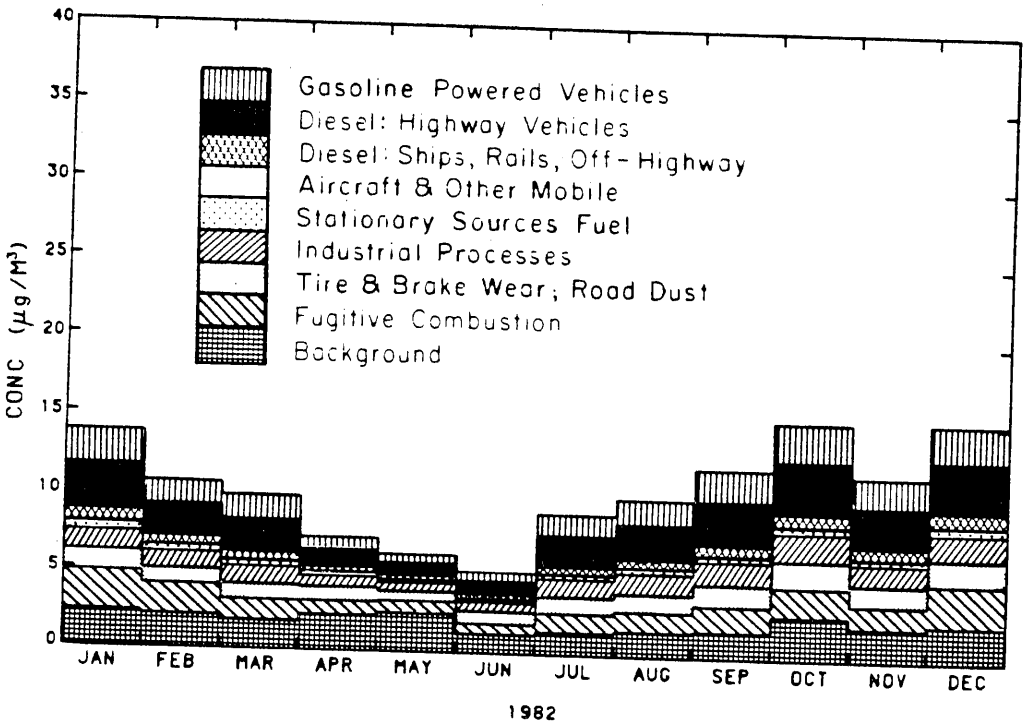

Figure 4.19b

MONTHLY MEAN TOTAL CARBON CONCENTRATION AT PASADENA

AIR QUALITY MODEL RESULTS VS. OBSERVED VALUES

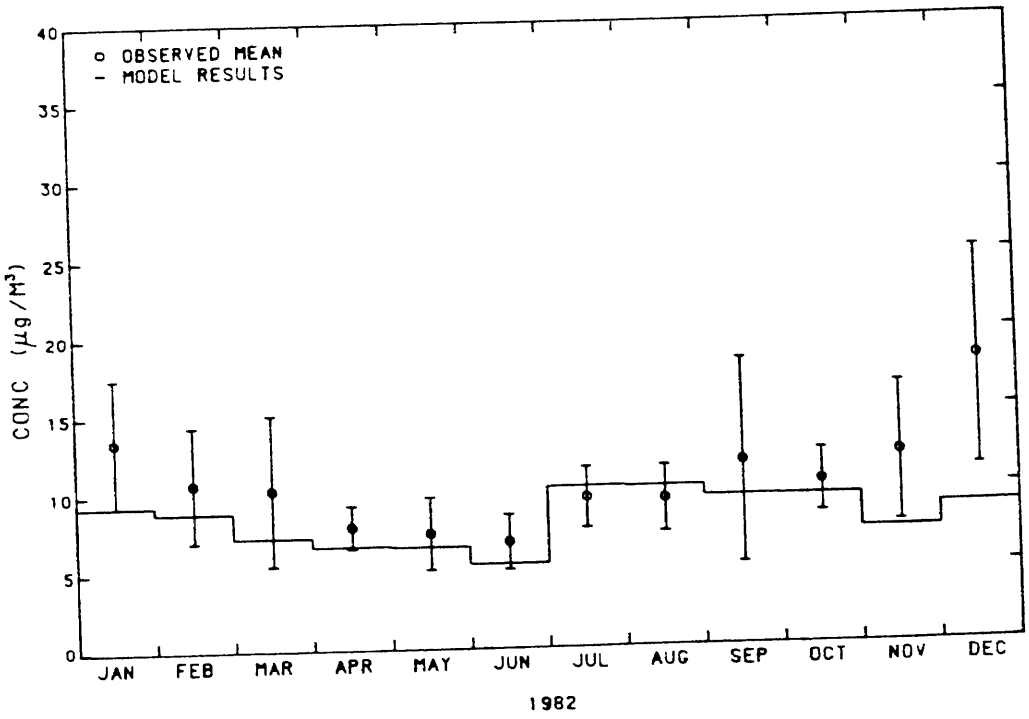

Figure 4.20a

SOURCE CLASS CONTRIBUTIONS TO TOTAL CARBON CONCENTRATIONS

AT PASADENA

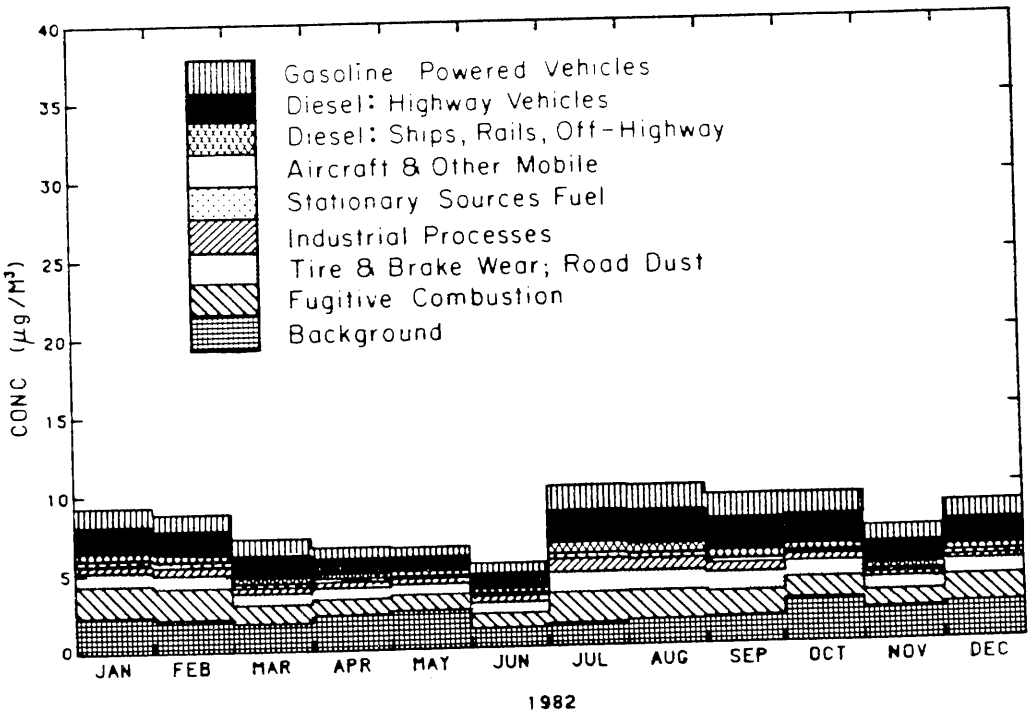

Figure 4.20b

MONTHLY MEAN TOTAL CARBON CONCENTRATION AT AZUSA

AIR QUALITY MODEL RESULTS VS. OBSERVED VALUES

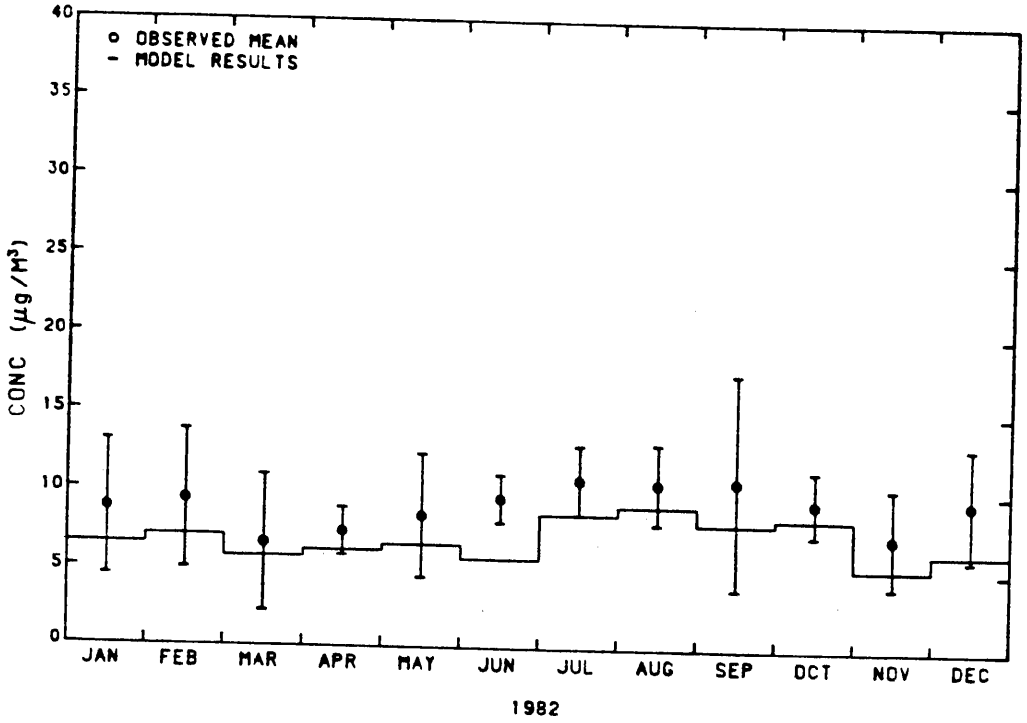

Figure 4.21a

SOURCE CLASS CONTRIBUTIONS TO TOTAL CARBON CONCENTRATIONS AT AZUSA

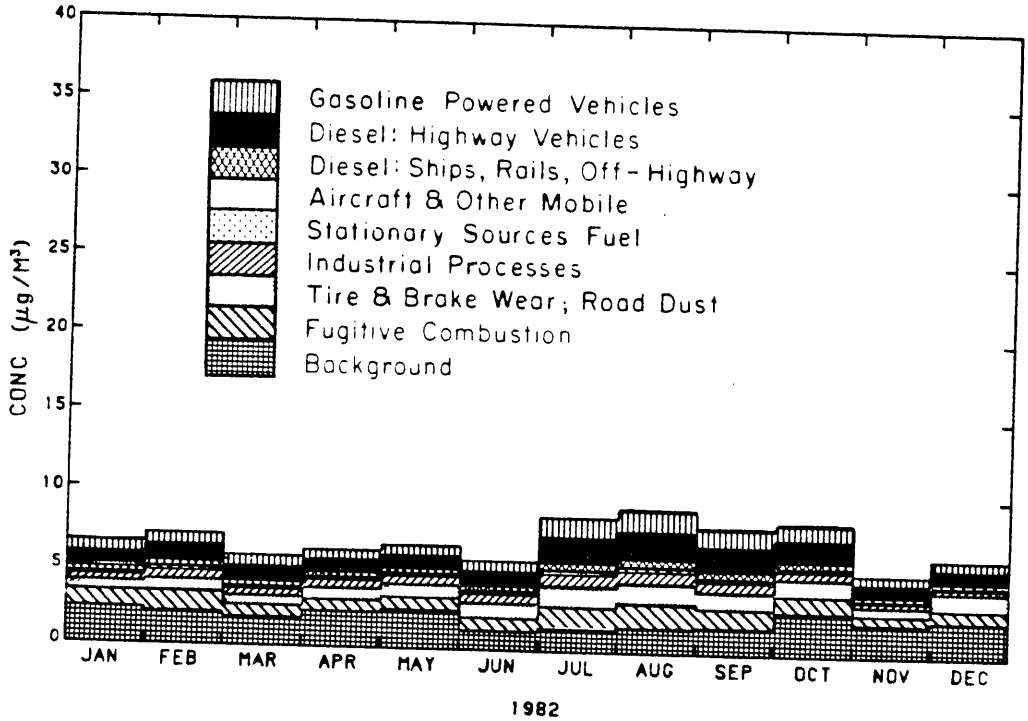

Figure 4.21b

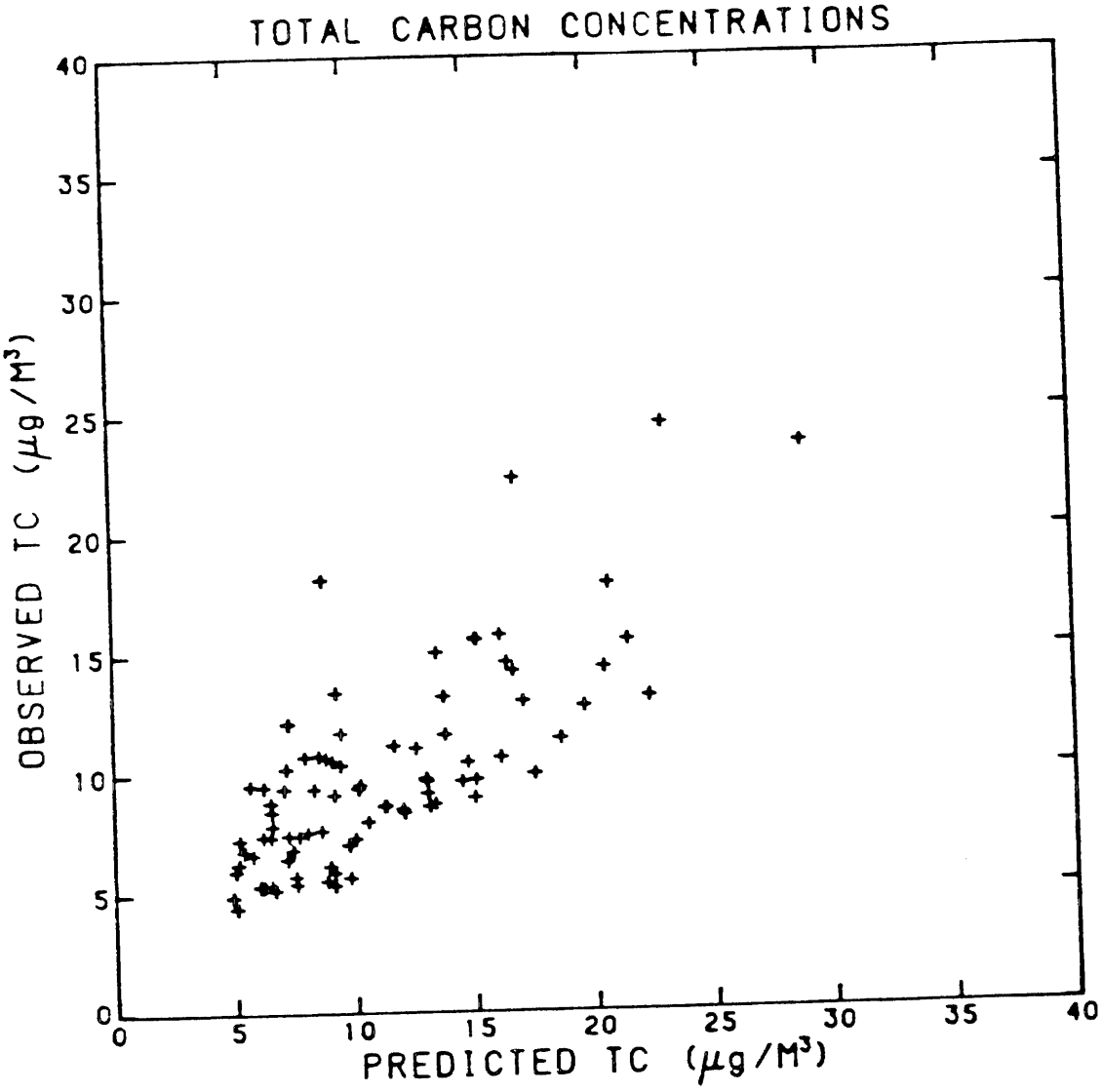

Figure 4.22 Observations of monthly average fine total carbon particle concentrations vs. predictions of fine primary total carbon particle concentrations at seven monitoring sites.

The primary total carbon emission inventory was matched to the air quality model, and primary total carbon concentrations were predicted for each month of the year 1982. Results at each of the seven monitoring sites are shown in Figures 4.15a through 4.21a. About 73% of the monthly average primary fine total carbon particle concentrations predicted by the model are within the error bounds of the observed monthly mean fine total carbon concentrations. It is seen that present estimates of primary total carbon emissions are sufficient to account for most of the observed concentrations and seasonal behavior of long-term average fine total carbon air quality during 1982.

The correlation between model-predicted primary fine total carbon concentrations and observed total carbon concentrations is shown in Figure 4.22. The predictions and observations of total carbon concentrations have a positive correlation coefficient of 0.76.

The goodness-of-fit test, which was performed on elemental carbon predictions in the previous section, also may be conducted to test the hypothesis that primary fine total carbon concentrations computed by the model may serve as accurate predictions of fine total carbon air quality. The comparison of predicted and observed annual average total carbon concentrations at the seven monitoring sites results in a goodness-of-fit statistic of 4.28, which is below $\chi^2_{.05} \simeq 105.0$ ($\nu = 83$). It may be concluded, therefore, that the model provides an accurate prediction of fine total carbon air quality.

4.3.4 Spatial Variations in Fine Carbon Particle Air Quality

Figures 4.23 and 4.24 show contour plots of the 1982 annual mean air quality predictions of fine primary total carbon and fine elemental carbon concentrations throughout the modeling region. The area surrounding the downtown Los Angeles central business district southwest of the central Los Angeles air monitoring site is subject to the highest annual mean concentrations of carbonaceous particulate matter.

Contour plots showing fine elemental carbon concentration predictions for each month of 1982 are presented in Figures 4.25 through 4.36. In January, winds from the northeast cause emissions to be pushed toward the southwestern portion of the modeling grid, with monthly averaged concentrations of elemental carbon reaching 6 $\mu g/m^3$ at the coastline. The direction of flow is similar in February and March; however, the magnitude of peak concentrations has decreased. As the weather warms, the net transport direction shifts and concentrations in the northeastern portion of the modeling region become as high as high as at the coast, as seen in April, May, and June. Overall concentration levels decrease drastically in the central portion of the air basin. In July, the peak elemental carbon concentrations increase, while the direction of flow is still predominantly from the west and southwest, causing higher concentrations in the eastern locations of the modeling grid. This trend continues through August and September. As the temperature cools, peak concentrations increase and the area most affected by

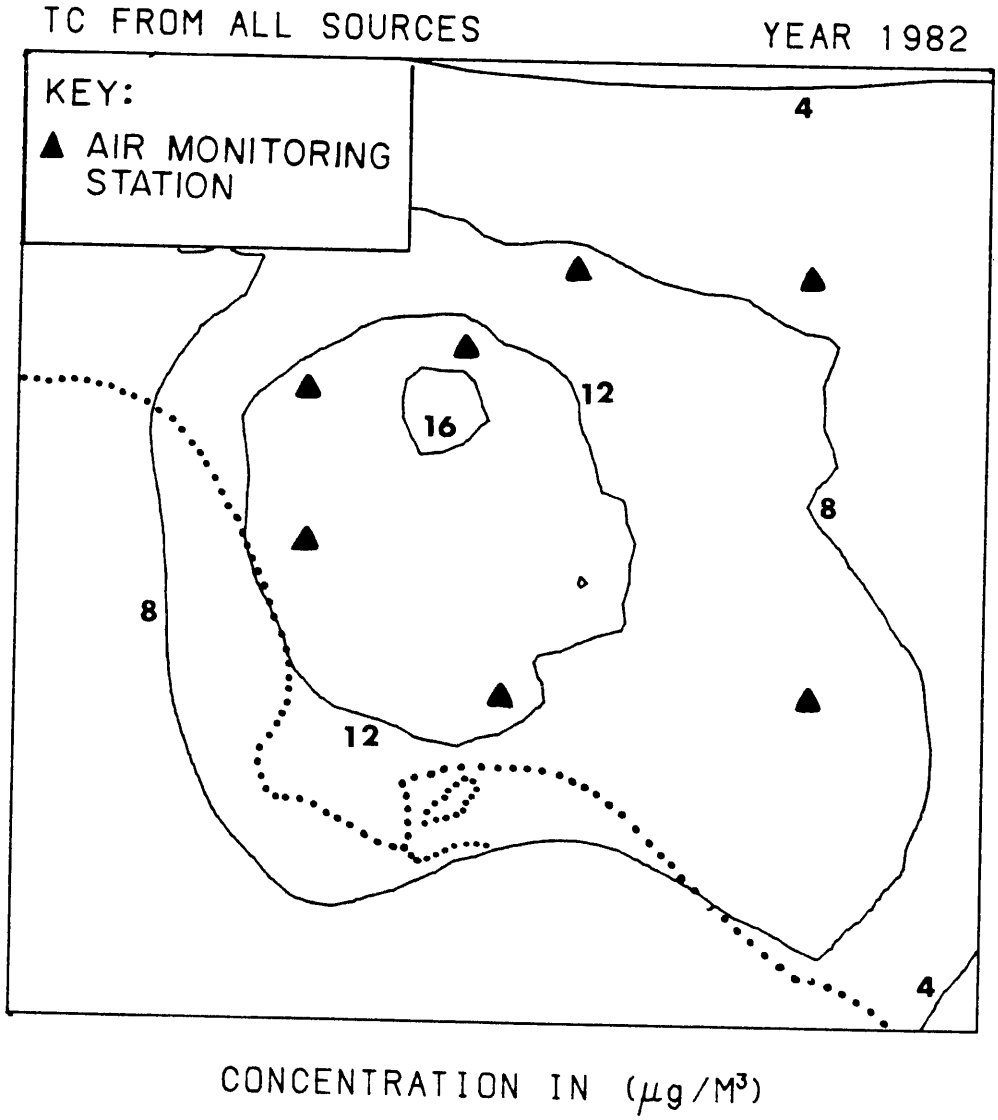

Figure 4.23 Annual mean fine primary total carbon concentration isopleths computed by the air quality model simulation.

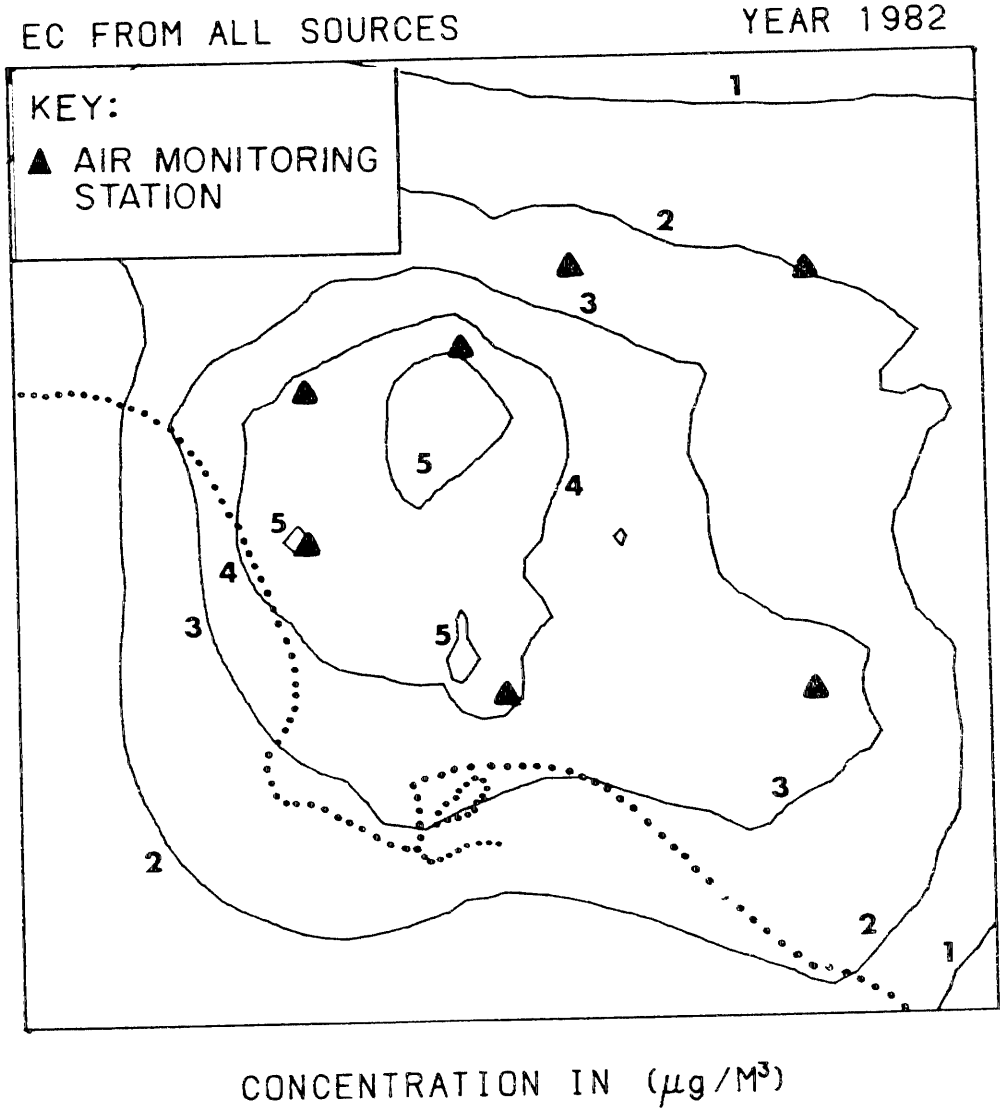

Figure 4.24 Annual mean fine elemental carbon concentration isopleths computed by the air quality model simulation.

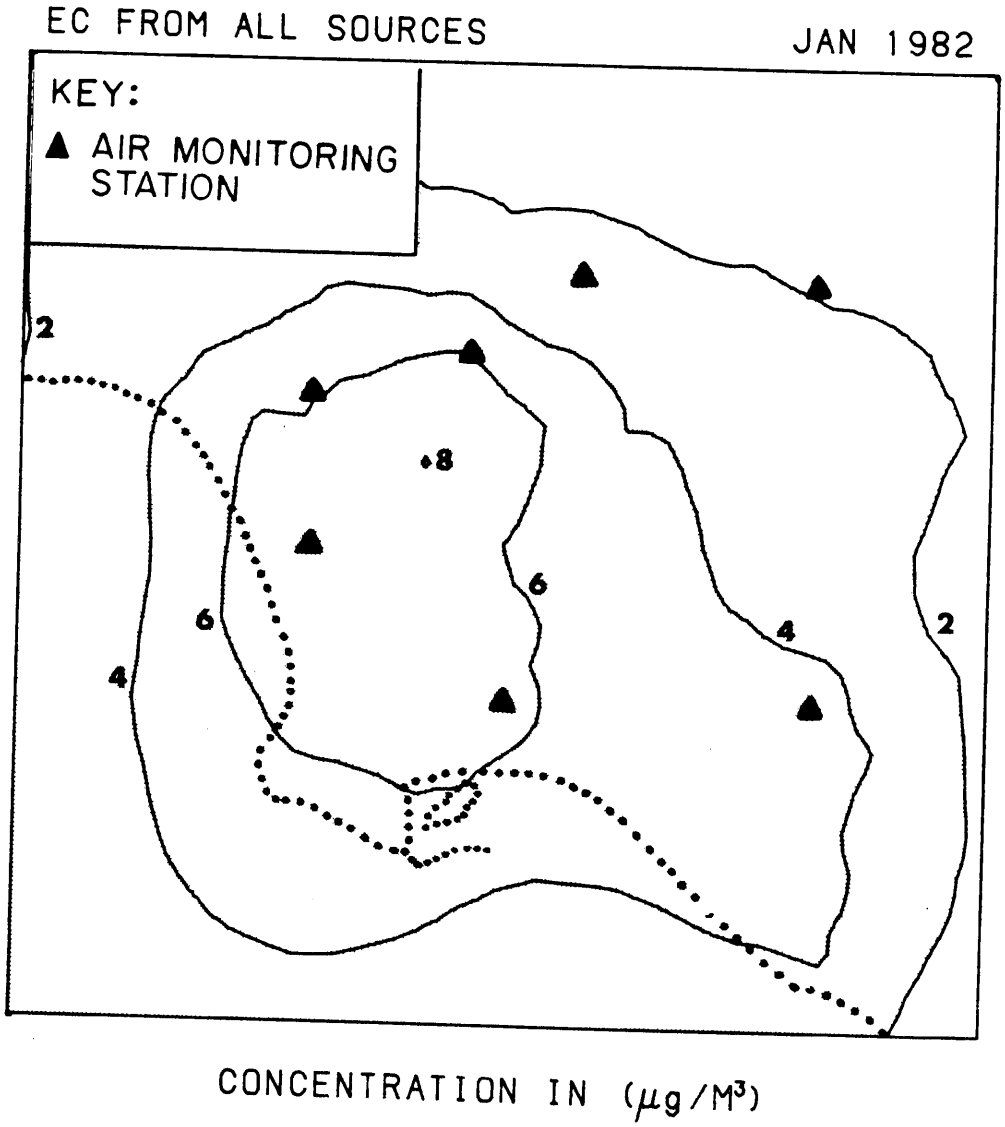

Figure 4.25 Monthly average fine elemental carbon concentration isopleths computed by the air quality model simulation--January 1982.

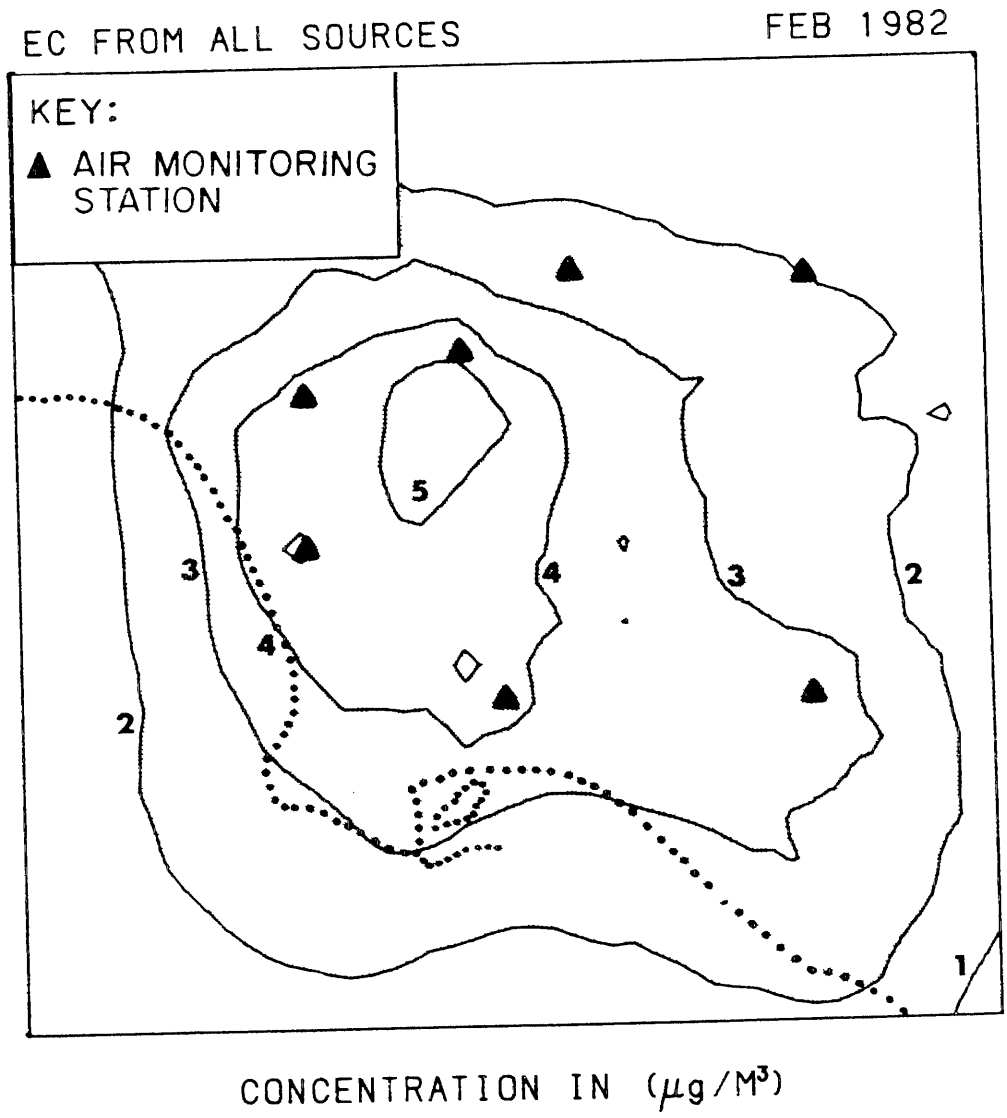

Figure 4.26 Monthly average fine elemental carbon concentration isopleths computed by the air quality model simulation--February 1982.

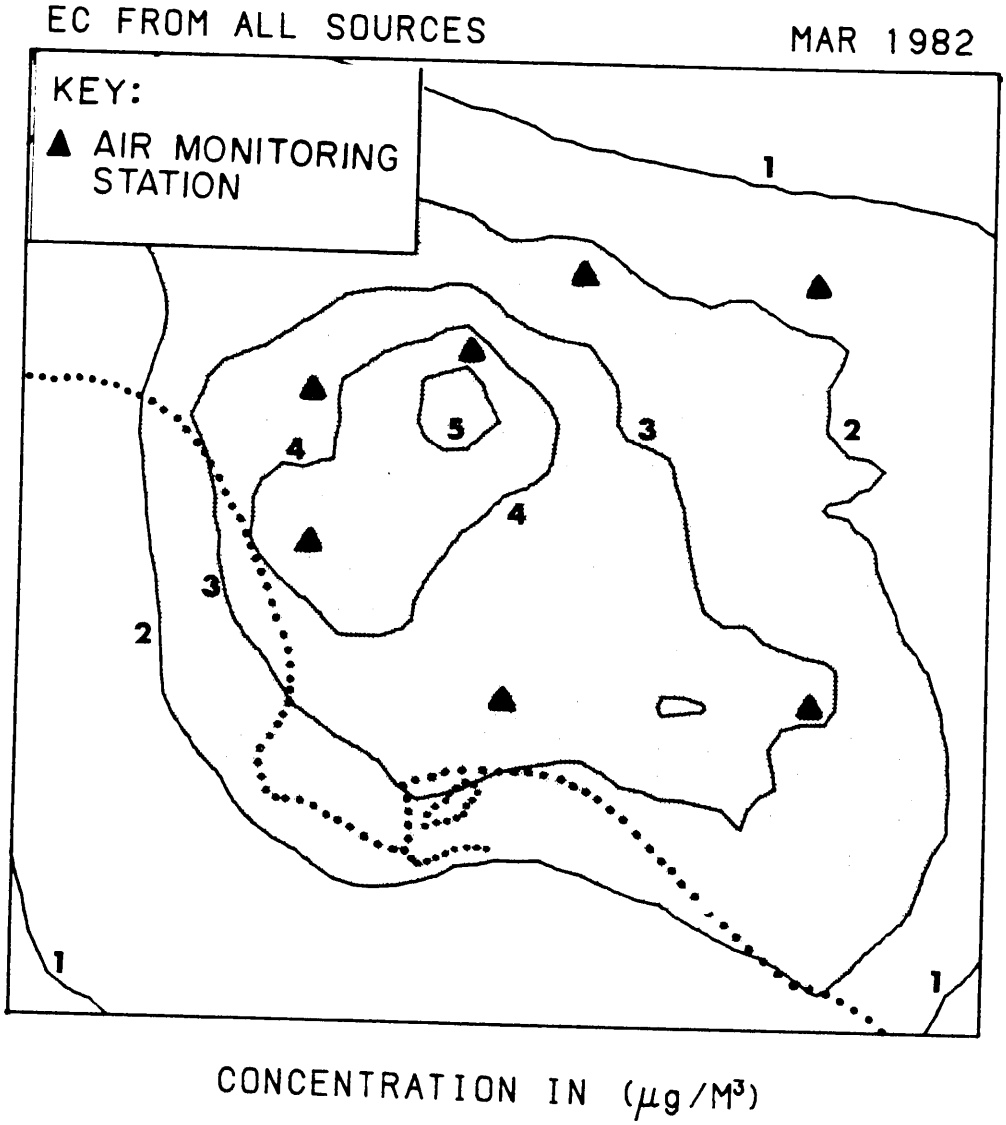

Figure 4.27 Monthly average fine elemental carbon concentration isopleths computed by the air quality model simulation--March 1982.

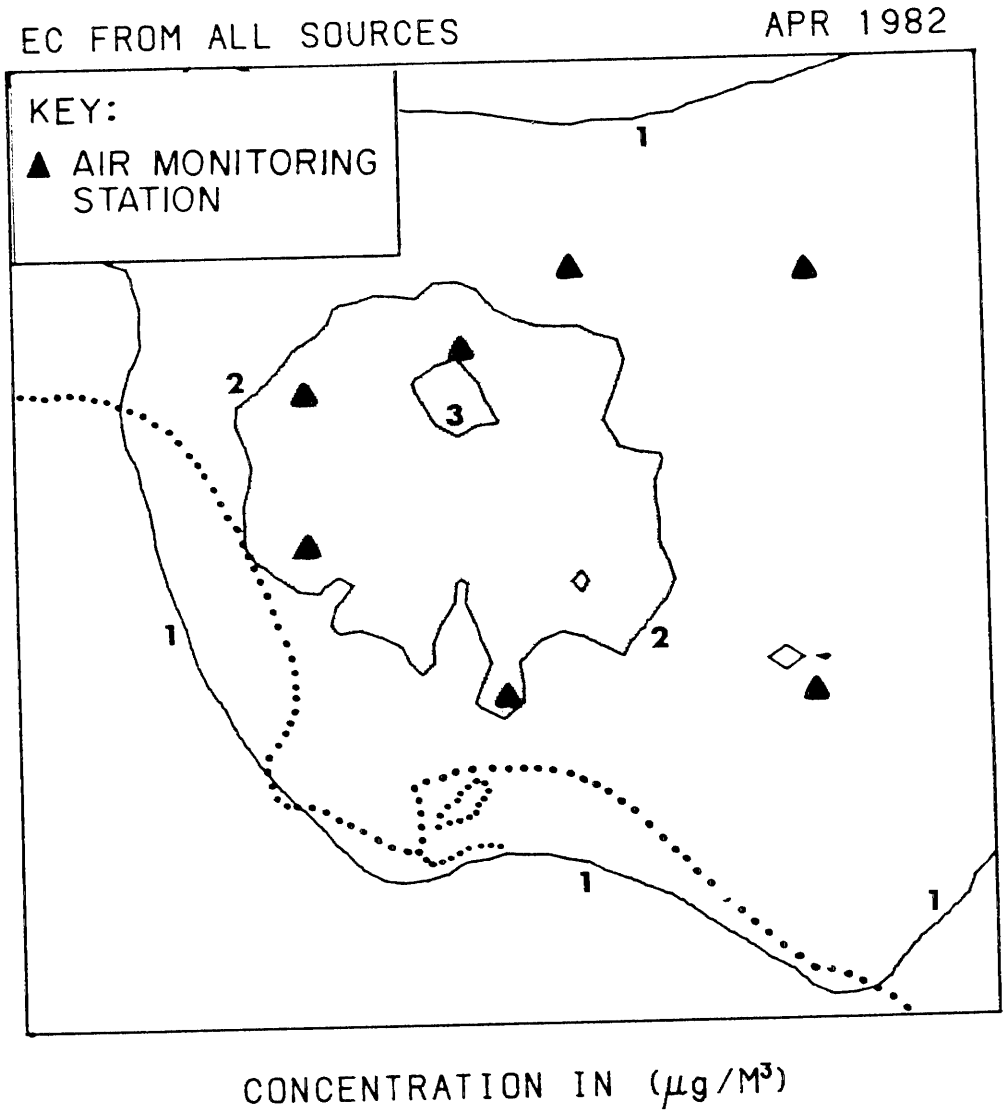

Figure 4.28 Monthly average fine elemental carbon concentration isopleths computed by the air quality model simulation--April 1982.

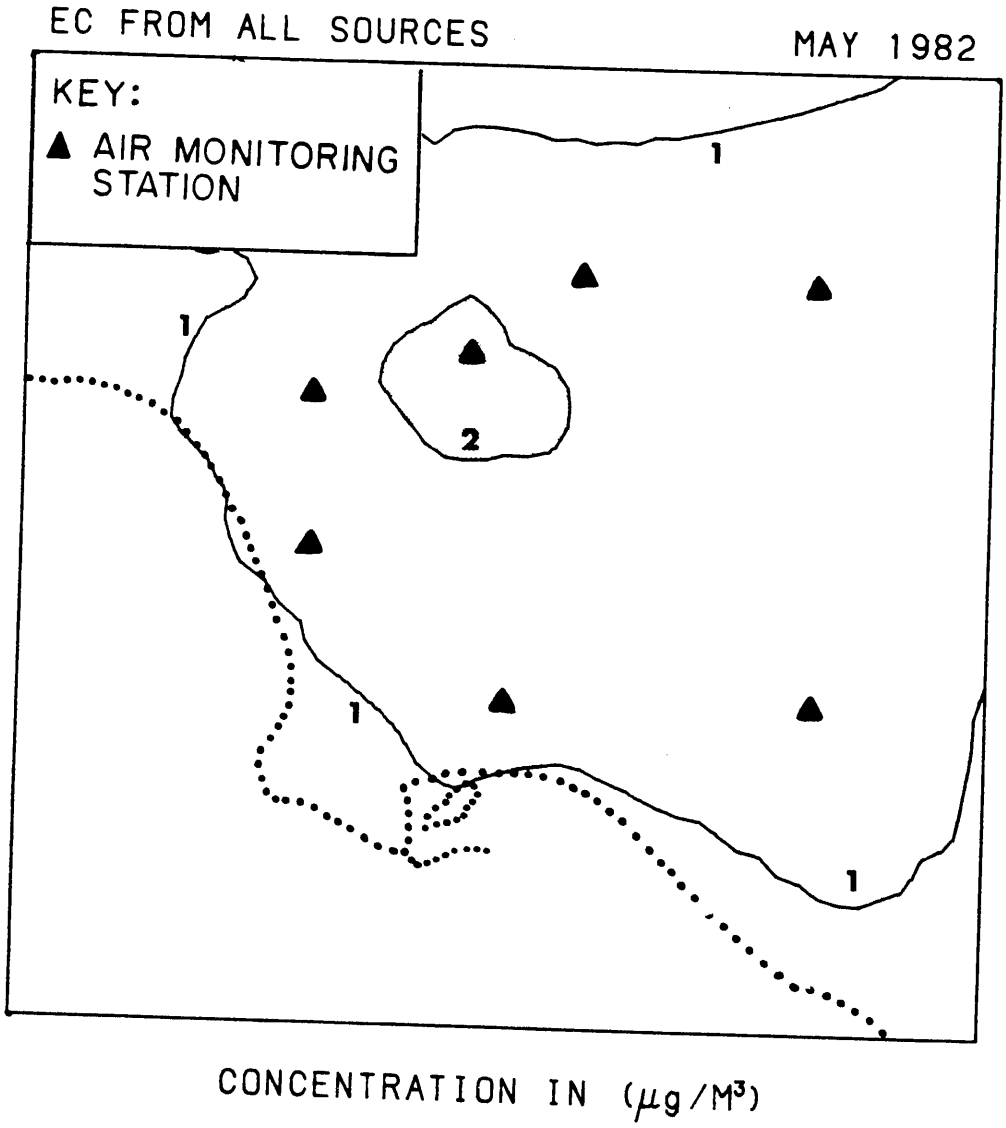

Figure 4.29 Monthly average fine elemental carbon concentration isopleths computed by the air quality model simulation--May 1982.

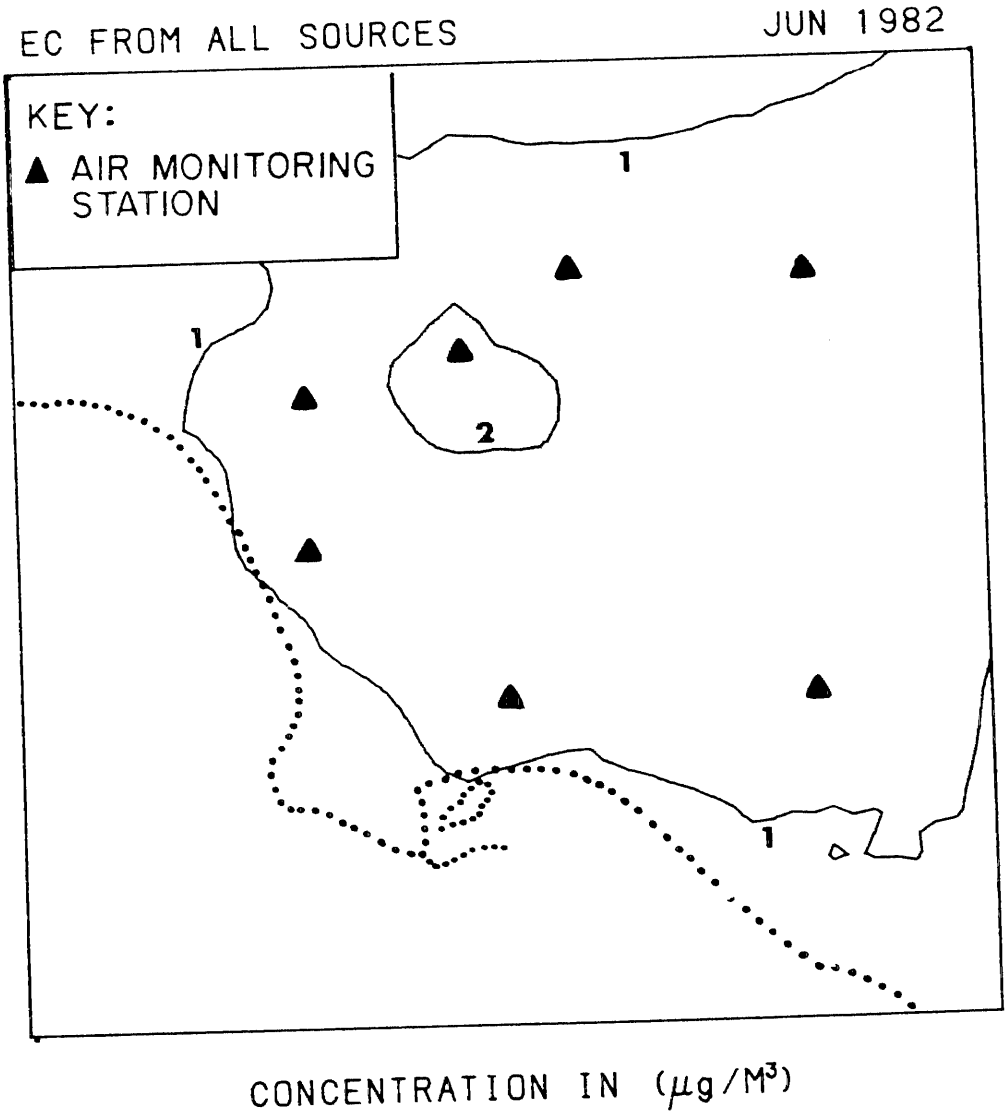

Figure 4.30 Monthly average fine elemental carbon concentration isopleths computed by the air quality model simulation--June 1982.

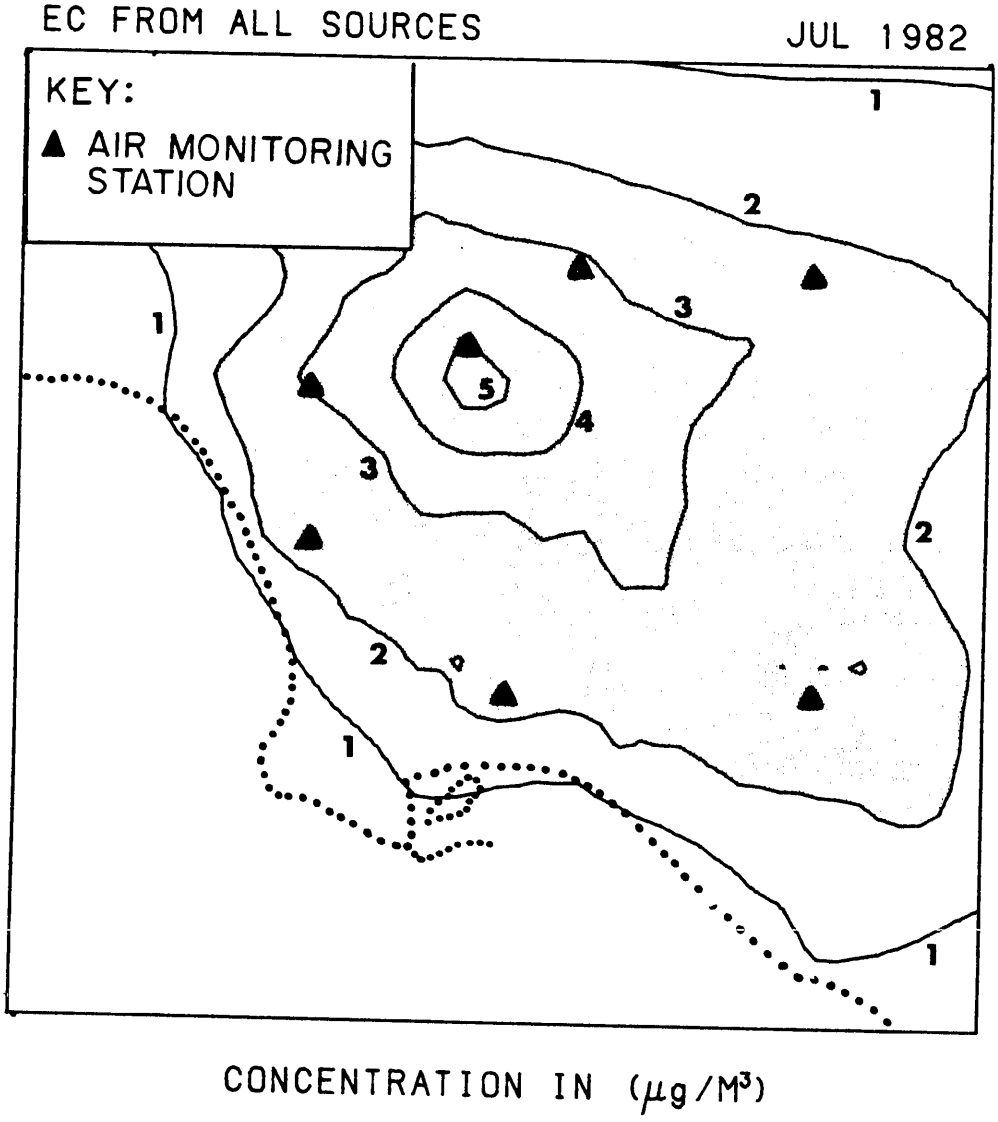

Figure 4.31 Monthly average fine elemental carbon concentration isopleths computed by the air quality model simulation--July 1982.

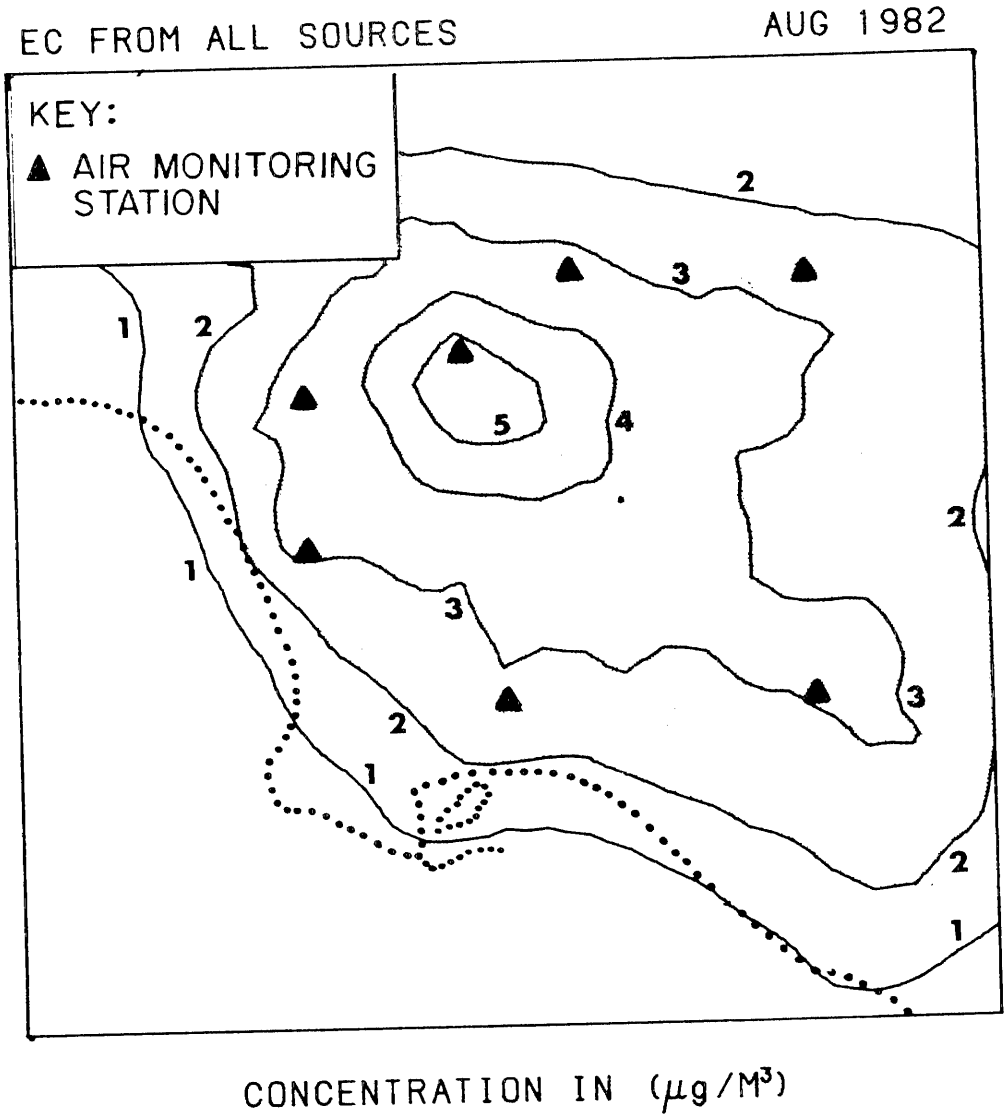

Figure 4.32 Monthly average fine elemental carbon concentration isopleths computed by the air quality model simulation--August 1982.

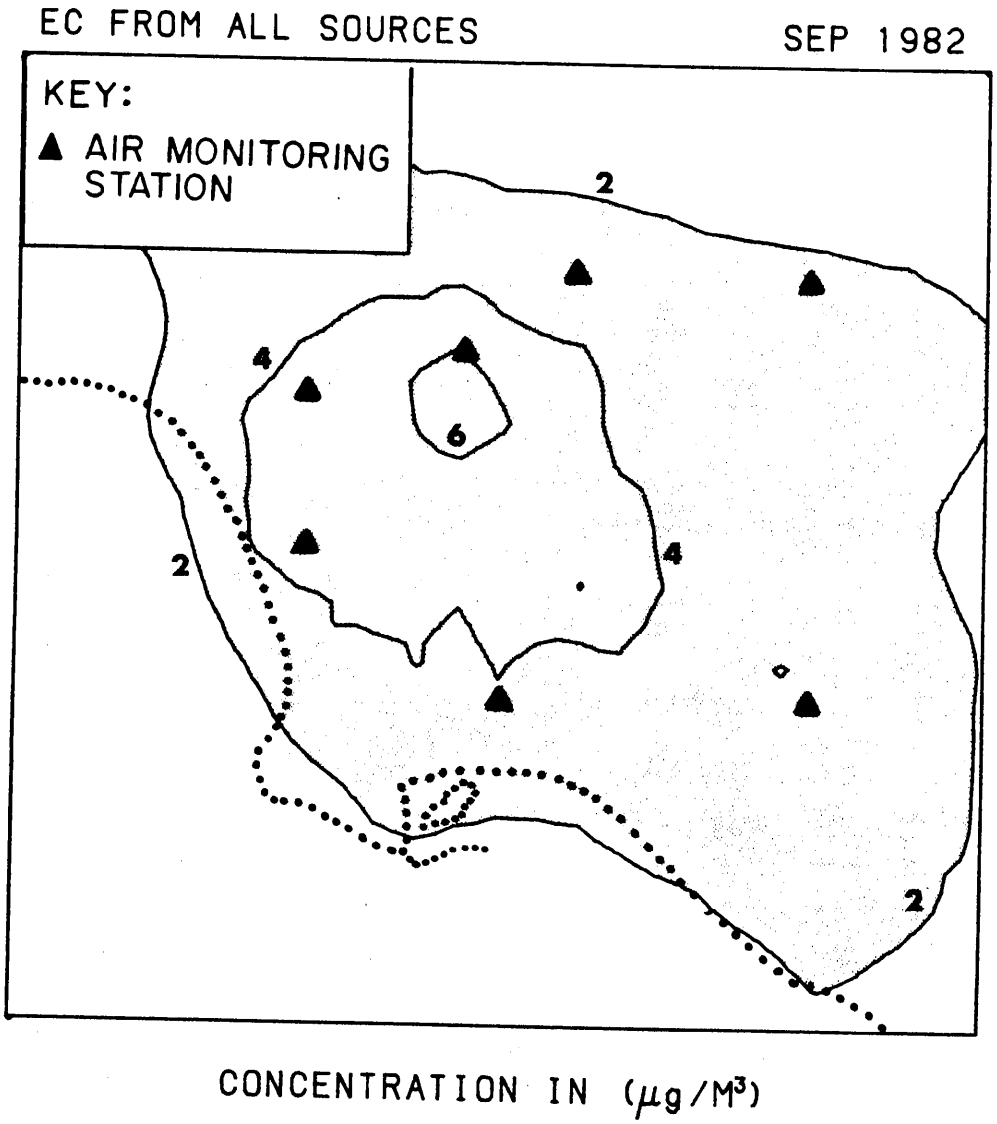

Figure 4.33 Monthly average fine elemental carbon concentration isopleths computed by the air quality model simulation--September 1982.

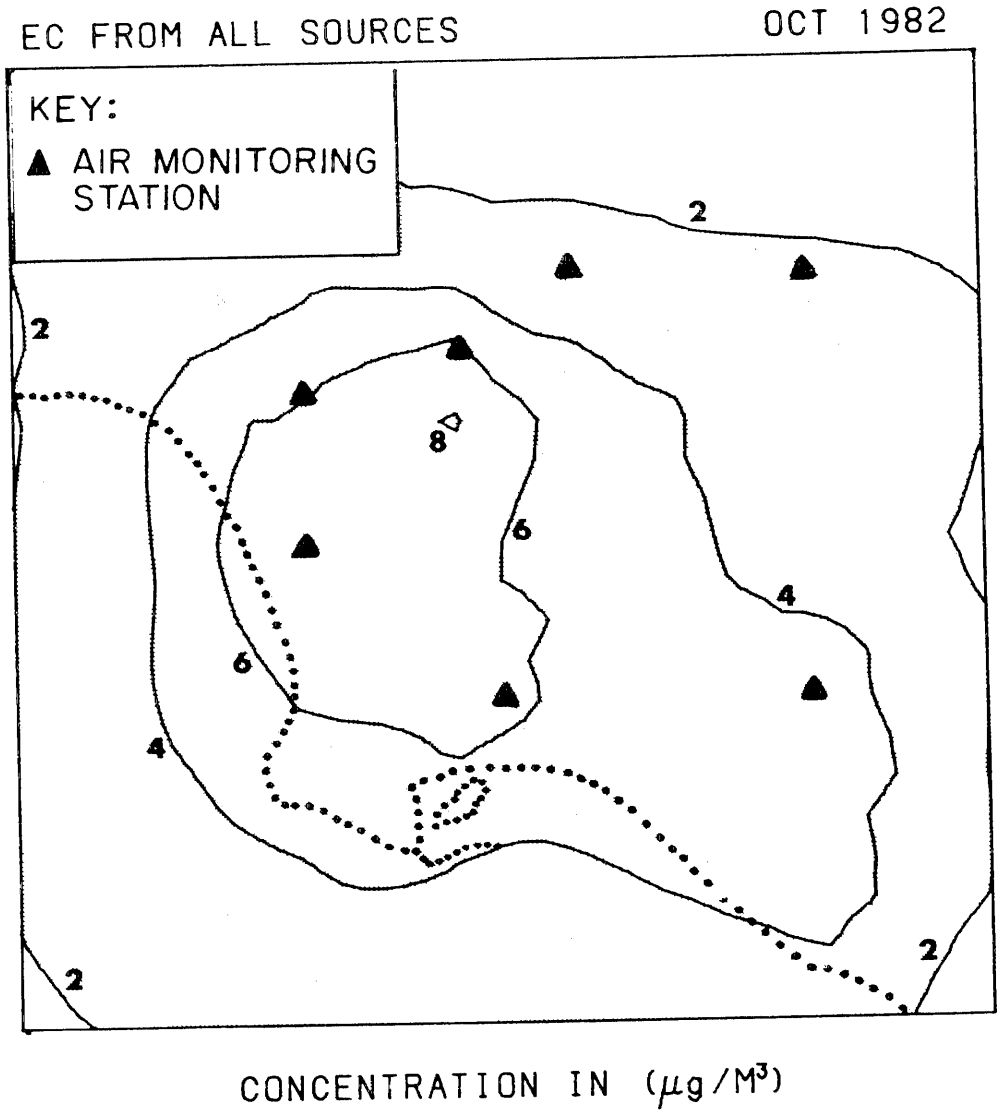

Figure 4.34 Monthly average fine elemental carbon concentration isopleths computed by the air quality model simulation--October 1982.

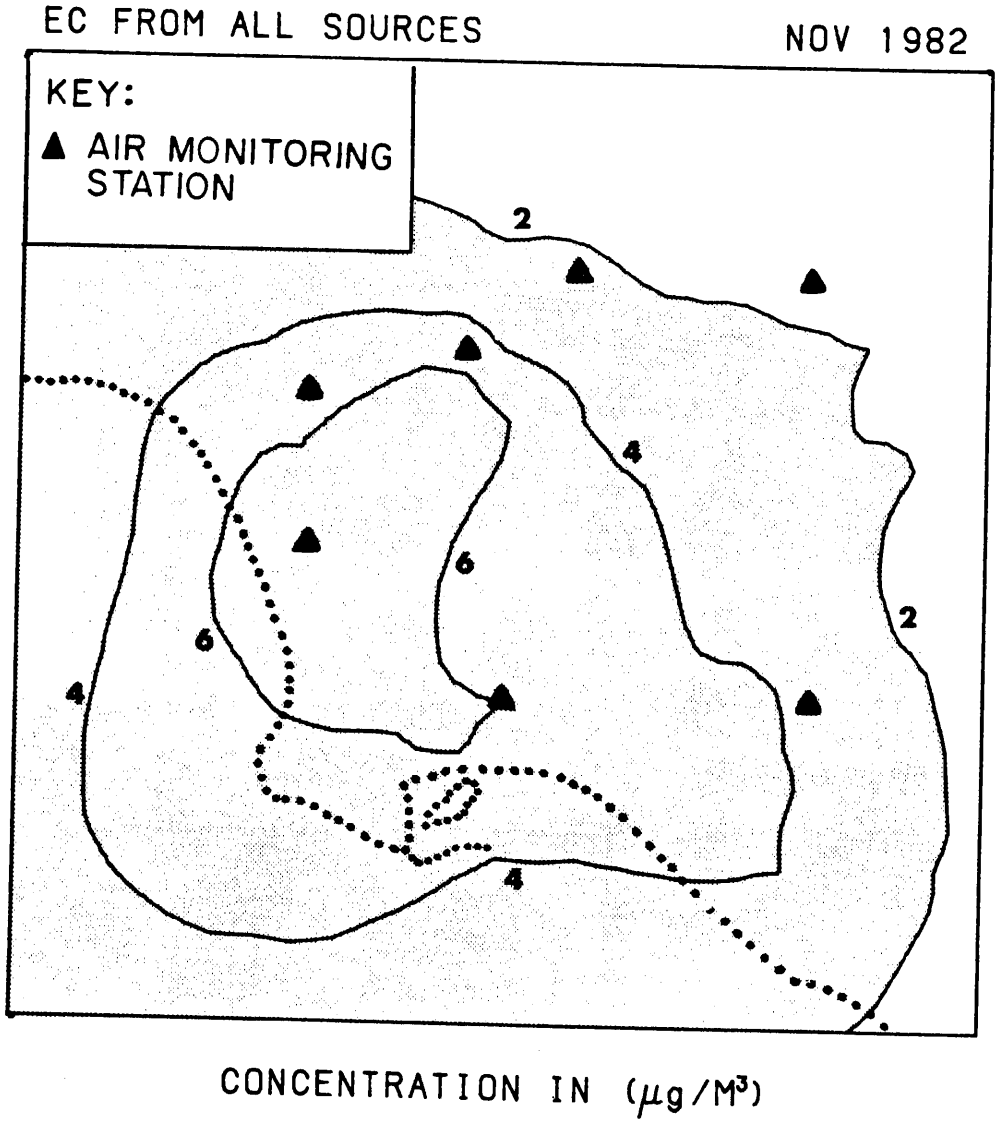

Figure 4.35 Monthly average fine elemental carbon concentration isopleths computed by the air quality model simulation--November 1982.

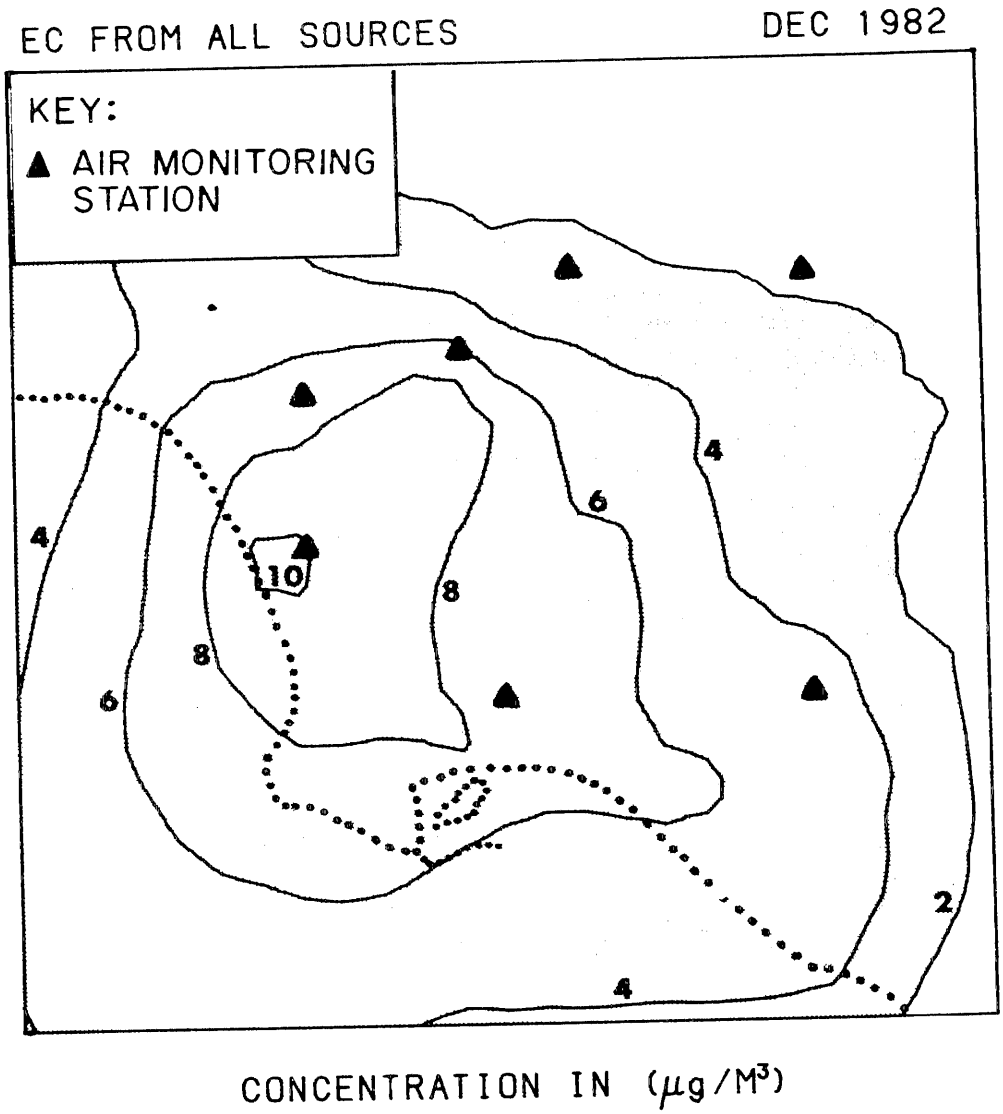

Figure 4.36 Monthly average fine elemental carbon concentration isopleths computed by the air quality model simulation--December 1982.

emissions shifts toward the southwest. By October, peak monthly averaged elemental carbon concentrations reach 8 $\mu g/m^3$ while seaward transport causes contours to extend off-grid to the southwest. This feature becomes more pronounced in November and December. In December, peak concentrations are predicted to be over 10 $\mu g/m^3$ in western Los Angeles County near the coast. The peak predicted and observed monthly average elemental carbon concentration value at any monitoring site occurs at Lennox in December 1982. Contours of high concentration extend out over the ocean.

The geographic region affected by elemental carbon concentrations in excess of 2 $\mu g/m^3$ during each month is represented in Figures 4.25 through 4.36. This area covers almost the entire 50X50-mile grid, with the exception of the northeast and east, during the months of October through January. In February, the turning of the general direction of transport has begun, and by April the region with concentrations above 2 $\mu g/m^3$ has shrunk considerably. In June, minimum monthly average concentrations of elemental carbon are reached. The following months show a larger region being affected by elemental carbon concentrations greater than 2 $\mu g/m^3$; however, the region extends much farther inland than in winter months. By September, that region appears to be turning toward the southwest and includes most of Orange County and the Los Angeles harbor area.

4.3.5 Source Class Contributions to Atmospheric Fine Carbon Particle Concentrations

The air quality model computes the contribution to pollutant loadings from each source type separately. Because the spatial distribution of emissions in the modeling region is different for each source type, the resulting contribution to air quality from each source type varies by location. Other characteristics of emission sources that vary between source types, such as effective stack height and diurnal cycle of release, also add to the disparity between source types with respect to the contribution to resulting air quality.

Contour plots of individual source class contributions to carbon particle air quality can be examined to further understand the impact on air quality from each source type. The increment to monthly average fine total carbon concentrations in June 1982 is shown in Figures 4.37 and 4.38 for diesel trucks and for petroleum refinery fuel burning. Contour plots showing the contribution to fine total carbon concentrations in December 1982 from these same two source types are displayed in Figures 4.39 and 4.40.

Emissions from heavy diesel trucks (air quality model source class no. 5; see Table D.38) are widespread throughout the Los Angeles air basin. All locations in the modeling region are affected to some extent by this large area source, emissions of which were assumed to be constant from month to month during 1982. In June, the effect is felt throughout the central and eastern portion of the modeling grid, with the peak contribution of 1.25 $\mu g/m^3$ near downtown Los Angeles.

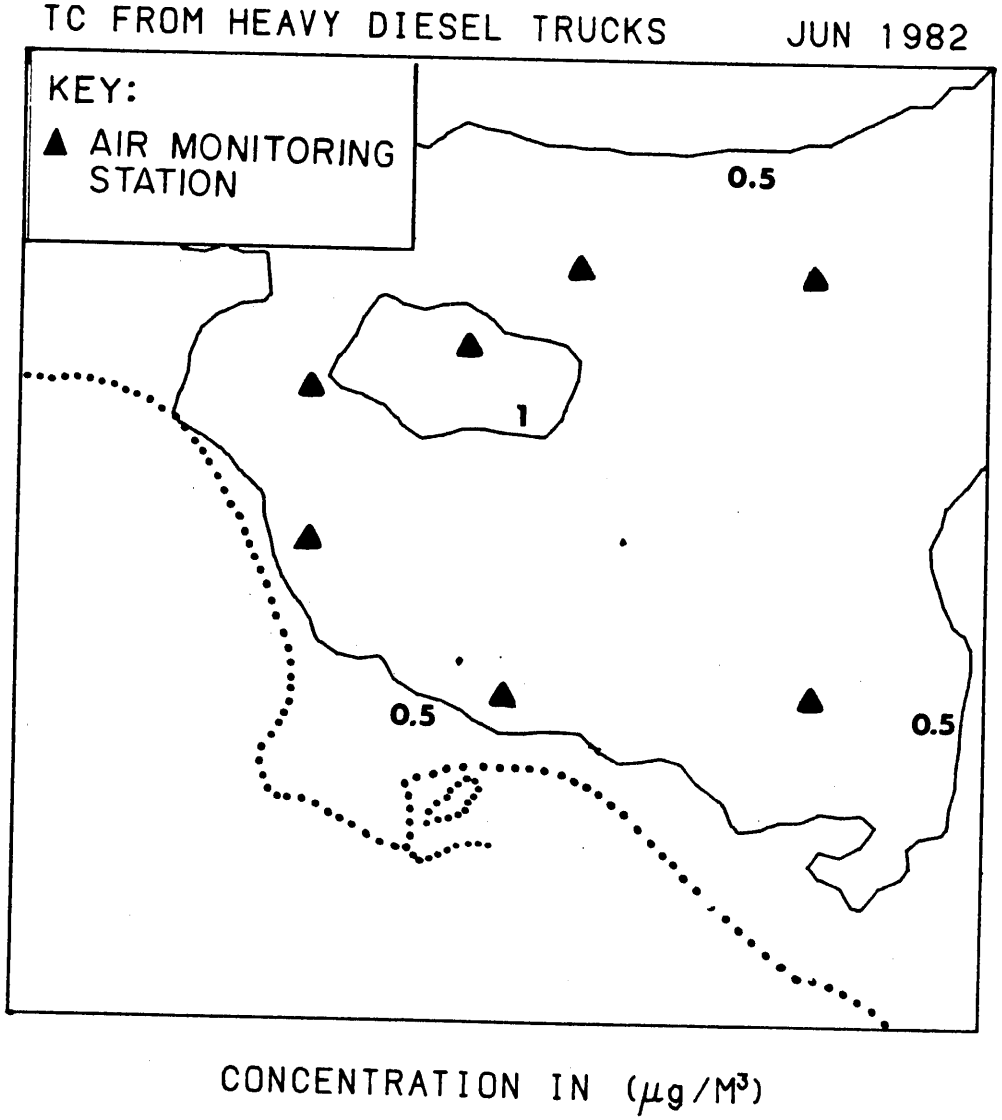

Figure 4.37 Fine primary total carbon air quality increment due to heavy diesel trucks--June 1982.

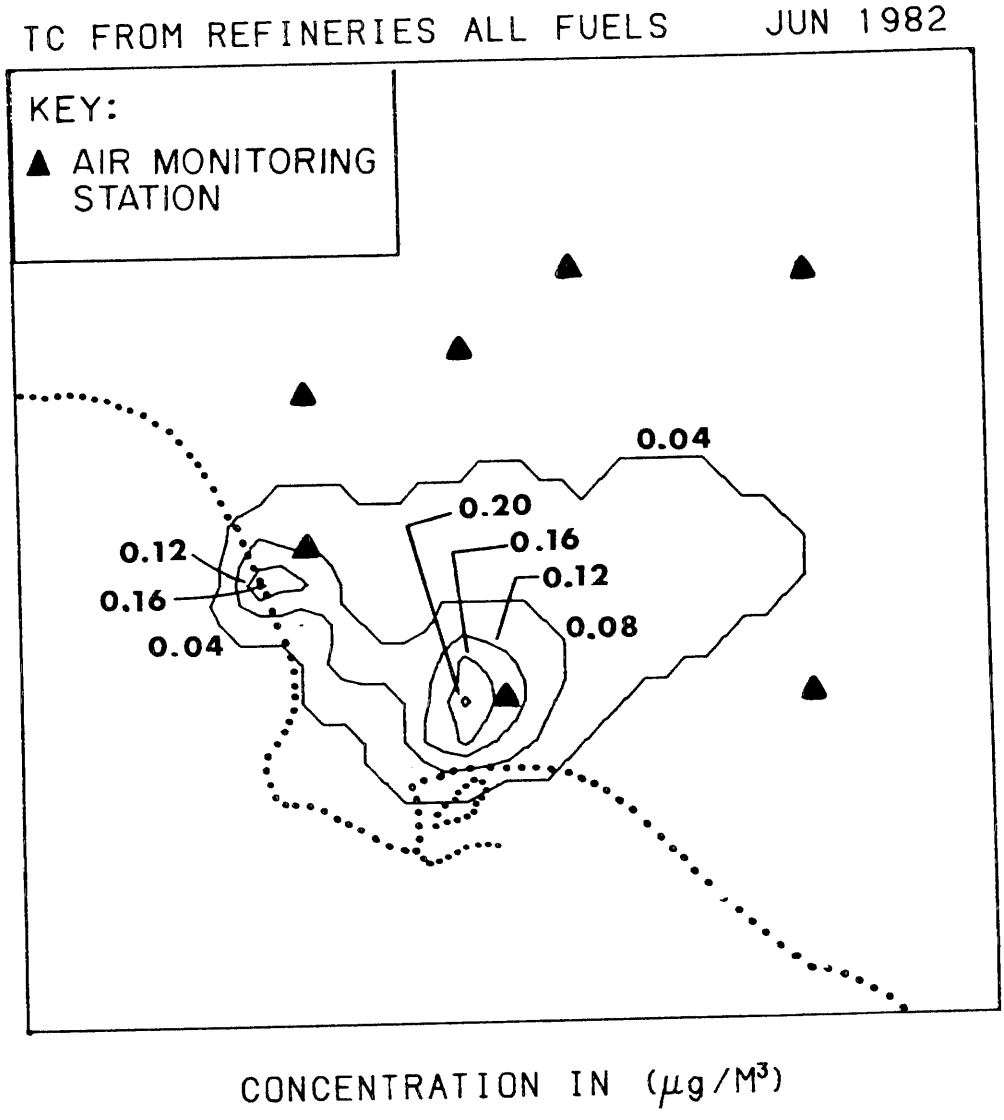

Figure 4.38 Fine primary total carbon air quality increment due to petroleum refinery fuel combustion--June 1982.

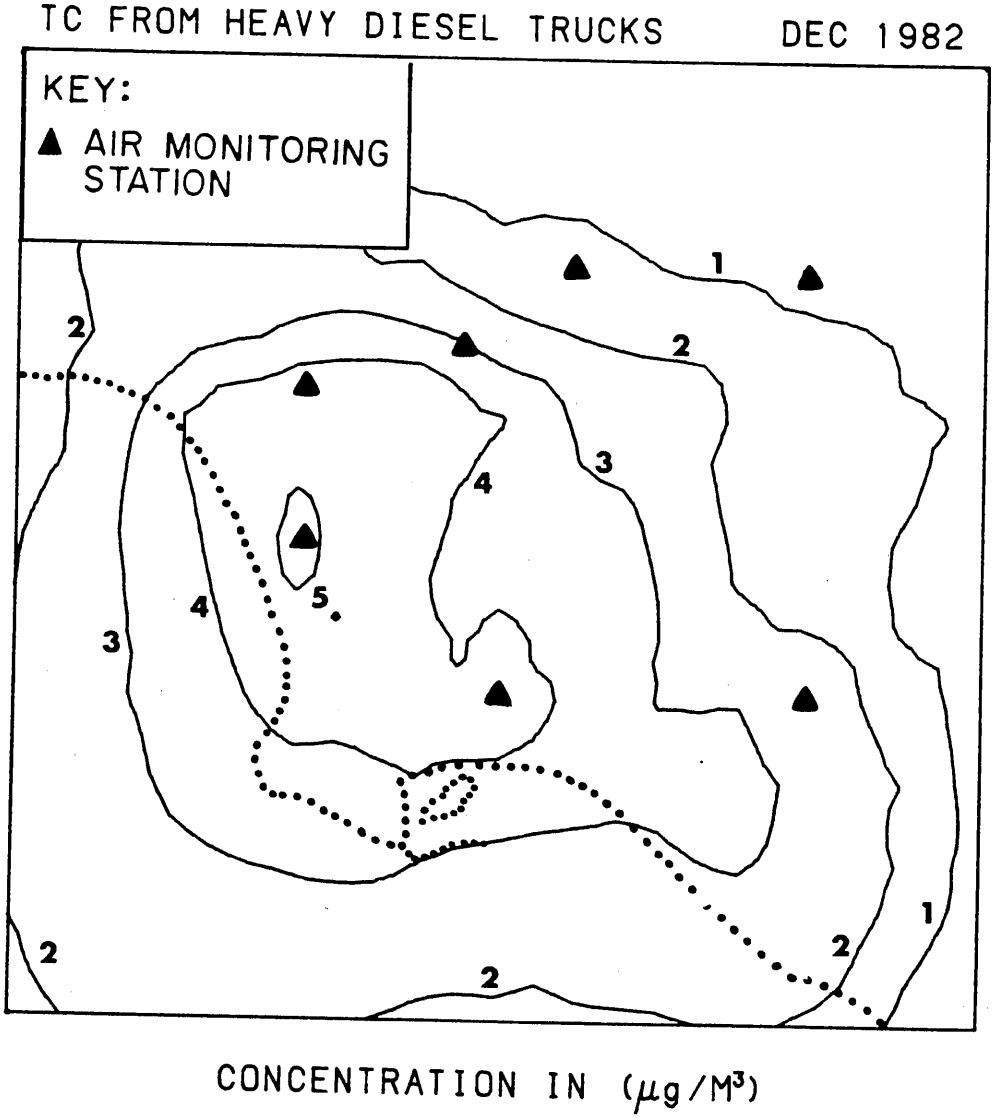

Figure 4.39 Fine primary total carbon air quality increment due to heavy diesel trucks--December 1982.

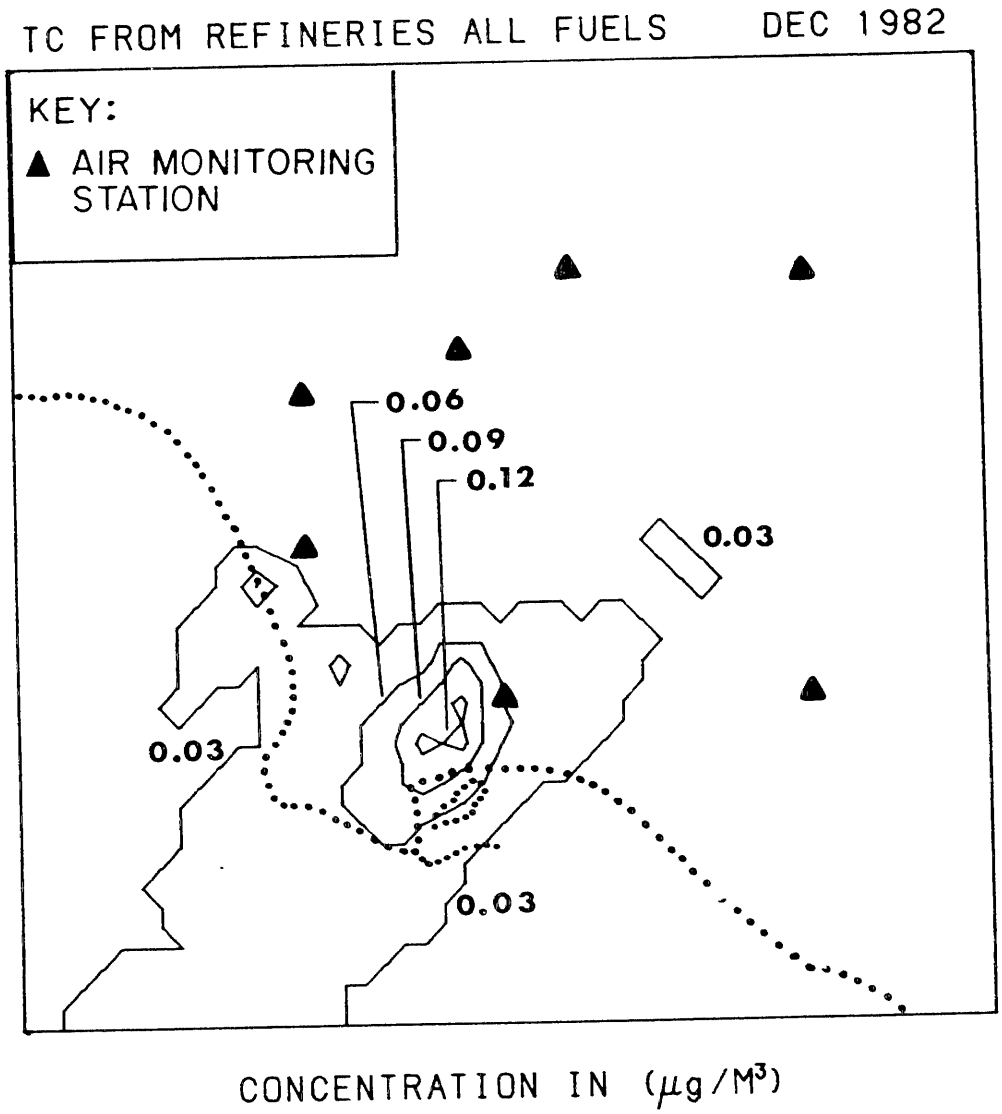

Figure 4.40 Fine primary total carbon air quality increment due to petroleum refinery fuel combustion--December 1982.

In December, the magnitude of total carbon concentrations due to heavy diesel trucks is much greater, with a peak increment of 5.23 $\mu g/m^3$ near Lennox. In winter months, predominant winds are from the northeast, thereby causing the areas of greatest impact to be the western portion of Los Angeles County and northern Orange County. Since this source type is the largest single source of total carbon emissions in the air basin, pollutant concentrations are largely affected by contributions from heavy diesel trucks. The contour plots for monthly averaged total carbon particulate concentrations from all sources in Figures 4.41 and 4.42 strongly resemble the contour plots representing the contribution to total carbon concentrations from heavy diesel trucks shown in Figure 4.37 and 4.39.

Figures 4.38 and 4.40 show the contribution to total carbon concentrations from fuel burning at refineries in June and December, respectively. Note that the magnitude of the contribution is very low, even in December. Refinery operations are located in the southwest of Los Angeles County, mostly near Long Beach, with other refineries located in Torrance and at El Segundo near Lennox. Overall transport of emissions from fuel combustion at refineries is offshore, towards the southwest, in December (Figure 4.40) and inland, towards the northeast, in June (Figure 4.38).

In Figures 4.7b through 4.13b and 4.15b through 4.21b, model-computed concentrations are divided into contributions from eight major source groups plus background concentrations at each of the monitoring locations. The spatial distribution of emissions is

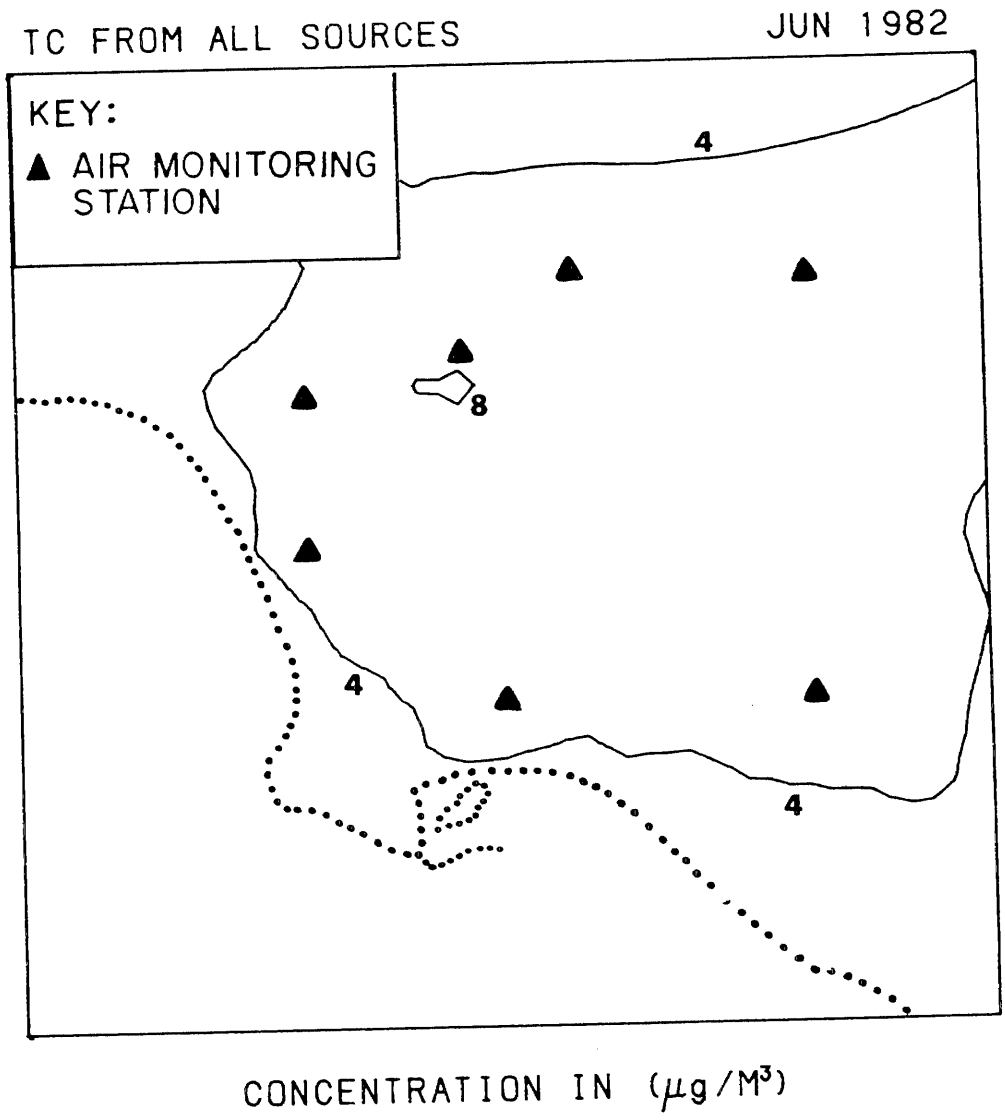

Figure 4.41 Monthly average fine primary total carbon concentration isopleths computed by the air quality model simulation--June 1982.

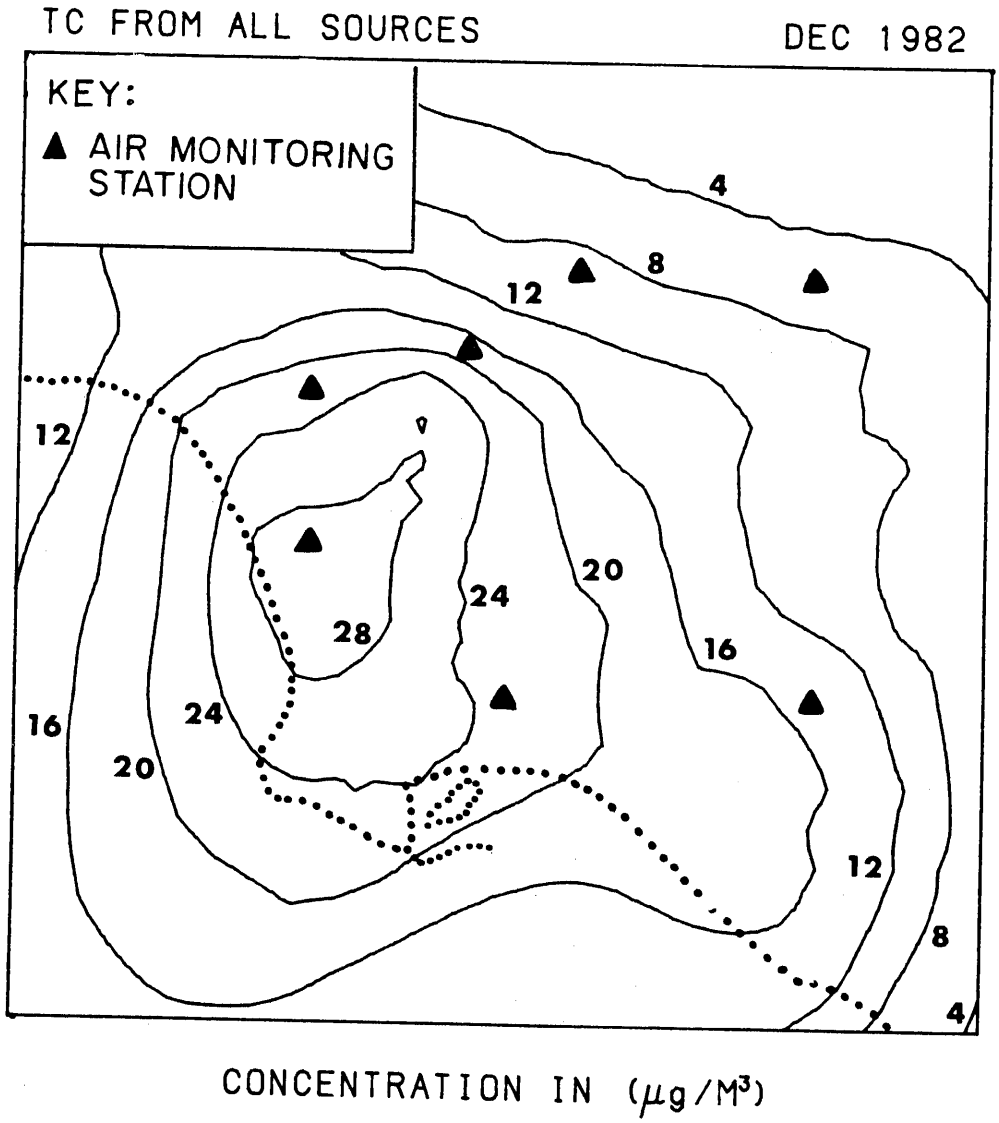

Figure 4.42 Monthly average fine primary total carbon concentration isopleths computed by the air quality model simulation--December 1982.

different for each source group. Hence, the relative importance of each source class varies by location.

As an extreme example, one may examine the contribution of aircraft emissions to atmospheric carbon particle concentrations. There is very little contribution at all sites except Lennox, which is near the Los Angeles International Airport. At Lennox, aircraft emissions are an important contributor, especially to elemental carbon concentrations (see Figure 4.7b).

At all stations, the largest single contribution to elemental carbon concentrations is due to emissions from diesel highway vehicles. This source class is responsible for between 40% to 50% of the elemental carbon concentrations in most months at most stations. At West Los Angeles, the contribution from highway diesels is near 60% for the later months of 1982. Other sources of elemental carbon emissions that contributed to a lesser extent were gasoline-powered vehicles and non-highway diesel fuel applications. These three mobile source classes were responsible for the overwhelming majority of elemental carbon concentrations at all sites.

On the other hand, total carbon concentrations are made up from contributions from a large number of varied source classes. The mobile sources, which were responsible for the majority of elemental carbon concentrations, are large contributors to fine total carbon particulate concentrations as well. However, there are other source

classes, such as charcoal broilers (within the fugitive combustion source category), which do not emit much elemental carbon but do emit particulate organic carbon and, therefore, contribute to the total carbon burden.

The sources responsible for pollutant concentrations have a direct bearing on the choice of an effective strategy for pollution control. If control of total carbon mass concentration is desired, then measures aimed at reducing emissions from many different sources must be considered. Diesel vehicle exhaust alone contributes the majority of the elemental carbon concentrations in Los Angeles. Therefore, if an effective control strategy for elemental carbon concentrations is sought, it must necessarily include measures which reduce particulate emissions from combustion of diesel fuel.

4.4 Summary

The Lagrangian air quality model, developed in Chapter 3, was applied to the task of predicting 1982 monthly average carbonaceous particulate concentrations in the Los Angeles air basin. An extensive fine particulate emissions inventory was assembled for the Los Angeles air basin. Other data requirements (e.g., meteorological) were outlined and satisfied. The model was employed to predict monthly average fine primary total carbon and fine elemental carbon concentrations at seven receptor locations that were monitored during 1982.

Concentration predictions were compared with observations of concentrations from the air monitoring network described in Chapter 2. The model appears to be a very good predictor of monthly average fine elemental carbon and total carbon particle concentrations. The model predicted seasonal trends that were very similar to those observed at most locations, and the correlation between predicted and observed monthly average concentrations was very high.

The model is accurate at predicting the magnitude and location of peak concentrations, which were generally at Los Angeles and Lennox. Concentration predictions may be improved in areas far from downtown Los Angeles (e.g., Azusa) by utilizing a more sophisticated wind field in the horizontal transport calculation.

The model, after having been validated, was used to determine source class contributions to both fine primary total carbon and fine elemental carbon concentrations at the seven receptor locations. These source-to-receptor transfer relationships may be used to predict the long-term average pollutant concentrations that would result from a different set of emission source strengths. Changes in emission strength can occur as a result of control measures being applied to a number of the source classes. Therefore, the model results may be used to determine the effect of strategies for control of fine carbonaceous particulate concentrations. This useful application of the modeling exercise is demonstrated in Chapter 5.

4.5 References for Chapter 4

Benjamin, J. R., and C. A. Cornell. 1970. Probability, statistics, and decision for civil engineers. New York: McGraw Hill.

Briggs, G. A. 1971. Plume rise: A recent critical review. Nuclear Safety 12, No. 1.

Cass, G. R. 1977. Methods for sulfate air quality management with applications to Los Angeles. Ph.D. thesis, California Institute of Technology, Pasadena.

Cass, G. R. 1981. Sulfate air quality control strategy design. Atmospheric Environment 15:1227-49.

Cass, G. R., and G. J. McRae. 1983. Source-receptor reconciliation of routine air monitoring data for trace metals: An emissions inventory assisted approach. Environmental Science and Technology 17:129-139.

Cass, G. R., M. H. Conklin, J. J. Shah, and J. J. Huntzicker. 1984. Elemental carbon concentrations: Estimation of an historical data base. Atmospheric Environment 18:153-62.

Davidson, C. I. 1977. Deposition of trace metal-containing aerosols on smooth, flat surfaces and on wild oat grass (Avena fatua). Ph.D. thesis, California Institute of Technology, Pasadena.

Drivas, P. J., and F. H. Shair. 1975. The chemistry, dispersion and transport of air pollutants emitted from fossil fuel power plants in California--transport of plumes associated with the complex coastal meteorology. California Institute of Technology, Division of Chemistry and Chemical Engineering. Pasadena. (Performed under California Air Resources Board contract no. ARB-915.)

Gifford, F. A. 1961. Uses of routine meteorological observations for estimating atmospheric dispersion. Nuclear Safety 2:47-51.

Gray, H. A., G. R. Cass, and B. Turpin. 1985. Source testing of road dust, cigarette smoke, roofing tar, and charcoal broilers. California Institute of Technology, Environmental Quality Laboratory Open File Report no. 85-1. Pasadena.

McElroy, J. L., and F. Pooler, Jr. 1968. St. Louis dispersion study. Vol. 2, Analysis. U.S. Public Health Service, National Air Pollution Control Administration Publication no. AP-53. Arlington, Virginia.

McRae, G. J. 1981 Mathematical modeling of photochemical air pollution. Ph.D. thesis, California Institute of Technology, Pasadena.

Pasquill, F. 1961. The estimation of the dispersion of windborne material. Meteorol. Mag. 90:33-49.

Phadke, M. E., G. C. Tiao, M. Grupe, S. C. Wu, A. Krug, and S. T. Liu. 1975. Los Angeles aerometric data on sulphur dioxide, particulate matter and sulphate 1955-1972. University of Wisconsin, Department of Statistics Technical Report no. 410. Madison.

Ranzieri, A. J., California Air Resources Board. Letter to author, 30 November 1983: Forwarded copy of magnetic tape AR3288 containing 1982 gridded emission inventory of South Coast Air Basin point and area sources.

Shair, F. H. 1977. Personal communication, 30 September 1977: Forwarded preliminary analyses of SF_6 tracer studies performed under California Air Resources Board contract no. A6-202-30.

South Coast Air Quality Management District. 1983a. Fuel use reports for 1982. El Monte, California.

South Coast Air Quality Management District. 1983b. 1982 wind data. El Monte, California.

South Coast Air Quality Management District. 1983c. Air quality and meteorology. Monthly reports for 1982. El Monte, California.

Turner, D. B. 1969. Workbook of atmospheric dispersion estimates. U.S. Public Health Service, National Air Pollution Control Administration Publication no. 999-AP-26. Cincinnati.

Walpole, R. E., and R. H. Meyers. 1978. Probability and statistics for engineers and scientists. 2d ed. New York: Macmillan Co.

CHAPTER 5

OPTIMAL STRATEGIES FOR THE CONTROL OF FINE PRIMARY PARTICULATE CARBON AIR QUALITY

5.1 Introduction

In the previous chapter, a Lagrangian air quality model was applied to the task of predicting monthly average fine primary particulate carbon concentrations in the Los Angeles area. Results from the model calculation may be combined with information on emission control measures and their costs in order to determine the optimal strategy for attaining any desired level of improved aerosol carbon air quality. The air quality model predicts the contribution to pollutant concentrations at seven monitoring sites from many different source types. The model's calculation scheme is linear in pollutant emissions. In other words, the model-computed contribution from any single source type is proportional to the basin-wide level of emissions from that source type. Therefore, a linear programming algorithm may be applied to determine the least costly combination of control measures that would achieve a given air quality goal simultaneously at the seven monitoring sites.

A linear program consists of an objective to be optimized, in the form of a function to be minimized or maximized, and a set of constraints, which take the form of a set of linear inequalities. The objective in this application is to minimize the cost of applying a

set of emission control measures. The most important constraint is that the air quality must improve. It is required that the annual average pollutant concentration be held at below a stated limit at each of the seven monitoring sites. To achieve this air quality goal, a trial set of emission control measures is selected. Results of the air quality model then are used to compute a hypothetical prediction of the 1982 annual average pollutant concentration at each site that would result from the pollutant emissions that remain after the given set of controls has been put in place. If the combination of control measures produces air quality which satisfies the constraints, then the strategy is feasible. The optimal control strategy is the feasible strategy that has the lowest cost.

Linear programming techniques often are used alongside air quality models to determine the least costly air pollution control strategy. Kohn (1970) minimized the cost of reducing basin-wide emissions in St. Louis using a linear rollback emissions to air quality model. Spatially resolved Gaussian plume models that attempt to account for atmospheric transport processes have been employed by researchers, in conjunction with linear programming techniques, to choose the least costly combination of control measures that will result in a required level of air quality improvement (Atkinson and Lewis 1974, Kohn 1974, Teller 1967). Burton and Sanjour (1970) combined a Gaussian plume air quality model with integer programming techniques (that guard against the choice of fractions of a control measure) to select strategies for control of particulate matter and

sulfur oxides in Washington, D.C., and Kansas City. Integer programming and linear programming techniques were compared by Gipson, Freas, and Meyer (1975) in case studies of three urban areas. Trijonis et al. (1975) used linear programming techniques to select least costly strategies for particulate matter control based on a non-linear emissions to air quality model that takes into account the secondary formation of particulate matter. Atkinson and Lewis (1974) and many others have indicated that the use of sophisticated air quality models to predict pollutant contributions from sources will result in a large cost savings when addressing the question of air quality control. A review of air quality modeling techniques that have been matched to optimization techniques may be found in Cass and McRae (1981).

In this chapter, a linear programming technique is stated that optimizes the choice of a strategy for regional air pollution control. The technique is applied to the control of fine primary carbonaceous particulate concentrations in the Los Angeles area. Since air quality standards do not exist at present for aerosol carbon species, no single air quality constraint can be considered at this point. Instead, the linear programming exercise can be run repeatedly for a variety of possible air quality objectives. By organizing those results, one can depict the least costly path toward air quality improvement, that is, the sequence in which the control measures are to be applied as air quality constraints are tightened. Optimal strategies for control of fine primary total aerosol carbon

concentrations are compared to optimal strategies aimed at controlling fine elemental carbon concentrations. The distinction between these two possible objectives is important. Total carbon control would be favored if reduction in aerosol mass loading is sought, while preferential control of elemental carbon would be favored as part of a strategy aimed at visibility improvement.

5.2 Formulation of the Linear Programming Technique

The control strategy which satisfies a regional air quality goal at the lowest cost can be identified by solving the following minimization problem:

Choose $x_1, x_2, \ldots, x_K$ to minimize:

$$C = \sum_{k=1}^{K} c_k x_k \tag{5.1}$$

Subject to:

$$\sum_{k=1}^{K} \sum_{j=1}^{J} t_{ij}\, r_{jk}\, x_k \geq q_i \qquad i = 1,\ldots,I \tag{5.2}$$

$$\sum_{k=1}^{K} d_{mk}\, x_k \leq s_m \qquad m = 1,\ldots,M \tag{5.3}$$

$$\sum_{k=1}^{K} b_{nk}\, x_k \leq 1 \qquad n = 1,\ldots,N \tag{5.4}$$

$$0 \leq x_k \leq 1 \qquad k = 1,\ldots,K \tag{5.5}$$

where

C is the total annual cost of the emission control strategy ($/year).

c_k is the cost of utilizing control measure k at all emission sources to which the control measure applies ($/year).

x_k is the level of application of control measure k. If $x_k = 0$ then control k is not used. If $x_k = 1$ then control k is applied to the maximum possible extent.

t_{ij} is a transfer coefficient from the air quality model which indicates the predicted annual average pollutant concentration increment at monitoring site i contributed by a single source class j ($\mu g/m^3$) at uncontrolled emission levels.

r_{jk} is the fractional reduction in pollutant emissions at source class j resulting from the application of control measure k. It is assumed that the fractional reduction in emissions, if control k is applied, is the same for all sources within single source class j. (Local emission control regulations generally apply uniformly to all sources of the same type in an air basin.)

q_i is the required air quality improvement at site i ($\mu g/m^3$). Note that $q_i = p_i - g$ where p_i is the present pollutant concentration at site i and g is the regional air quality goal.

d_{mk} is the amount of scarce resource m which is required if control measure k is adopted as part of the control strategy.

s_m is the limited supply of scarce resource m which is available for control strategy use.

b_{nk} is a compatibility parameter. The purpose of inequalities (5.4) is to prevent the simultaneous application of two or more incompatible control measures. For example, if control measure α conflicts with control measure β, then the requirement $x_\alpha + x_\beta \leq 1$ would prevent the application of both control measures to the same source. Emission control measures that conflict with one another will be grouped. All control measures k falling in the same group of conflicting controls are assigned values $b_{nk} = 1$; otherwise, $b_{nk} = 0$.

I is the number of air monitoring sites at which the air quality goal must be satisfied.

J is the number of source classes.

K is the number of control measures.

M is the number of different scarce resources required by the set of K control measures.

N is the number of groups of conflicting control measures among the universe of K control measures.

It is desired to solve for the control strategy, $(x_1, x_2, \ldots, x_K)$ which will minimize the overall cost, as shown in equation (5.1), while meeting the required air quality goal as expressed in the inequalities of (5.2). Constraints (5.3) are used to limit the consumption of resources, each of which is needed by one or more of the control measures. The inequalities of (5.4) are used to prevent the simultaneous application of conflicting control measures and the inequalities of (5.5) require that each x_k lie in the interval between 0 and 1 (between zero use and 100% application).

The minimization problem stated in (5.1) through (5.5) may be rewritten using matrices and vectors as follows:

Minimize

$$C = \underset{\sim}{c}^T \underset{\sim}{x} \tag{5.1'}$$

subject to:

$$T\underset{\sim}{R}\underset{\sim}{x} \geq \underset{\sim}{q} \tag{5.2'}$$

$$\underset{\sim}{D}\underset{\sim}{x} \leq \underset{\sim}{s} \tag{5.3'}$$

$$\underset{\sim}{B}\underset{\sim}{x} \leq \underset{\sim}{e} \tag{5.4'}$$

$$\underset{\sim}{x} \geq \underset{\sim}{0} \tag{5.5'}$$

where

$\underset{\sim}{c}, \underset{\sim}{x}, \underset{\sim}{q}$, and $\underset{\sim}{s}$ are vectors whose elements are the values c_k, x_k, q_k, and s_m, respectively, as described in (5.1) through (5.5).

T, R, and D are matrices whose elements are the values t_{ij}, r_{jk} and d_{mk}, respectively, as described in (5.1) through (5.5).

B serves two purposes. As in (5.4), it requires that $x_\alpha + x_\beta + \ldots + x_\gamma \leq 1$ for controls $\alpha, \beta, \ldots, \gamma$ which cannot be applied simultaneously. Since all $x_k \geq 0$, this is a stricter constraint than each of $x_\alpha \leq 1, x_\beta \leq 1, \ldots + x_\gamma \leq 1$ which are required by (5.5). Therefore, the constraints $x_k \leq 1$ of (5.5) may be incorporated into the matrix B in the following manner. B is constructed by starting with the identity matrix I $(k \times k)$, followed by adding a row for each conflict group n, such that $b_{nk} = 1$ if control k is in the group (0 otherwise), and then finally removing each row k of the original identity matrix if control k was specified in any conflict group. Therefore a 1 should appear at least once in each column of B.

$\mathbf{e}$ is a vector whose elements, e_n, all equal 1, i.e., $\mathbf{e}^T = (1,1,\ldots,1)$.

$\mathbf{0}$ is a vector whose elements are all zero, i.e., $\mathbf{0}^T = (0,0,\ldots,0)$.

The problem stated in (5.1) through (5.5) or in (5.1′) through (5.5′) may be solved directly by linear programming techniques. Linear programming is the study of systems of linear inequalities. In general, any equality, $x = a$, may be represented by two inequalities, $x \geq a$ and $x \leq a$. Therefore linear algebra, which is the study of systems of linear equalities, is merely a special case of linear programming. In 1902, Julius Farkas proved an important theoretical result concerning the existence of solutions to linear programming problems. However, not until the computer age began did efficient methods of finding solutions arrive. In 1951, George Dantzig's simplex method appeared (Dantzig 1951, Franklin 1980). The simplex method enables one to find the optimal feasible solution (if a feasible solution exists) to the following general problem (stated in canonical form):

$$\mathbf{A}\mathbf{x} = \mathbf{b}, \quad \mathbf{x} \geq \mathbf{0}, \quad \mathbf{c}^T\mathbf{x} = \min \tag{5.6}$$

The simplex algorithm may be found in any introductory text on linear programming (e.g., Gale [1960] or Franklin [1980]).

It remains to convert the system of (5.1′) through (5.5′) into the form of the canonical minimization problem (5.6). An inequality

$x \leq a$ may be transformed into an equality by introducing a slack variable z. Then $x + z = a$ together with $z \geq 0$ implies $x \leq a$. Introducing slack variables to the set of inequalities (5.2′) through (5.5′) yields:

$$(-TR)\underset{\sim}{x} + \underset{\sim}{z}^{(1)} = -\underset{\sim}{q} \tag{5.7}$$

$$D\underset{\sim}{x} + \underset{\sim}{z}^{(2)} = \underset{\sim}{s} \tag{5.8}$$

$$B\underset{\sim}{x} + \underset{\sim}{z}^{(3)} = \underset{\sim}{e} \tag{5.9}$$

$$\underset{\sim}{x} \geq 0, \ \underset{\sim}{z} \geq 0 \tag{5.10}$$

The matrix equations (5.7) through (5.9) may be rewritten as one partitioned matrix equation:

$$\begin{bmatrix} -TR & \\ D & I \\ B & \end{bmatrix} \begin{pmatrix} \underset{\sim}{x} \\ \underset{\sim}{z} \end{pmatrix} = \begin{bmatrix} -\underset{\sim}{q} \\ \underset{\sim}{s} \\ \underset{\sim}{e} \end{bmatrix} \tag{5.11}$$

and (5.10) becomes:

$$\begin{pmatrix} \underset{\sim}{x} \\ \underset{\sim}{z} \end{pmatrix} \geq \begin{pmatrix} \underset{\sim}{0} \\ \underset{\sim}{0} \end{pmatrix} \tag{5.12}$$

where

$$\underset{\sim}{z}^{T} = (\underset{\sim}{z}^{(1)T}, \underset{\sim}{z}^{(2)T}, \underset{\sim}{z}^{(3)T})$$

If equation (5.1′) is restated to minimize

$$C = (\underline{c}^T, \underline{0}^T) \begin{pmatrix} \underline{x} \\ \underline{z} \end{pmatrix} \tag{5.13}$$

then (5.11) through (5.13) are in the canonical form of (5.6) and are equivalent to the minimization problem presented in (5.1′) through (5.5′). It now requires only the application of the simplex method to determine if there exists a strategy $\underline{x}$ which satisfies (5.11) and (5.12) (feasibility), and if there is, to compute the optimal control strategy, $\underline{x}$.

5.3 Application of the Linear Programming Technique for Control of Fine Primary Carbonaceous Particulate Air Quality in the Los Angeles Area

5.3.1 Introduction

In this section, the linear programming technique discussed in Section 5.2 is applied to the task of computing the optimal strategy for controlling fine primary carbonaceous particulate air quality in the Los Angeles area. The calculation is performed using 1982 emissions data extracted from Chapter 4 of this work.

If a given set of emission control measures, which were not being used in 1982, had been in place during that year, then an improvement in air quality would have resulted. A prediction of what the 1982 air quality would have been, in the presence of an additional

set of emission controls, may be made by using the source class contributions to 1982 fine primary carbonaceous particulate concentrations computed by the air quality model in Chapter 4. A feasible set of emission control measures is sought, which would have resulted in a desired level of air quality improvement at a minimum cost.

Solving the fine particulate air quality problem in Los Angeles is difficult. In the last few decades, control devices have been installed at almost all industrial process sources that emit particulate matter. Despite these efforts, fine particulate matter concentrations in ambient air remain high. At downtown Los Angeles the 1982 annual average fine particulate matter concentration was measured to be 32.5 $\mu g/m^3$ and the peak monthly averaged fine particulate concentration was 58.2 $\mu g/m^3$ during December 1982. About 40% of the fine particulate was observed to be carbonaceous (see Chapter 2). The regional Air Quality Management Plan for the Los Angeles area (South Coast Air Quality Management District, 1982) does not offer much hope for future particulate air quality improvement. It contains only a few control measures for particulate emissions, and the emissions reductions are small.

In order to solve an air pollution problem, those sources responsible for the problem must be identified. In Chapter 4, Section 4.3.5, it was discovered that highway-related emissions are responsible for the majority of the fine carbonaceous particulate matter concentrations in the Los Angeles area. Therefore, it is

necessary to control these sources if a substantial improvement in fine carbonaceous particulate air quality is to be achieved.

5.3.2 Data Requirements

In order to solve the linear program of (5.11) through (5.13) to determine fine carbon particle control strategies, the matrices T, R, D and B and the corresponding requirement vectors $\underset{\sim}{q}$ and $\underset{\sim}{s}$ must be specified. Also the unit control cost vector, $\underset{\sim}{c}$, must be assembled.

The source to receptor transfer coefficient matrix, T, is constructed from the results of the air quality model calculation which was presented in Chapter 4. Each t_{ij} represents the predicted annual average pollutant concentration increment ($\mu g/m^3$) at site i due to emissions from source type j (at uncontrolled 1982 emission levels). Model concentration predictions made at seven air monitoring station sites resulting from emissions from 74 source types will be employed in the linear programming calculation (i.e. I = 7, J = 74). The increments to both fine primary total carbon and fine elemental carbon concentrations at each of these air monitoring sites from each source type are presented in Appendix F. Model results from all months of 1982 were averaged, weighted by the number of days in each month, to arrive at the predicted contributions to annual average fine primary total carbon and fine elemental carbon concentrations from each source.

Potential control measures for fine particulate carbon were inventoried, resulting in a list of 33 control measures (i.e., K =

33). Measures were sought which are technically feasible and the existence of which are reasonably certain. Generally, only control measures which involve some technological change were considered during this study, for example: control devices which are applied to emissions sources or the switching of grades of fuel. Control measures which require a political or social restructuring were not considered, for example: the changing of driving habits.

Detailed estimates of the costs and emission reduction capabilities of each of the 33 control measures appear in Appendix D. This information is summarized in Table 5.1. The costs are stated as an equivalent annual cost of operation plus allowance for amortization of capital investments in 1982 dollars per year. Estimation of the costs of control often is difficult. In recent years fuel prices have fluctuated greatly. The ultimate price of a new technology that has, to date, been demonstrated only at the prototype stage often is not known exactly. The price of a control device or resource may change drastically when demand is increased. It should be understood that the purpose of this exercise is to demonstrate the utility of the proposed linear programming calculation procedure, and that the calculations may be rerun when more reliable data on emission control measures and their costs become available.

The linear programming objective function, (5.13), assumes that the cost of a control is proportional to its application level, which may not always hold true. Some control cost functions may be non-linear. A non-linear cost function could be used to replace (5.13);

Table 5.1

Costs and Emissions Reductions of Control Measures Used in This Study

No.	Control Measure	Annual Cost ($10^6$$/year)	Fine Carbon Emissions Reductions (T/day)		Source Types Affected (a)	Conflicts
			Total Carbon	Elemental Carbon		
D.2	Catalysts on Non-catalyst Autos and Light Trucks	236.352	3.7387	0.7053	non-cat light duty vehicles(3,4)	
D.3	#1 Diesel Fuel Use by Light-duty Diesel Vehicles	4.317	0.2475	0.1896	light duty diesel vehicles(6,7)	D.4,D.5
D.4	Particle Traps on Light-duty Diesel Vehicles	8.148	0.9900	0.7583	light duty diesel vehicles(6,7)	D.3,D.5
D.5	Particle Traps & #1 Diesel Fuel Use for Lt-duty Diesel Vehicles	12.465	1.0395	0.7962	light duty diesel vehicles(6,7)	D.3,D.4
D.7	Catalysts on Non-Catalyst Medium & Heavy Gas Vehicles	66.453	1.1026	0.2080	non-cat medium/heavy vehicles(9,10)	
D.8	#1 Diesel Fuel Use by Heavy-duty Diesel Vehicles	38.523	1.4808	1.1343	heavy diesel vehicles(11)	D.9,D.10
D.9	Particle Traps on Heavy-duty Diesel Vehicles	36.240	6.6637	5.1044	heavy diesel vehicles(11)	D.8,D.10
D.10	Particle Traps & #1 Diesel Fuel for Heavy-duty Diesel Vehicles	74.763	6.8118	5.2178	heavy diesel vehicles(11)	D.8,D.9
D.11	Air Taxi Modification (Towing)	0.000	0.1354	0.1053	aircraft surface(12)	
D.12	0.5%S Residual Oil for Shipping — Berthing Operations	2.253	0.0442	0.0088	shipping residual oil(16)	
D.13	#1 Diesel Fuel Use by Railroads	5.011	0.2858	0.2189	railroad diesel(18)	
D.14	#1 Diesel Fuel Use in Off-road Diesel Engines	8.725	0.4771	0.3654	off-road diesel(19)	D.15,D.16
D.15	Particle Traps on Off-road Diesel Engines	19.535	2.0827	1.5953	off-road diesel(19)	D.14,D.16
D.16	Particle Traps & #1 Diesel Fuel Use for Off-road Diesel Engines	28.260	2.1432	1.6417	off-road diesel(19)	D.14,D.15
D.18	Catalysts on Off-road Gasoline Engines	15.615	0.0831	0.0157	off-road gasoline(20)	
D.19	Use of 0.10%S Residual Oil by Utilities	30.442	0.1232	0.0247	utility residual oil(23)	D.34
D.20	Use of 0.10%S Residual Oil by Refineries	1.367	0.0056	0.0011	refinery residual oil(28)	D.35
D.21	Use of 0.25%S Residual Oil in Industrial Boilers	0.445	0.0047	0.0009	industrial boiler residual oil(31)	D.22,D.36
D.22	Use of 0.10%S Residual Oil in Industrial Boilers	2.404	0.0100	0.0020	industrial boiler residual oil(31)	D.21,D.36
D.24	Catalysts on Gasoline Large Industrial IC Engines	0.113	0.0013	0.0001	industrial IC gasoline engine(35)	
D.25	#1 Diesel Fuel Use in Diesel Industrial IC Engines	1.566	0.0057	0.0057	industrial IC diesel engine(36)	D.26,D.27
D.26	Particle Traps on Diesel Industrial IC Engines	4.796	0.0257	0.0257	industrial IC diesel engine(36)	D.25,D.27
D.27	Particle Traps & #1 Fuel in Diesel Industrial IC Engines	6.362	0.0263	0.0263	industrial IC engine diesel(36)	D.25,D.26
D.28	Use of 0.25%S Residual Oil by Residential/Commercial	3.094	0.0248	0.0049	residential/commercial residual oil(39)	D.37
D.29	Paved Road Flushing	430.689	—	—	paved road dust(61)	D.30
D.30	Paved Road Flushing and Broom Sweep	556.628	—	—	paved road dust(61)	D.29
D.31	Radial Tire Use on Light-duty Vehicles	0.0	0.1167	0.0385	tire attrition(62)	
D.32	Use of Gas Logs in Fireplaces	23.897	4.2394	0.7199	fireplace(65)	
D.33	Charcoal Broiler Control	4.370	4.8541	0.0728	charcoal broilers(68)	
D.34	Substitute Natural Gas for Residual Oil in Utility Boilers	0.0	0.1971	0.0411	utility residual oil(23)	D.19
D.35	Substitute Natural Gas for Residual Oil in Refineries	0.0	0.0063	0.0019	refinery residual oil(28)	D.20
D.36	Substitute Natural Gas for Residual Oil in Industrial Boilers	0.0	0.0098	0.0027	industrial boiler residual oil(31)	D.21,D.22
D.37	Substitute Natural Gas for Residual Oil in Residential/Commercial	0.0	0.0245	0.0016	residential/commercial residual oil(39)	D.28
	Fine Particle Emissions in the Entire 4-County South Coast Air Basin		52.1055	14.5071		

(a) See Appendix D, Table D.38 for the numerical list of 74 source types.

however, more information would be needed concerning the market prices of a number of items. Some control measures may be indivisible (they must be used completely or not at all). Integer programming could be used to search for the optimal solution where each x_k is confined to take a value of 1 or 0 only. However, most of the control measures listed in Table 5.1 can be applied to a fraction of the source class population (e.g., half of the city busses, half of the paved road surfaces) without taxing the feasibility of the control program. Therefore, execution of the more difficult integer programming problem was not deemed to be necessary.

In several cases, additional benefits would be attained from the use of a control technique, beyond the carbonaceous particulate emission reduction, which make that control measure more attractive than pictured in Table 5.1. For example, catalytic converters have been required on automobiles primarily to reduce CO, NO_x, and hydrocarbon emissions, although some particulate emission reductions also occur. In formulating the present problem, a choice is faced. Either the catalysts on automobiles are viewed as "costless" since they will be required for other reasons, or the merits of the catalytic converter may be assessed as if it were a particulate control technique. In the calculations that follow, the latter course is taken. The determination of whether the cost of utilizing a control measure is justified will be based only on its effect on carbon particle air quality. If one wishes to consider that catalysts placed on light-duty vehicles are a sunk cost, then it is a simple

matter to delete their cost from the cost of the aerosol carbon control program.

The column of annual costs in Table 5.1 contains the unit cost, c_k, of each control measure k. These values make up the unit cost vector $\underline{c}$. If a control measure has a level of application of one unit, it is being applied uniformly to all sources in the four-county South Coast Air Basin even if the source is located outside the 50X50-mile air quality modeling grid. That is done in recognition of the fact that it is administratively impractical to separate the western Los Angeles basin, where the air quality modeling grid resides, from the remainder of the airshed.

The reduction of fine total carbon and elemental carbon emissions in the South Coast Air Basin which would result from each control measure is presented in Table 5.1. These values were obtained by multiplying the fraction reduction (found in Appendix D) by the rate of emissions in the South Coast Air Basin (from Appendix C) for each source type that the control measure affects. Estimates of the 1982 actual fine total carbon and elemental carbon emissions from all sources in the South Coast Air Basin are presented at the bottom of Table 5.1, for comparison. The maximum reduction of total carbon emissions is 24.86 T/day, attainable if every control measure in Table 5.1 is adopted (excluding the very expensive paved road dust controls; if more than one control measure is in conflict, the measure which produces the largest reduction is used). This amounts to 48% of the 1982 total carbon emissions in the South Coast Air Basin. The cost for that maximum reduction of total carbon emissions

is estimated to be 481×10^6\$/yr. Approximately the same cost produces the maximum elemental carbon emissions reduction of 9.83 T/day, which amounts to 68% of the 1982 total for elemental carbon emissions in the air basin.

The emission reduction matrix, R, is constructed from the values presented in Appendix D, for total carbon (TC) and elemental carbon (EC) emissions reductions. A separate R matrix is developed for total carbon emissions and for elemental carbon emissions, and these two matrices are intended for use in separate linear programming calculations. Each r_{jk} is the fractional emissions reduction due to the application of control measure k at source type j. Since each control measure affects, at most, only a few source types, many of the r_{jk} are zero. The value of r_{jk} is non-zero if source type r is listed under control measure k in Table 5.1 (or Appendix D).

The multiplication of matrices T and R results in the matrix, TR, whose elements, $(tr)_{ik}$, represent the reductions in pollutant concentration at site i due to control measure k. A separate TR matrix was constructed for fine total primary carbon and fine elemental carbon concentration reductions.

The first 9 rows of the matrix B are constructed from the 9 groupings of incompatible controls listed in Table 5.2 (i.e., $N_1 = 9$). The n^{th} row contains the coefficients, b_{nk}, which equal 1 if control measure k is a member of conflict group n (0 otherwise). Subsequent rows are added to B for each control measure not included in any conflict group. Of the 33 control measures, only ten are not included

Table 5.2

Groupings of Incompatible Control Measures

Group 1:	LT-DUTY DIESELS
	D.3 #1 DIESEL FUEL USE BY LIGHT-DUTY DIESEL VEHICLES
	D.4 PARTICLE TRAPS ON LIGHT-DUTY DIESEL VEHICLES
	D.5 PARTICLE TRAPS & #1 DIESEL FUEL USE FOR LT-DUTY DIESELS
Group 2:	HEAVY DIESEL TRUCKS
	D.8 #1 DIESEL FUEL USE BY HEAVY DIESEL TRUCKS
	D.9 PARTICLE TRAPS ON HEAVY-DUTY DIESEL TRUCKS
	D.10 PARTICLE TRAPS & #1 DIESEL FUEL FOR HEAVY DIESEL TRUCKS
Group 3:	OFF-ROAD DIESELS
	D.14 #1 DIESEL FUEL USE IN OFF-ROAD DIESEL ENGINES
	D.15 PARTICLE TRAPS ON OFF-ROAD DIESEL ENGINES
	D.16 PARTICLE TRAPS & #1 FUEL FOR OFF-ROAD DIESEL ENGINES
Group 4:	UTILITY BOILERS - RESIDUAL OIL
	D.19 USE OF 0.10%S RESIDUAL OIL BY UTILITIES
	D.34 SUBSTITUTE NATURAL GAS FOR RESIDUAL IN UTILITY BOILERS
Group 5:	REFINERY BOILERS - RESIDUAL OIL
	D.20 USE OF 0.10%S RESIDUAL OIL BY REFINERS
	D.35 SUBSTITUTE NATURAL GAS FOR RESIDUAL IN REFINERIES
Group 6:	INDUSTRIAL BOILERS - RESIDUAL OIL
	D.21 USE OF 0.25%S RESIDUAL OIL IN INDUSTRIAL BOILERS
	D.22 USE OF 0.10%S RESIDUAL OIL IN INDUSTRIAL BOILERS
	D.36 SUBSTITUTE NATURAL GAS FOR RESIDUAL IN INDUS BOILERS

Table 5.2 (continued)

Group 7:	DIESEL STAT IC ENGINES
	D.25 #1 DIESEL FUEL USE IN DIESEL INDUSTRIAL IC ENGINES
	D.26 PARTICLE TRAPS ON DIESEL INDUSTRIAL IC ENGINES
	D.27 PARTICLE TRAPS & #1 FUEL IN DIESEL INDUSTRIAL IC ENGINE
Group 8:	RES/COM BOILERS - RESIDUAL OIL
	D.28 USE OF 0.25%S RESIDUAL OIL BY RESIDENTIAL/COMMERCIAL
	D.37 SUBSTITUTE NATURAL GAS FOR RESIDUAL IN RES/COM BOILERS
Group 9:	PAVED ROAD DUST
	D.29 PAVED ROAD FLUSHING
	D.30 PAVED ROAD FLUSHING AND BROOM SWEEP

in any conflict group (10 columns of the first 9 rows of B contain no non-zero values), so ten additional rows are added to B (i.e., N_2 = 10, $N = N_1 + N_2 = 19$). Only one element, b_{nk}, is non-zero in each of these additional six rows. A value of 1 is placed in each additional row, such that every column k of the final B matrix has at least one non-zero value.

The linear program has the capacity to limit the availability of scarce resources needed by control measures. Examination of control measure D.34 (see Appendix D) reveals that costs and pollutant emissions may be lowered by burning natural gas rather than residual oil. However, natural gas is not always available for use as a boiler fuel. Two cases are examined. In the first case, it is assumed that no additional natural gas is available for boiler fuel beyond that which was actually burned in 1982. In the second case, an unlimited natural gas supply is allowed at 1982 prices. Both cases make use of matrix D, which contains only one row (i.e., M = 1), with elements, $d_{mk} = d_{1k}$, equal to the amount of natural gas required by control measure k, beyond that consumed in 1982. The natural gas supply required by control measures D.34 through D.37 is listed in Appendix D.

The vector $\underline{s}$ contains only one value, $s_m = s_1$, which represents the natural gas available for the control strategy. For the limited natural gas case, $s_1 = 0$, whereas for the unlimited natural gas case, s_1 is set to a value which is larger than $\sum_{k=1}^{k} d_{mk}$ (the total natural gas required by all control measures).

The minimum cost of control to achieve an air quality goal under the two cases of natural gas supply may be compared. This comparison is useful in determining how much the availability of additional natural gas is worth, with respect to the improvement of carbon particle air quality. The air quality model shows that stationary fuel combustion sources were not responsible for a large fraction of the carbon particle concentration, so it is expected that the difference between control strategy costs in these two cases will not be large.

Finally, the vector of required air quality improvements $\underset{\sim}{q}$ must be constructed. Recall that each value, q_i, representing the air quality improvement required at site i, is equal to $p_i - g$, where p_i is the present pollutant concentration at site i, and g is the air quality goal to be met at all locations. The linear program will be solved a number of times with progressively stricter air quality goals. Initially, g is set near the present maximum annual average concentration at all sites. For each subsequent linear programming calculation, g is decreased by Δg until no feasible solution exists. For fine primary total carbon concentration control, Δg is set to be $(-)0.4\ \mu g/m^3$, while the decrement of the fine elemental carbon concentration limit is $(-)0.2\ \mu g/m^3$. By solving a number of successive linear programs, each with a slightly stricter air quality goal, a relationship will be developed between the cost of control and the concentration limit that could be met simultaneously at all receptor sites.

5.3.3 Results

The source to receptor transfer coefficients produced by the air quality model were used to determine the optimal control strategies for fine total carbon and fine elemental carbon particulate air quality in the Los Angeles area. The linear program of (5.11) through (5.13) was solved using the simplex method as implemented by a modified version of a computer code provided by Sandia National Laboratories (1979). The solution is the least costly set of control measures which would cause air pollutant concentrations to fall to or below a required concentration limit simultaneously at every receptor site.

The linear programming minimization problem was solved repeatedly, each time with a progressively stricter air quality requirement. The results are displayed in Figure 5.1 for fine primary total carbon control and in Figure 5.2 for fine elemental carbon control (limited natural gas case). Control measures are listed as each becomes a part of the optimal control strategy. (The number in parentheses next to each control measure in Figures 5.1 and 5.2 refers to the control measure number in Appendix D). As the allowable pollutant concentration limit is reduced, more and more controls become necessary.

Control measures are selected for inclusion in the optimal control strategy based on their cost and effectiveness in reducing ambient pollutant levels. Therefore control measures with zero costs were selected first, even though concentration reductions from these

Figure 5.1

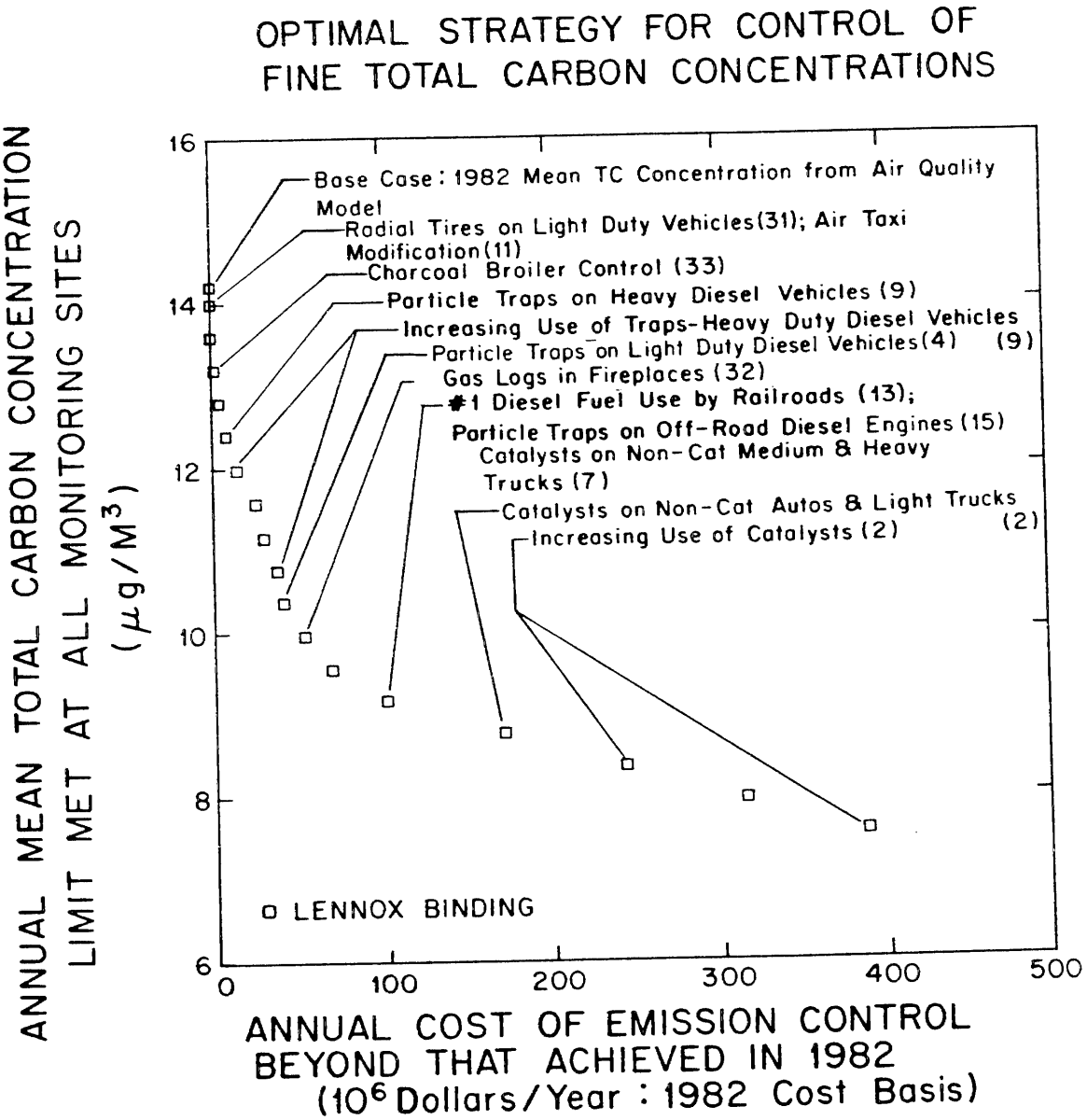
OPTIMAL STRATEGY FOR CONTROL OF FINE TOTAL CARBON CONCENTRATIONS
ANNUAL MEAN TOTAL CARBON CONCENTRATION LIMIT MET AT ALL MONITORING SITES ($\mu g/M^3$)
16
14
12
10
8
6
0
100
200
300
400
500
Base Case: 1982 Mean TC Concentration from Air Quality Model
Radial Tires on Light Duty Vehicles(31); Air Taxi Modification(11)
Charcoal Broiler Control (33)
Particle Traps on Heavy Diesel Vehicles (9)
Increasing Use of Traps-Heavy Duty Diesel Vehicles (9)
Particle Traps on Light Duty Diesel Vehicles(4)
Gas Logs in Fireplaces (32)
#1 Diesel Fuel Use by Railroads (13);
Particle Traps on Off-Road Diesel Engines (15)
Catalysts on Non-Cat Medium & Heavy Trucks (7)
Catalysts on Non-Cat Autos & Light Trucks (2)
Increasing Use of Catalysts (2)
□ LENNOX BINDING
ANNUAL COST OF EMISSION CONTROL BEYOND THAT ACHIEVED IN 1982
(10^6 Dollars/Year : 1982 Cost Basis)

Figure 5.2

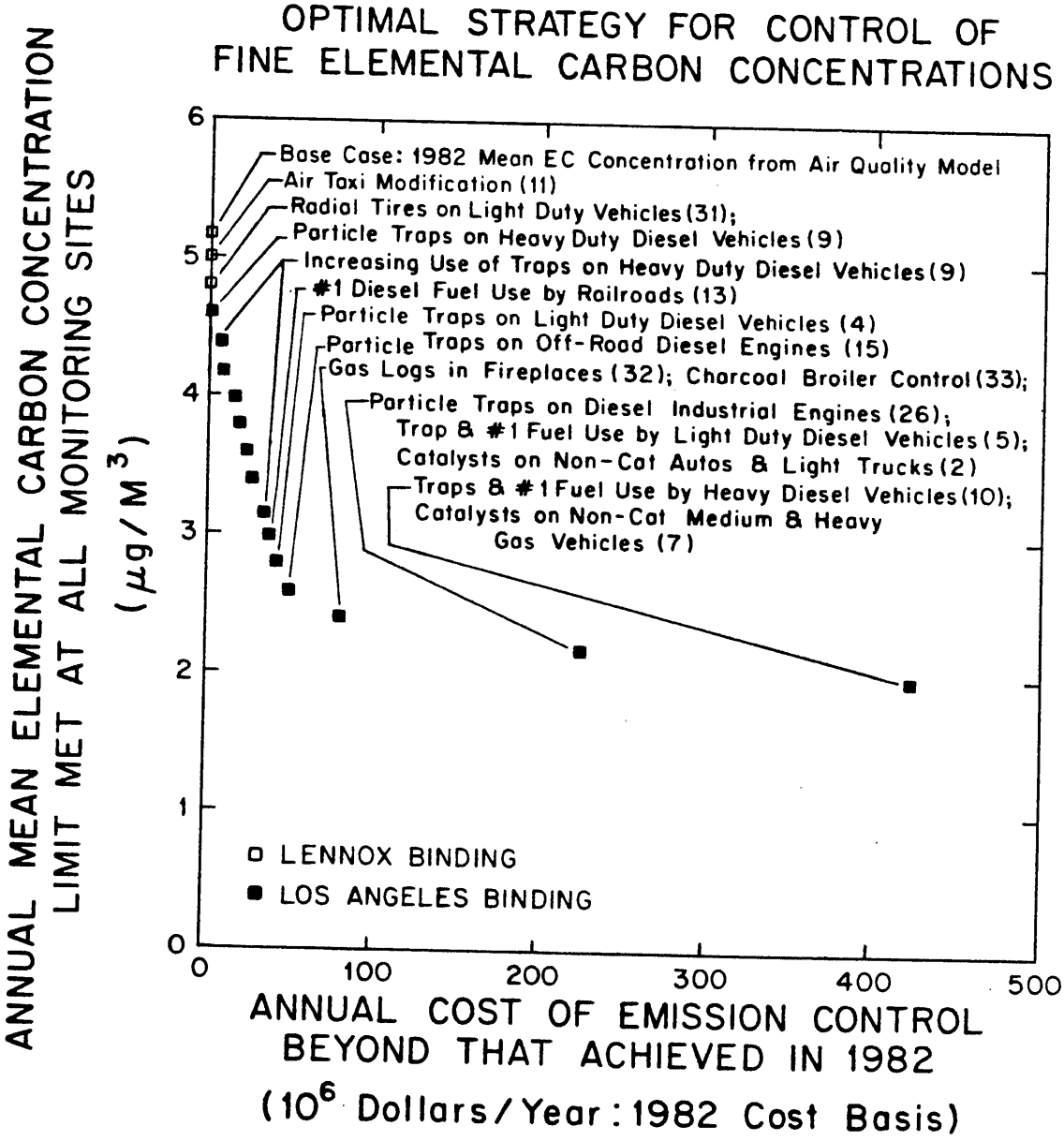
OPTIMAL STRATEGY FOR CONTROL OF
FINE ELEMENTAL CARBON CONCENTRATIONS
ANNUAL MEAN ELEMENTAL CARBON CONCENTRATION
LIMIT MET AT ALL MONITORING SITES
(μg/M³)
Base Case: 1982 Mean EC Concentration from Air Quality Model
Air Taxi Modification (11)
Radial Tires on Light Duty Vehicles (31);
Particle Traps on Heavy Duty Diesel Vehicles (9)
Increasing Use of Traps on Heavy Duty Diesel Vehicles (9)
#1 Diesel Fuel Use by Railroads (13)
Particle Traps on Light Duty Diesel Vehicles (4)
Particle Traps on Off-Road Diesel Engines (15)
Gas Logs in Fireplaces (32); Charcoal Broiler Control (33);
Particle Traps on Diesel Industrial Engines (26);
Trap & #1 Fuel Use by Light Duty Diesel Vehicles (5);
Catalysts on Non-Cat Autos & Light Trucks (2)
Traps & #1 Fuel Use by Heavy Diesel Vehicles (10);
Catalysts on Non-Cat Medium & Heavy
Gas Vehicles (7)
LENNOX BINDING
LOS ANGELES BINDING
0
1
2
3
4
5
6
0
100
200
300
400
500
ANNUAL COST OF EMISSION CONTROL
BEYOND THAT ACHIEVED IN 1982
(10⁶ Dollars/Year: 1982 Cost Basis)

controls are small. The additional cost of radial tires over bias-ply tires is offset by the longer life of radial tires (see Appendix D.31). The South Coast Air Quality Management District states that a fuel savings would occur if jet aircraft were towed when in taxi mode by special purpose vehicles (see Appendix D.11). Since these two control measures have no net cost, they are the most cost effective.

The next most cost effective control measures have non-zero costs, but result in large concentration reductions at all locations. These measures are aimed entirely at diesel engines in the case of fine elemental carbon particle control (see Figure 5.2). The annual cost of placing particle trap systems on all light and heavy duty diesel vehicles and off-road diesel engines, and switching from #2 diesel fuel to #1 diesel fuel in railroad use was estimated to be about 69×10^6 \$/yr (see Appendices D.4, D.9, D.13, and D.15). These four control measures would have reduced the 1982 annual average fine elemental carbon concentrations at downtown Los Angeles by approximately 2.24 $\mu g/m^3$, which represents almost a 50% concentration reduction at that location.

The four diesel control measures are also an effective choice for reducing fine primary total carbon concentrations. Two additional controls on charcoal broilers and on fireplace emissions (see Appendices D.33 and D.32), which reduce emissions from large sources of fine organic carbon, are included near the beginning of the total carbon control strategy list (see Figure 5.1). It is estimated that

these six controls would have reduced 1982 annual average fine total carbon concentrations at Lennox by about 4.3 $\mu g/m^3$ at an annual cost of less than 100×10^6 \$/yr.

As the concentration limit is further reduced, more costly (less cost-effective) control measures are added to the least cost control strategy. Although several hundred million dollars per year is needed to produce the largest possible concentration reduction, a very large reduction is possible at a fraction of that cost, if only the most cost-effective control measures are employed. It is estimated that for a cost of 102×10^6 \$/yr, the maximum annual average fine primary total carbon concentration may be reduced from above 14 $\mu g/m^3$ to 9.2 $\mu g/m^3$. The maximum annual average fine elemental carbon concentration may be reduced from above 5 $\mu g/m^3$ to 2.4 $\mu g/m^3$ at a cost of only 80×10^6 \$/yr.

The two cases of natural gas supply were examined. The control measures, D.34 through D.37, requiring a natural gas supply in excess of 1982 levels have zero costs and hence are included immediately into the control strategies when the unlimited natural gas supply case is considered. The concentration reductions resulting from these four control measures are very small (annual average elemental carbon concentration reductions less than 0.006 $\mu g/m^3$ at all locations; total carbon concentration reductions less than 0.035 $\mu g/m^3$ at all locations) so that the control strategies produced with and without a further increase in natural gas levels are almost identical.

The control strategy optimization for annual average pollutant

concentrations was compared to the same calculation for determining optimal control strategies for abatement of the peak monthly average pollutant concentrations. Transfer coefficients from the December 1982 air quality model calculation were used to compute optimal strategies for controlling peak monthly fine primary total carbon and fine elemental carbon concentrations. The linear programming results for peak monthly average concentrations were almost identical to those for annual average concentrations. Control measures were included in optimal control strategies in the same order for 1982 annual average concentrations as for December 1982 concentrations. It is expected therefore, that a control strategy which is chosen to be the most effective at reducing annual average carbon particle concentrations will also be optimal or near optimal for reducing peak monthly average carbon particle concentrations.

Optimal control strategies have been found for the reduction of annual average fine primary total carbon and fine elemental carbon concentrations in the Los Angeles area, as shown in Figures 5.1 and 5.2. These two strategies are similar, including mostly controls on diesel fuel combustion sources. These strategies do differ in some details. As mentioned previously, the emphasis on total carbon versus elemental carbon abatement should depend on the goal of the control program. A goal emphasizing mass concentration reduction favors total carbon control, while visibility improvement would be served best by a heavier emphasis on preferential removal of elemental carbon.

The effect of choosing between control strategies that

emphasize fine elemental carbon control versus fine total carbon control is illustrated in Figure 5.3. The solid line represents the optimal strategies for controlling fine elemental carbon concentrations. It was constructed from the points in Figure 5.2. For a given number of dollars spent, that curve determines the lowest possible elemental carbon concentration limit, which is attainable by adopting the optimal set of control measures as prescribed in Figure 5.2. If, however, the optimal strategy for total carbon concentration reduction is adopted, higher elemental carbon concentrations would result at some levels of expenditure as shown by the dashed line in Figure 5.3.

The difference between the two strategies is largest when control costs are in the vicinity of $69 million per year. At this cost, optimization for total carbon control would result in a maximum annual elemental carbon concentration of about 2.72 $\mu g/m^3$. At the same cost, the optimal strategy for elemental carbon control would produce a maximum annual elemental carbon concentration of approximately 2.44 $\mu g/m^3$.

The maximum annual average total carbon concentrations which would result from the optimal control strategies for elemental carbon are shown on the dashed line in Figure 5.4. If $50 million per year is spent on control measures to produce the lowest possible maximum annual average elemental carbon concentration, then the maximum annual average total carbon concentration at any location would be about 10.8 $\mu g/m^3$. Adoption of the optimal strategy for total carbon

Figure 5.3 Control of elemental carbon concentration: comparison of optimal strategy for EC reduction to EC concentrations that result from optimal strategy for TC reduction.

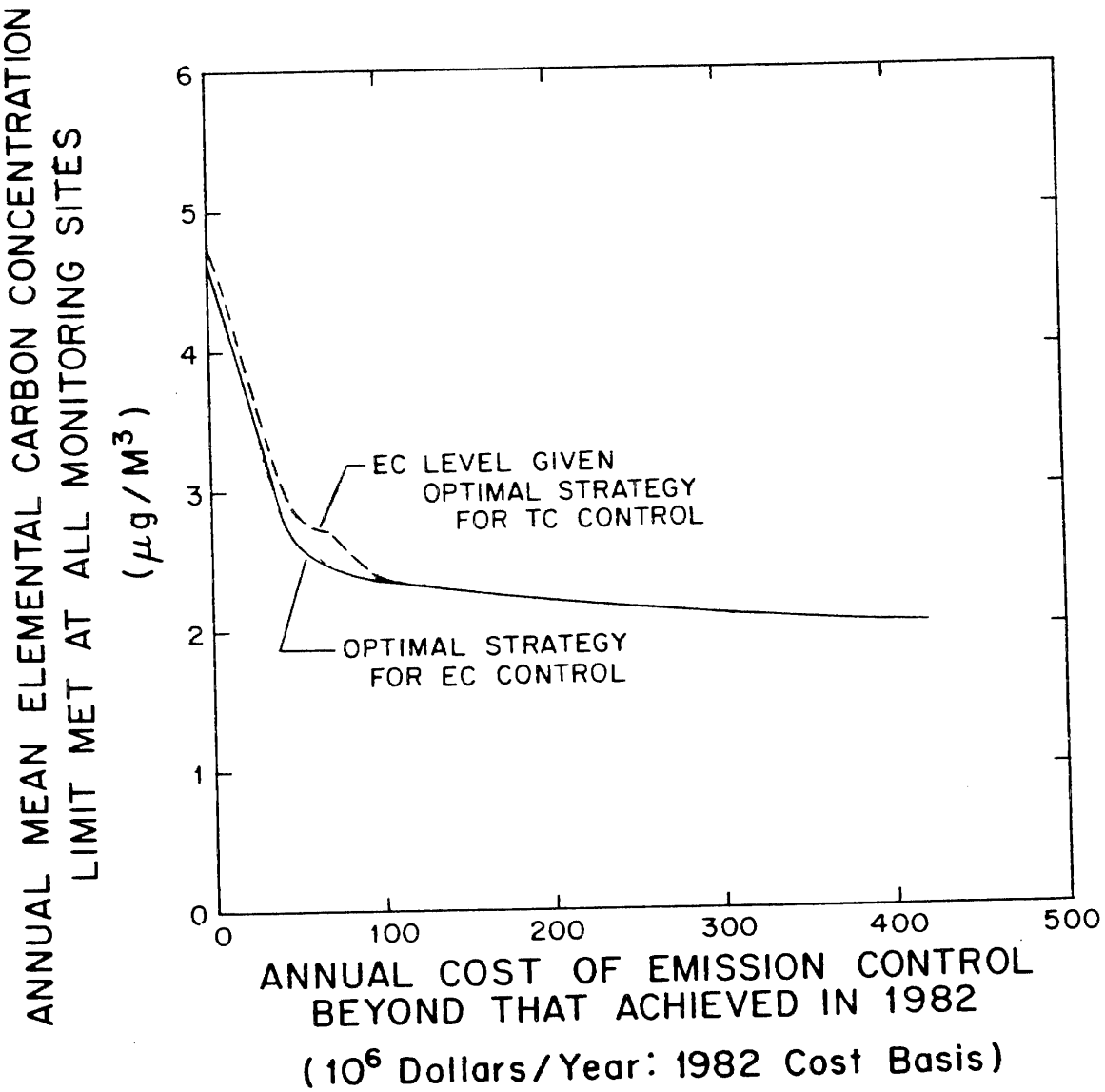

Figure 5.4 Control of total carbon concentration: comparison of optimal strategy for TC reduction to TC concentrations that result from optimal strategy for EC reduction.

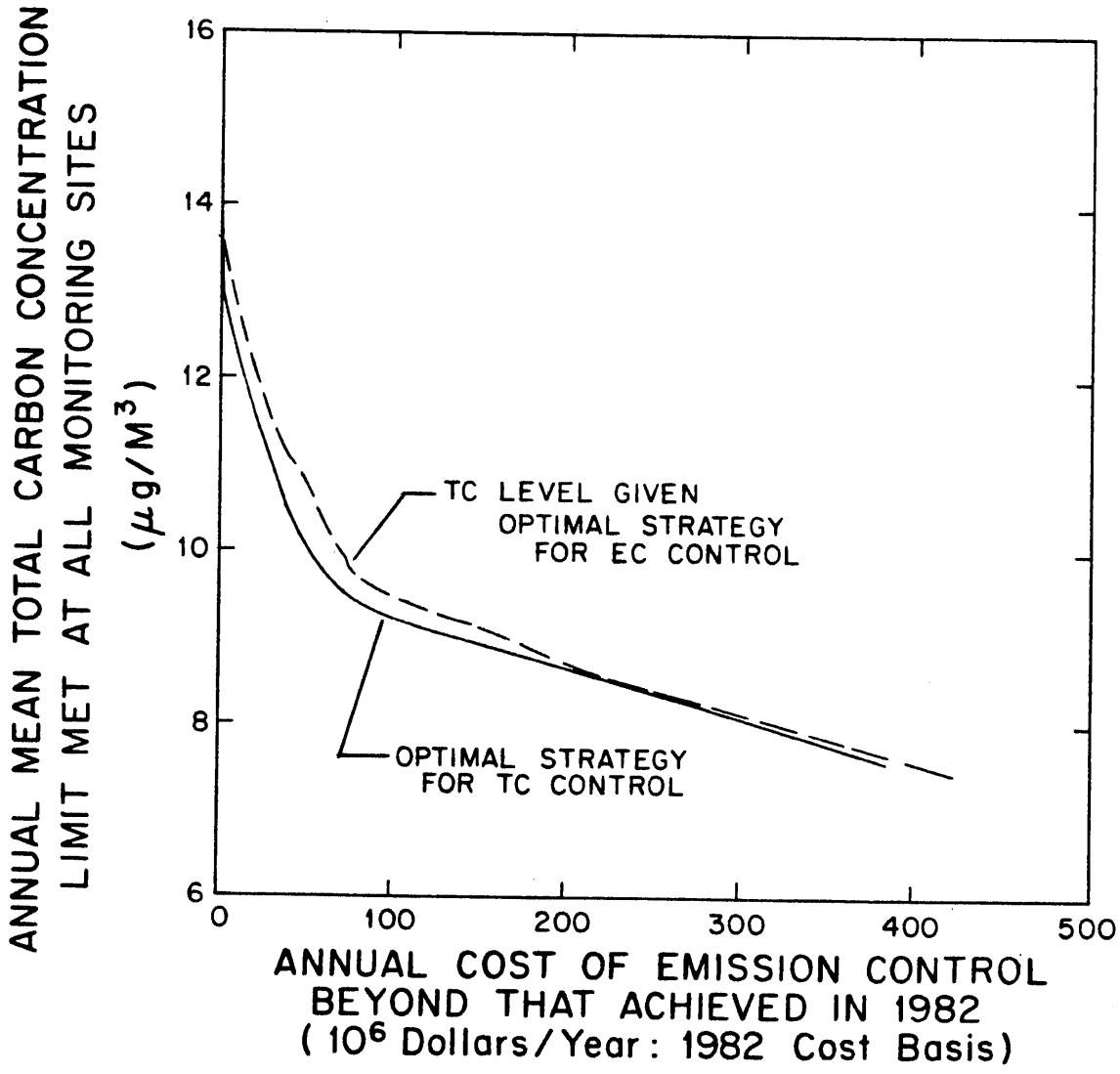

control, at the same cost, would result in a maximum annual average total carbon concentration slightly higher than 10.0 $\mu g/m^3$.

Either of the two optimal control strategies, for costs greater than $100 million, produce similar maximum annual average elemental carbon concentrations, as shown in Figure 5.3. Overall, the greatest difference between the effects of the two control strategies is on maximum annual total carbon concentrations, as seen in Figure 5.4. Controls on charcoal broilers and fireplace emissions (controls D.33 and D.32) are absent from low cost strategies aimed at reducing elemental carbon concentrations. The largest discrepancy in the two curves of Figure 5.4 disappears beyond a cost of about $220 million.

During the course of this project, two successive generations of cost estimates were supplied to the linear programming model. It was found that the order of preference for various control measures was virtually unchanged in spite of a complete review of the cost data which resulted in about a 25% increase in the total estimated cost of control.

5.4 Summary and Conclusions

In this chapter, a linear programming technique for air pollution control strategy optimization was applied to the problem of aerosol carbon control in the Los Angeles area. The technique combines source to receptor information derived from the air quality modeling study of Chapter 4 with data on the cost and emission reduction capabilities of a variety of control measures to determine

the least costly combination of controls that would result in a required air quality improvement.

Source to receptor coefficients are supplied in the form of source class contributions to fine elemental carbon and total carbon concentrations from the air quality model application presented in Chapter 4. A set of 33 control measures were defined in terms of their costs and emission reduction effectiveness. The linear program was solved for both fine elemental carbon (EC) and fine total carbon (TC) control, for a number of different levels of air quality improvement.

It was found that, while a 68% basin-wide fine elemental carbon emissions reduction could be achieved at an annual cost of near $500 million, resulting in peak annual average EC concentrations under 2.0 $\mu g/m^3$ at all locations, it is possible to reduce the annual average EC concentrations from the 1982 peak of over 5 $\mu g/m^3$ to 2.4 $\mu g/m^3$ at a cost of only $80 million/year. Annual average primary fine TC concentrations may be reduced from the 1982 peak of over 14 $\mu g/m^3$ to 9.2 $\mu g/m^3$ at a cost of $102 million/year. More than triple that cost is required to produce a reduction of peak annual average primary TC concentration to 7.6 $\mu g/m^3$ (see Figures 5.1 and 5.2).

The control measures included in the optimal strategies for fine elemental carbon control are aimed almost entirely at reducing emissions from diesel fuel combustion applications. These control measures on diesel emissions are also cost-effective measures for fine

primary total carbon control; however, the addition of several low cost control measures that produce large reductions in organic carbon emissions is needed as part of the optimal TC control strategies. The trade-offs implied by the choice of control strategy for TC versus EC were investigated. It has been determined that a control strategy that is optimal for TC control may be near-optimal for EC control (see Figure 5.3), whereas an emissions control strategy designed to optimize for EC control may produce peak TC concentrations that exceed those which would result from a control strategy optimized for TC by as much as 0.8 $\mu g/m^3$ annual mean (see Figure 5.4).

The effect of an increased availability of natural gas in the Los Angeles area was examined. Since the base case (1982) carbonaceous particulate emissions from boilers burning residual oil contribute only a small increment to overall aerosol carbon concentrations, the effect of an increased availability of natural gas on aerosol carbon concentrations is insignificant.

Optimal control strategies, designed to reduce 1982 annual average carbon particle concentrations, are almost identical to the optimal strategies for reducing aerosol carbon concentrations during the peak month of 1982 (December). Therefore, the control strategies that are most effective at reducing annual average carbon particle concentrations will be as effective as possible at reducing the peak monthly average concentrations.

The control strategy optimization technique described in this chapter was demonstrated to be a valuable tool for understanding how

to control air pollution. In a complex multiple source urban setting, emission control costs for even a modest air quality improvement program can be enormous. By employing the combination of field experiments, air quality model development and control cost optimization procedures described in this study, air pollution control strategies for aerosol carbon in Los Angeles can be identified that cost less than about $100 million per year which will perform nearly as well as other strategies costing at least three times as much.

5.5 References for Chapter 5

Atkinson, S. E., and D. H. Lewis. 1974. A cost-effectiveness analysis of alternative air quality control strategies. J. Environmental Economics and Management 1:237-50.

Burton, E. S., and W. Sanjour. 1970. A simulation approach to air pollution abatement program planning. Socio-Economic Planning Science 4:147-59.

Cass, G. R., and G. J. McRae. 1981. Minimizing the cost of air pollution control. Environmental Science and Technology 15:748-57.

Dantzig, G. B. 1951. Maximization of linear functions of variables subject to linear inequalities. In Activity analysis of production and allocation, ed. T. C. Koopmans, 339-47. New York: Wiley.

Franklin, J. N. 1980. Methods of mathematical economics. Springer-Verlag.

Gale, D. 1960. The theory of linear economic models. New York: McGraw Hill.

Gipson, G. L., W. Freas, and E. L. Meyer, Jr. 1975. Evaluation of techniques for obtaining least-cost regional strategies for control of SO_2 and suspended particulates. Environmental Science and Technology 9:354-59.

Kohn, R. E. 1970. Linear programming model for air pollution control: A pilot study of the St. Louis airshed. J. Air Pollut. Control Assoc. 20:78-82.

Kohn, R. E. 1974. Industrial location and air pollution abatement. J. Regional Science 14:55-63.

Sandia National Laboratories. 1979. SAND78-2322, unlimited release. (Printed August.)

South Coast Air Quality Management District and Southern California Association of Governments. 1982. Air quality management plan 1982 revision. Appendix no. 7-A, Short range tactics for the South Coast Air Basin.

Teller, A. 1967. Air pollution abatement: Economic rationality and reality. Daedalus (Fall): 1082-98.

Trijonis, J. C., G. Richard, K. Crawford, R. Tan, and R. Wada. 1975. An implementation plan for suspended particulate matter in the Los Angeles region. TRW Transportation and Environmental Engineering Operations, Redondo Beach, California. (March edition.)